DIFFRACTION STUDIES OF

HYDRAZINIUM COMPOUNDS

DIFFRACTION STUDIES OF

HYDRAZINIUM COMPOUNDS

by

MARTIN ROUSSELANGE ANDERSON, B.Sc.

A Thesis

Submitted to the Faculty of Graduate Studies

in Partial Fulfilment of the Requirements

for the Degree

Doctor of Philosophy

McMaster University

July, 1973

SCOPE AND CONTENTS:

A neutron diffractometer has been designed and used to investigate the mechanism of the supposed ferroelectric switching in $Li(N_2H_5)SO_4$. This was done by studying the effect of the anomalous scattering of neutrons from ^6Li on the structure factors of Bijvoet pairs. The absence of any observable change confirms that $Li(N_2H_5)SO_4$ is not ferroelectric.

The crystal structures of $Li(N_2H_5)BeF_4$, $Li(NH_3OH)SO_4$ and $(N_2H_6)BeF_4$ have been determined, and an accurate redetermination of the crystal structure of $Li(N_2H_5)SO_4$ has been made: all by X-ray diffraction. The structure of $Li(N_2H_5)BeF_4$ has also been studied by neutron diffraction. In the crystal structure determinations, all hydrogen atoms were located and hydrogen bonding schemes proposed; these were verified by the method of bond-strength summations.

ACKNOWLEDGEMENTS

I would like to thank my supervisor Dr. I. D. Brown for his encouragement and many valuable discussions throughout this research. I am also indebted to the other members of the crystallography group, especially Dr. C. Calvo and Dr. H. D. Grundy for their friendly assistance.

Finally, I wish to thank Donna MacDonald for typing this thesis.

TABLE OF CONTENTS

INDEX OF TABLES

x

INDEX OF ILLUSTRATIONS

Plates

Figures

CHAPTER I

GENERAL INTRODUCTION

This work is an investigation by X-ray and neutron diffraction of the crystal structures of sulphate and fluoroberyllate compounds containing: hydrazinium, $N_2H_5^+$; hydroxylammonium, NH_3OH^+; and hydrazonium, $N_2H_6^{2+}$. There are many reasons why these compounds are of interest to crystallographers, solid state physicists and chemists.

The compound lithium hydrazinium sulphate, $Li(N_2H_5)SO_4$, was first prepared by Sommer and Weise (1916). Pepinsky, Vedam, Okaya & Hoshino (1958) reported that it was a room temperature ferroelectric, likening it to the other ferroelectric sulphates: ammonium hydrogen sulphate, $(NH_4)HSO_4$ (Pepinsky et al., 1958a) and ammonium sulphate, $(NH_4)_2SO_4$ (Matthias and Remeika, 1956). They also correctly reported the space group and lattice parameters. Subsequently, $Li(N_2H_5)SO_4$ was extensively investigated crystallographically, spectroscopically and dielectrically (cf. Chapter IV); but no further evidence was found of ferroelectricity, nor of the existence of a ferroelectric to paraelectric phase change, nor as to what the possible switching mechanism would be. Neutron diffraction has played an important part in the understanding of hydrogen

bonded ferroelectrics. The small shifts in atomic positions, and especially those which are involved in the hydrogen bonding, can be studied by comparing the crystal structures of the ferroelectric and paraelectric phases. From these shifts, the nature of the phase transition is determined. Examples of such studies are the order-disorder phase transitions in potassium dihydrogen phosphate, KH_2PO_4 (Bacon & Pease, 1955); and colemanite, $CaB_3O_4(OH)_3.H_2O$ (Hainsworth & Petch, 1965); and the phase transition in ammonium sulphate (Schlemper and Hamilton, 1966) in which the hydrogen bonding configuration is stronger in the ferroelectric phase. This method is impossible with $Li(N_2H_5)SO_4$ as no paraelectric phase has been found between $77^{\circ}K$ and the decomposition temperature of $560^{\circ}K$. Our approach was to investigate the ferroelectric switching mechanism whereby the direction of spontaneous polarisation is reversed by the application of a suitable electric field. This was to be accomplished by designing and constructing a neutron diffractometer (Chapter III) and by studying the anomalous neutron scattering from a single crystal of $^6Li(N_2H_5)SO_4$ (Chapter IV).

Compounds of the form $LiMSO_4$ and $LiMBeF_4$, where M is a monovalent cation, show interesting structural configurations. $LiSO_4^-$ and $LiBeF_4^-$ often form three-dimensional frameworks of corner-sharing oxygen or fluorine tetrahedra which are distorted forms of either the

tridymite (space group $P6_3/mmc$) or tridymite-derivative structure (space group Icmm). These structures are characterised by a six-member ring of alternating LiO_4, SO_4 or LiF_4, BeF_4 tetrahedra. In the former space group, alternate members of the ring point in opposite directions from the plane of the ring; and in the latter, three adjoining tetrahedra point above the plane, while the remaining three point below the plane; these are shown in their ideal symmetry form in Figure 1-1. It can be seen that large cavities are formed between the layers made up of the six-membered rings, and these cavities contain the cations. With potassium as the cation (ionic radius[*] 1.33 Å), both $LiKSO_4$ (Bradley, 1925) and $LiKBeF_4$ (Le Roy and Aléonard, 1972) take on a distorted form of the tridymite structure with space group $P6_3$. The introduction of rubidium (ionic radius 1.47 Å) does not affect the fluoroberyllate structure which retains the pseudo-tridymite space group $P6_3$, but the sulphate changes to $P2_1/n$, a distorted form of the Icmm space group (Hahn, Lohre & Chung, 1969). The space group $P2_1cn$ occurs with the ammonium ion compounds (ionic radius 1.43 Å): $Li(NH_4)SO_4$ (Dollase, 1969) and $Li(NH_4)BeF_4$ (Chung & Hahn, 1972). The caesium compounds (ionic radius 1.67 Å) $LiCsSO_4$ (Wells, 1954) and $LiCsBeF_4$ (Chung & Hahn, 1972) have the

---

[*]The source of the quoted ionic radii is the Handbook of Chemistry and Physics (1970).

Figure 1-1.

The configuration of the six-membered rings in

a) tridymite framework, P6_3/mmc, and

b) tridymite-derivative framework, Icmm.
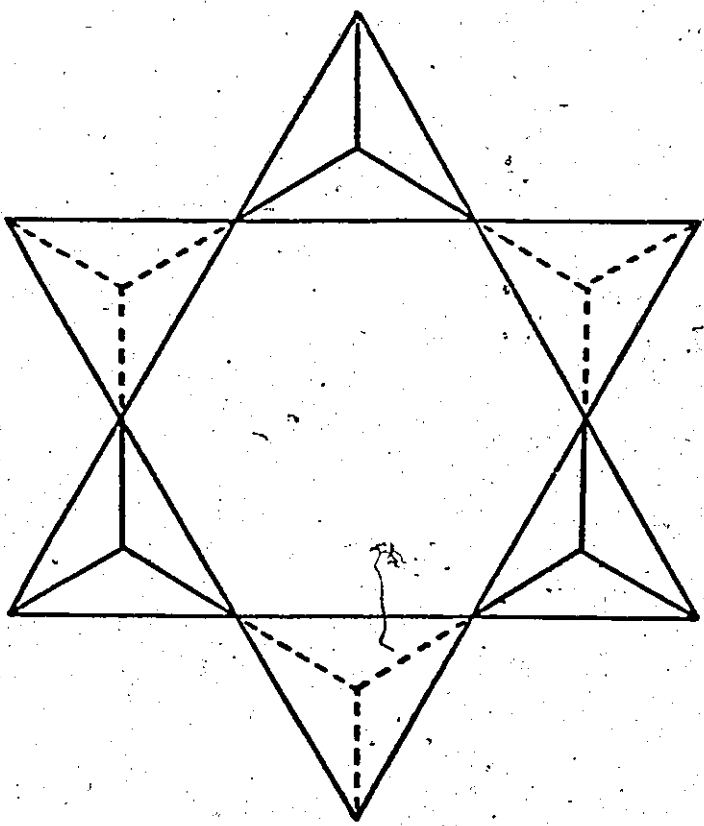
a
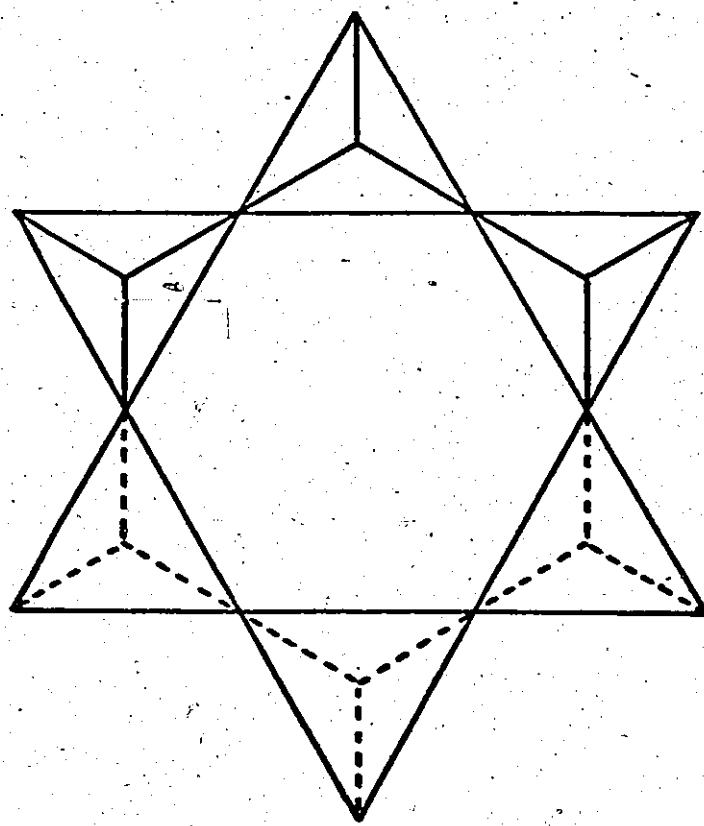
b

space groups $P2_1cn$ and $P2_1/n$ respectively. Thus, the introduction of progressively larger monovalent cations modifies the structure from tridymite to tridymite-derivative, the transition occurring between $LiRbBeF_4$ and $LiRbSO_4$; and this would indicate that $Li(N_2H_5)BeF_4$ would be isostructural to the corresponding sulphate which has a distorted form of the Icmm space group $Pna2_1$. We wished to confirm this prediction by determining the crystal structure of $Li(N_2H_5)BeF_4$ and wished also to investigate that of $Li(NH_3OH)SO_4$ to see if the hydroxylammonium cation would create a distortion of the Icmm space group or whether a completely different structure would result.

If $Li(N_2H_5)BeF_4$ and $Li(N_2H_5)SO_4$ proved to be isostructural, then they would be the only two known structures with chains of hydrazinium ions where the $-NH_2$ group was both the donor and acceptor of the hydrogen bonds forming the chain. The alternative type of chain is one in which a hydrogen bond donated by the $-NH_3^+$ group is accepted by the $-NH_2$ group; these two possible configurations are shown in Figure 1-2. A number of compounds form chains of the second type: $(N_2H_5)Cl$; $(N_2H_5)Br$ (Sakurai & Tomiie, 1952); $(N_2H_5)Ac$ (Liminga, 1968); $(N_2H_5)H_2PO_4$ (Liminga, 1965); and $(N_2H_5)HC_2O_4$ (Ahmed, Liminga & Olovsson, 1968). There are also hydrazinium compounds which do not form chains; examples of this type are $(N_2H_5)_2SO_4$ (Liminga & Lundgren, 1965) and $(N_2H_5)ClO_4 \cdot \tfrac{1}{2}H_2O$ (Liminga, 1967).

Figure 1-2.

The two possible configurations of hydrogen bonded chains of hydrazinium ions: a) $-NH_2$ as both donor and acceptor; b) $-NH_3^+$ as donor and $-NH_2$ as acceptor.
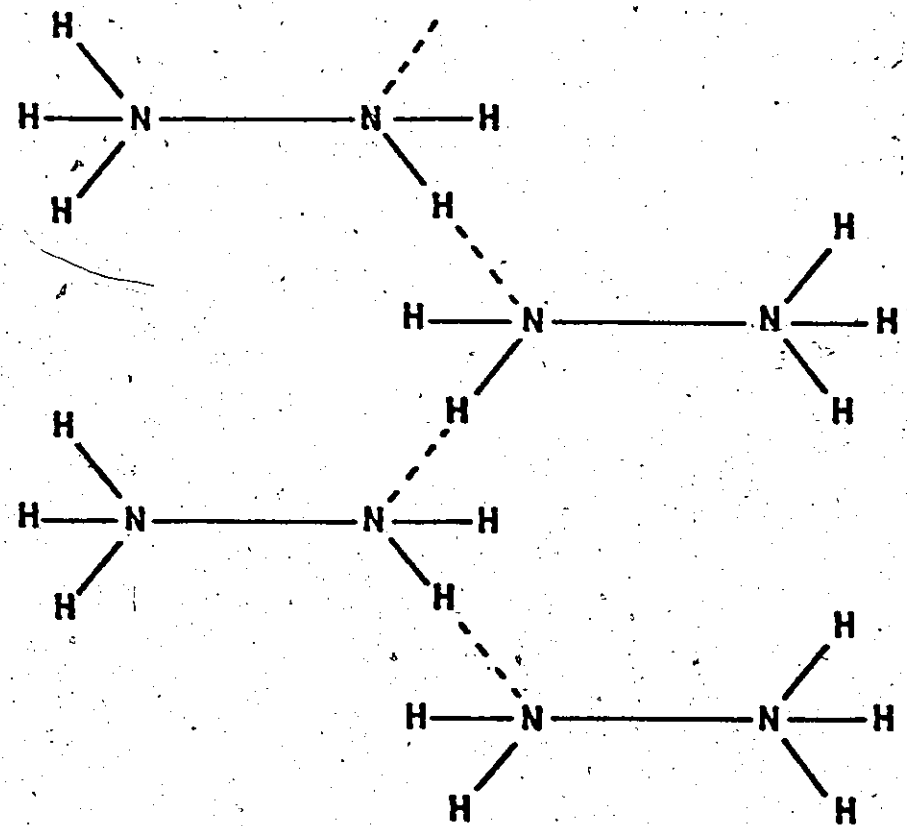
a

b
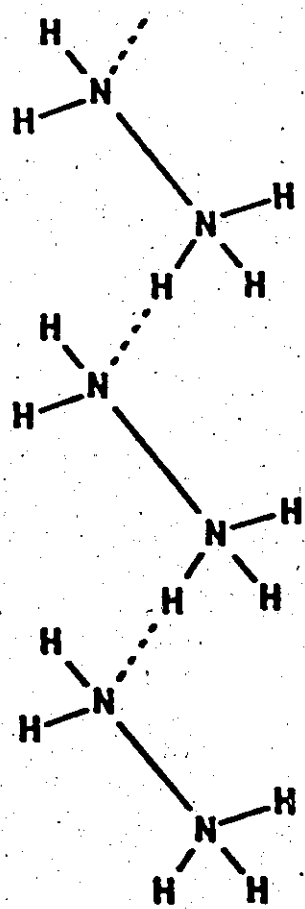
Another aspect of the crystallography of this type
of compound that we wished to investigate was the conformation
and hydrogen bonding networks of the hydrazinium,
hydroxylammonium and hydrazonium ions. We have pointed out
above that the hydrazinium ion can act as both donor and
acceptor of hydrogen bonds; when such a chain of hydrazinium
ions is formed, there are four remaining hydrogen atoms
which form bonds to fluorine or oxygen atoms of the
tetrahedral frameworks. In general, there will be more than
four potential acceptors competing for these bonds. In such
a situation, complex hydrogen bonding networks arise with
the occurrence not only of single but of bifurcated and
trifurcated hydrogen bonds. To study these systems properly,
accurate structure determinations are needed, either by X-ray
diffraction in which the hydrogen atoms are correctly
located or, preferably, by neutron diffraction with its
higher resolution of the hydrogen atoms. For this reason,
the structure of $Li(N_2H_5)BeF_4$ was examined by both methods,
and those of $Li(N_2H_5)SO_4$, $Li(NH_3OH)SO_4$ and $(N_2H_6)BeF_4$ were
determined from accurate X-ray diffraction measurements made
on a diffractometer.

If the positions of the hydrogen atoms are not
known, it is still possible to predict their positions.
Baur (1965) proposed a method where a simple point-charge
model is used to predict the hydrogen bonds from the water
molecules of inorganic hydrates by searching for hydrogen

positions giving a minimum in electrostatic energy. He has
also extensively studied the bond geometries of several
species of hydrogen bond and uses this to calculate the best
position for probable hydrogen bonds (Baur, 1972). These
methods are quite useful in compounds with few active
hydrogen atoms but are of little value in our case. Recently,
Brown and Shannon (1973) have shown that the existence of a
hydrogen bond can be predicted from the sum of bond-strengths
around oxygen atoms. This is very useful when bifurcated
and trifurcated bonds exist as it indicates the relative
amount of bonding received by each of the acceptors.
Brown (1973) has extended this scheme for bond-strength
sums around fluorine but, as very few accurate H-F bonds
have been reported, has not yet refined an H-F bond-strength
curve. It was hoped that with the two fluoroberyllate
structures, $Li(N_2H_5)BeF_4$ and $(N_2H_6)BeF_4$, an H-F
bond-strength curve could now be refined.

CHAPTER II

DIFFRACTION THEORY AND ITS APPLICATION TO

CRYSTAL STRUCTURE ANALYSIS

In this chapter a brief outline of the diffraction processes in crystals will be given along with a discussion of the methods of structure analysis used in subsequent chapters. Attention will be drawn to the differences and relative merits of X-ray and neutron diffraction; these will be exemplary, not exhaustive; a more thorough account of this and other aspects of crystallography is given in the many texts available (e.g. Stout & Jensen, 1968; Bacon, 1962; Woolfson, 1961).

Diffraction by a Crystal

A crystal lattice can be defined as a regular array of points in a crystal such that the atomic arrangement around each point is identical. The fundamental translation vectors, $\underline{a}$, $\underline{b}$ and $\underline{c}$, are such that if $\underline{r}'$ is the position vector of a lattice point, then all other lattice points, $\underline{r}$, are given by:

$$\underline{r} = \underline{r}' + n_1\underline{a} + n_2\underline{b} + n_3\underline{c} \qquad (2-1)$$

where n_1, n_2 and n_3 are integers. If $\underline{a}$, $\underline{b}$ and $\underline{c}$ are chosen

such that the volume $\underline{a} \times \underline{b}.\underline{c}$ is a minimum, then $\underline{a}$, $\underline{b}$ and $\underline{c}$ are said to be primitive. The parallelopiped formed by $\underline{a}$, $\underline{b}$ and $\underline{c}$ is called the unit cell which is often, but is not always, chosen to be primitive.

Symmetry operations exist which when applied to the lattice leave it unaltered. The translation operators:

$$\underline{T} = n_1\underline{a} + n_2\underline{b} + n_3\underline{c} \qquad (2-2)$$

where n_1, n_2 and n_3 are integers, are one set of such symmetry operators. At each lattice point there can exist a number of other symmetry operations which leave the atomic arrangement unaltered; these define the lattice point group and can include operations such as rotations, mirror planes, inversions, screw rotations and glide planes. There are fourteen basic kinds of lattice (the Bravais lattices) based on the seven distinct crystal systems. When these are combined with the 32 possible lattice point groups, one gets the 230 distinct space groups (International Tables for X-ray Crystallography, Vol. I, 1952).

Diffraction of a beam of X-rays or neutrons by a crystal occurs because the scattered radiation from the atoms of the crystal have a well-defined phase difference and hence interfere with each other. The incident beam can be considered as a plane wave, of wavevector $\underline{k}$ ($|\underline{k}| = 1/\lambda$), and the diffracted beam, with wavevector $\underline{k}'$, far outside the crystal is given by:

$$F(\underline{k}'-\underline{k}) = \int_{crystal} \rho(\underline{r}) e^{2\pi i (\underline{k}'-\underline{k}) \cdot \underline{r}} d\underline{r} \qquad (2-3)$$

where $\rho(\underline{r})$ is the scattering density at a point $\underline{r}$ in the unit cell. We define the scattering vector $\underline{s}$ to be $\underline{k}'-\underline{k}$:
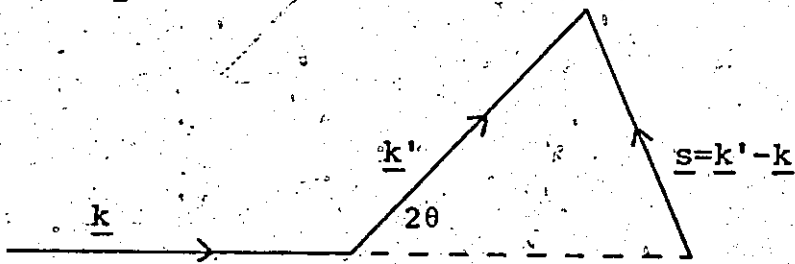
where θ is called the Bragg angle.

It can be shown that a diffraction peak will only occur when the scattering vector, $\underline{s}$, is equal to a reciprocal lattice vector $\underline{G}$ defined by:

$$\underline{G} = m_1 \underline{A} + m_2 \underline{B} + m_3 \underline{C} \qquad (2-4)$$

where m_1, m_2 and m_3 are integers and

$$\underline{A} = \frac{\underline{b} \times \underline{c}}{\underline{a} \cdot \underline{b} \times \underline{c}} \qquad \underline{B} = \frac{\underline{c} \times \underline{a}}{\underline{a} \cdot \underline{b} \times \underline{c}} \qquad \underline{C} = \frac{\underline{a} \times \underline{b}}{\underline{a} \cdot \underline{b} \times \underline{c}} \qquad (2-5)$$

The vectors $\underline{A}$, $\underline{B}$ and $\underline{C}$ are the basis vectors of the set of reciprocal lattice points $\{\underline{G}\}$. The vector $\underline{G}$ is perpendicular to lattice planes in the real cell and its magnitude is inversely proportional to the inter-planer spacing in the real cell denoted by $d_{hk\ell}$, where $hk\ell$ are the Miller indices of the plane. Thus for elastic scattering, $|\underline{k}| = |\underline{k}'|$, the

magnitude of the scattering vector is:

$$|\underline{s}| = 2|\underline{k}|\sin\theta = |\underline{G}|$$
$$= \frac{2}{\lambda}\sin\theta = \frac{1}{d_{hk\ell}}$$

therefore
$$2d_{hk\ell}\sin\theta = \lambda \qquad (2\text{-}6)$$

which is Bragg's law.

The intensity of a diffraction peak (often called a Bragg reflection) is given by:

$$I(\underline{G}) = C(\underline{G})\underline{F}(\underline{G}).\underline{F}^*(\underline{G}) \qquad (2\text{-}7)$$

where $C(\underline{G})$ is a constant involving various known fundamental quantities which depend on the scattered radiation and the scattering mechanism, $\underline{F}(\underline{G})$ is the amplitude of the diffracted beam (the structure factor) and $\underline{F}^*(\underline{G})$ its complex conjugate. From equation (2-3) and the diffraction condition $(\underline{k}'-\underline{k} \equiv \underline{s} = \underline{G})$, $\underline{F}(\underline{G})$ is given by:

$$\underline{F}(\underline{G}) = \int_{cell} \rho(\underline{r})e^{2\pi i\underline{G}.\underline{r}}d\underline{r}. \qquad (2\text{-}8)$$

The scattering density of the cell is usually expressed in terms of the individual contributions of the atoms in the cell. We define an atomic form factor by:

$$f_i(\underline{G}) = \int \rho_i(\underline{r})e^{2\pi i\underline{G}.\underline{r}_i}d\underline{r}_i \qquad (2\text{-}9)$$

where $\rho_i(\underline{r})$ is the scattering density of the ith atom at rest
at the origin. Because of thermal motion, the atoms are not
at rest and we define a temperature factor, $T_i(\underline{G})$ (the
Debye-Waller factor), to account for the difference between
the scattering density at rest and that due to thermal motion.
Various models of thermal motion can be used, the simplest
being isotropic harmonic motion where $T_i(\underline{G})$ is given by:

$$T_i(\underline{G}) = e^{-8\pi^2 U_i (\sin\theta/\lambda)^2} \tag{2-10}$$

where U_i is the mean square amplitude of the vibration. The
structure factor (2-8) can now be written as:

$$\underline{F}(\underline{G}) = \sum_{i=1}^{N} f_i(\underline{G}) T_i(\underline{G}) e^{2\pi i \underline{G}.\underline{r}_i} \tag{2-11}$$

where N is the number of atoms in the cell and $\underline{r}_i$ is the
position of the ith atom in the cell.

We have now expressed the intensity of a Bragg
reflection $I(\underline{G})$ in terms of the atomic positions, the atomic
form factors and the temperature factors. In the next
sections we shall develop the relationships between the
fundamental scattering processes of X-rays and neutrons and
the atomic scattering factors.

X-ray Scattering

X-rays, being electromagnetic radiation, are

scattered by charged particles. Classically, the fraction
of the incident radiation, I_0, scattered by a free charge is
given by:

$$I_{scattered} = \left(\frac{\mu_0}{4\pi}\right)^2 \frac{e^2}{m^2} I_0 \left(\frac{1+\cos^2 2\theta}{2}\right) \qquad (2-12)$$

where e and m are the charge and mass of the scatterer and
2θ is the scattering angle. The presence of the m^2 term in
the denominatior of equation (2-12) allows us to neglect
scattering by the nucleus and consider only scattering by
atomic electrons. The above expression is the Thomson
formula and accounts for the radiation emitted by an
accelerating charge in the driving field of the incident
radiation. It involves no transfer of energy or momentum to
the charge; thus, the incident and scattered radiation are of
the same wavelength.

In crystals where the electrons are bound to the
nuclei, the intensity of the coherent scattering, I_c, from a
single atom is given by:

$$I_c = I_{scattered} f^2 \qquad (2-13)$$

where f is the electronic form factor (cf. equation 2-9). For
an atom, i, with n electrons the atomic form factor, $f_i(\underline{G})$,
can be expressed in terms of the individual electron wave
functions ψ; and equation (2-9) becomes:

$$f_i(\underline{G}) = \sum_{j=1}^{n} \int \psi_j \psi_j^* e^{i\underline{G}\cdot\underline{r}_i} d\underline{r}_i . \qquad (2-14)$$

Thus, we have shown that the atomic form factors, $f_i(\underline{G})$, involved in the structure factor expression, equation (2-11), can be calculated from the electron wave functions for the case of X-ray scattering. The values of $f_i(\underline{G})$ can be calculated by Hartree or Self-Consistent Field methods (Cromer & Mann, 1968).

Neutron Scattering

The neutron, having zero charge, is not scattered by the Coulomb potential of the electrons or nucleus but is scattered by the nuclear potential. The neutron does interact weakly with the electrons by way of their magnetic moments, but this aspect of neutron scattering will not be discussed since it can only be observed for unpaired electrons which were not present in this work.

In crystal structure analysis, wavelengths of the order of 1Å are used. At this wavelength the scattering of the neutrons by the nucleus is purely s wave; that is, the neutron wavelength is large compared with the nuclear size parameter. This effective hard sphere potential would suggest that the scattering should vary as $A^{1/3}$, where A is the atomic mass number of the nucleus, but there are resonance effects caused by both nuclear size and neutron capture excitation levels. The size resonance produces a

small change in the scattering cross-section and the absorption re-emission, via virtual energy levels, introduces large deviations from the hard sphere values.

The coherent scattering will also be affected by both spin and isotope incoherence. If the spin of the scatterer is non-zero, then there are two spin states, $I \pm \frac{1}{2}$, available for the compound nucleus, their probabilities being:

$$g = \frac{I+1}{2I+1} \qquad I+\tfrac{1}{2} \text{ state}$$

$$1-g = \frac{I}{2I+1} \qquad I-\tfrac{1}{2} \text{ state.} \tag{2-15}$$

As the two states may have different resonance levels and widths, the coherent scattering will be altered. It is also evident that as different isotopes will have different scattering lengths, these must be summed according to their isotopic abundances, P_n.

For a nucleus with a single resonance level, E_r, of width Γ, the coherent scattering length is given by the Breit-Wigner formula:

$$b = \frac{gP \lambda_r \Gamma_n/2 (E - E_r)}{(E - E_r)^2 + \Gamma^2/4} - \frac{igP \lambda_r \Gamma_n/2 \, \Gamma/2}{(E - E_r)^2 + \Gamma^2/4}$$

$$+ \left[\sum_i \frac{gP \lambda_r \Gamma_n/2}{(E - E_r) + i\Gamma/2} + R \right]. \tag{2-16}$$

where Γ_n is the width for neutron emission of the resonance level, E is the energy at which the measurement is made, λ_r is the resonant wavelength divided by 2π and R is the mean nuclear radius. The summation is over the various nuclides of the species. Thus at a particular wavelength for a specific isotope, the coherent neutron scattering length can be expressed as a complex number:

$$b = b' + ib''. \tag{2-17}$$

It should be pointed out that the b_i's which take the place of the $f_i(\underline{G})$'s in the structure factor, equation (2-11), are independent of $\underline{G}$ and hence of the scattering angle. Figure 2-1 shows a comparison of the effective neutron and X-ray scattering lengths as a function of $\sin\theta/\lambda$ for two elements, and Figure 2-2 shows the dependence of the X-ray scattering length on A for two scattering angles and the non-systematic behaviour of the neutron scattering length with A.

The decrease in the X-ray atomic form factor with scattering angle arises because the X-ray wavelength is of the same order as the spatial extent of the electrons and interference occurs between scattering from different parts of the atom. The neutron wavelength is very long compared with the nuclear radii so that the nucleus can be considered as a point scatterer.

Figure 2-1.

A comparison of the X-ray and neutron scattering lengths
as a function of scattering angle.
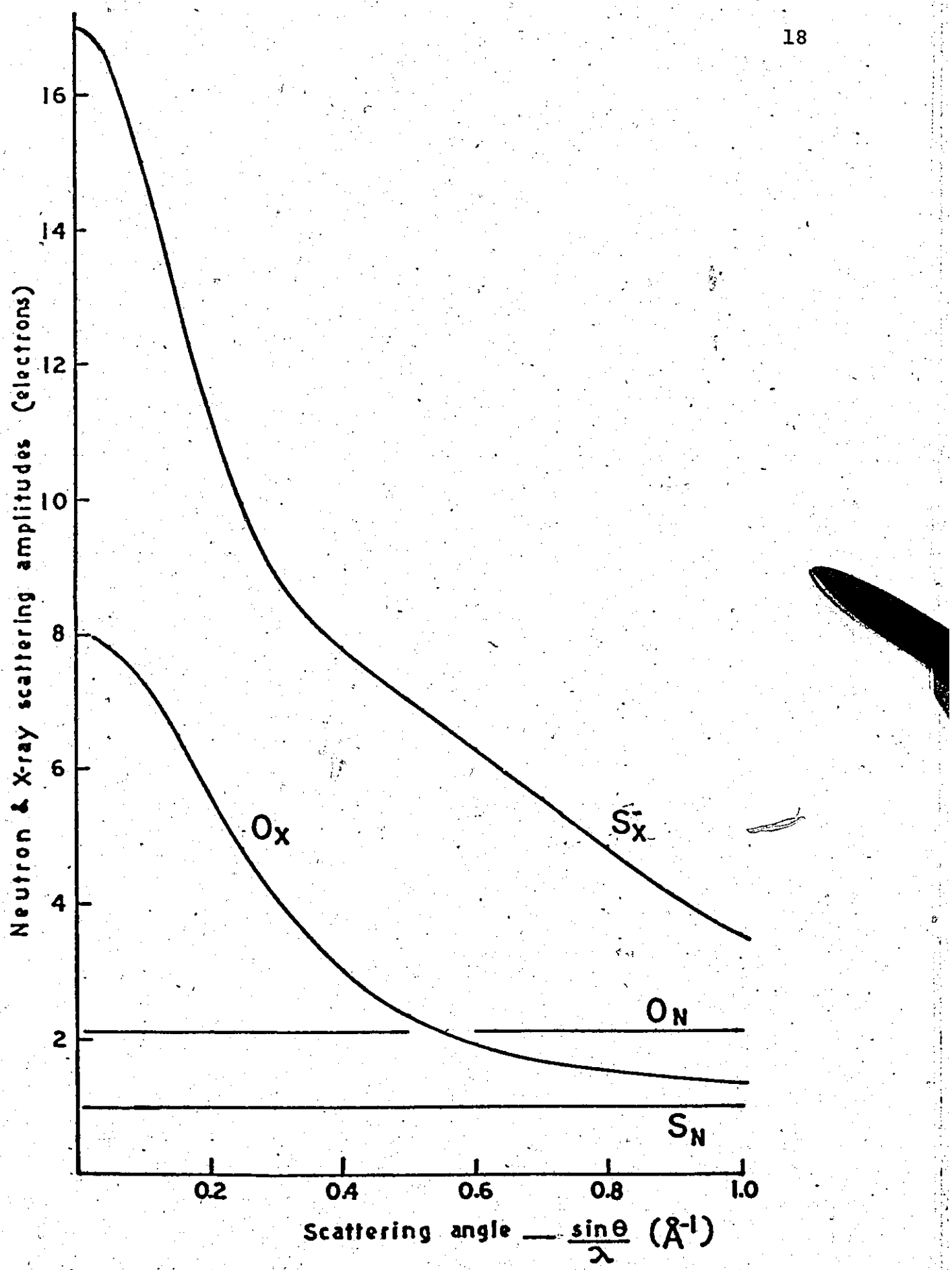
Figure 2-2.

The dependence of the scattering lengths on atomic number.
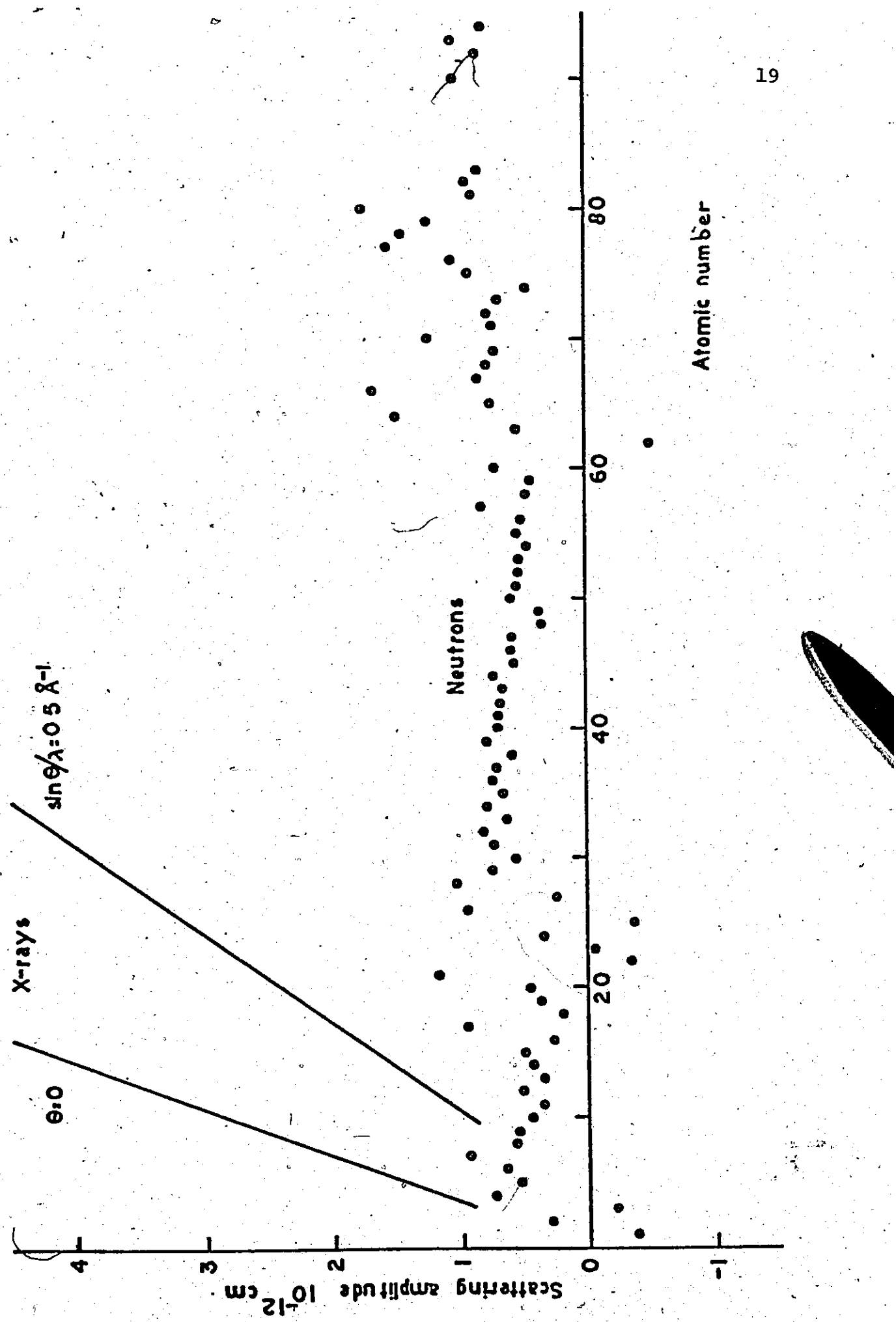
The non-systematic variation of the neutron scattering length with A can be of advantage in locating light elements in crystal structures and for distinguishing between atoms of adjacent atomic number; but for most purposes, X-rays remain the preferred radiation because of the availability of inexpensive high flux X-ray sources.

Crystal Structure Determination

It was stated at the beginning of this chapter that a crystal lattice, whose lattice spacings are comparable to the wavelength of an X-ray or neutron beam, will form a diffraction pattern whose intensities, $\{I(\underline{G})\}$, can be measured. It was also stated that the amplitude and phase of the structure factors are related, by their Fourier transform, to the atomic positions in the unit cell (cf. equations 2-9 and 2-11). It is also clear from equation (2-7) that as we measure the intensities, $\{I(\underline{G})\}$, we can only obtain the magnitudes of $\underline{F}(\underline{G})$ since:

$$I(\underline{G}) \propto \underline{F}(\underline{G}).\underline{F}^{*}(\underline{G}) = |\underline{F}(\underline{G})|^{2} \qquad (2\text{-}18)$$

and the phase information is lost. Thus it is impossible to obtain the atomic positions directly from the intensities; this is called the phase problem in crystallography.

One method of overcoming this problem was suggested by Patterson (1934). He showed that the convolution of the scattering density, $P(\underline{u})$, (the Patterson function) was

independent of the phases. The Patterson function is defined as:

$$P(\underline{u}) = V \int_{cell} \rho(\underline{r}) \rho(\underline{r}+\underline{u}) d\underline{r} \qquad (2-19)$$

The scattering density, $\rho(\underline{r})$, is periodic with a volume interval of the unit cell and can be written as a Fourier series:

$$\rho(\underline{r}) = V^{-1} \Sigma \underline{F}(\underline{G}) e^{-2\pi i \underline{G} \cdot \underline{r}} . \qquad (2-20)$$
$$\text{all } \underline{G}$$

Substituting for $\rho(\underline{r})$ in equation (2-19) we have:

$$P(\underline{u}) = \frac{1}{V} \int^{cell} \sum_{\underline{G}} \sum_{\underline{G}'} \underline{F}(\underline{G}) e^{-2\pi i \underline{G} \cdot \underline{r}} \cdot \underline{F}(\underline{G}') e^{-2\pi i \underline{G}' \cdot \underline{r}} e^{-2\pi i \underline{G}' \cdot \underline{u}} d\underline{r}$$

$$= \frac{1}{V} \sum_{\underline{G}} \underline{F}(\underline{G}) \cdot \underline{F}(-\underline{G}) e^{2\pi i \underline{G} \cdot \underline{u}}$$

$$= \frac{1}{V} \sum_{\text{all } \underline{G}} |\underline{F}(\underline{G})|^2 e^{2\pi i \underline{G} \cdot \underline{u}} . \qquad (2-21)$$

All the quantities in the R.H.S. of equation (2-21) are measurable, and the function $P(\underline{u})$ will have peaks at all points $\underline{u}$ where the vectors $\underline{u}$ correspond to interatomic vectors in the crystal. Furthermore, the value of P at such a peak will be proportional to the product of the scattering factors of the two atoms. If there are N atoms in the unit

cell, the Patterson function will in general have N^2 peaks
N of which are superposed at the origin; and so it is usual
to locate only those interatomic vectors between heavy
scatterers. Sometimes when all the atoms are approximately
the same size, it is not possible to locate any vectors with
certainty because of the high amount of overlap.

The peaks of the Patterson function are intrinsically
much broader than those of the scattering density function;
this accentuates the problem of overlapping of peaks and to
avoid this, the Patterson is sharpened and the large
superposition of peaks at the origin removed. To sharpen
the Patterson, the structure factors are multiplied by a
factor which changes the diffraction pattern to that
expected from a set of point scatterers:

$$F_{point}(\underline{G}) = \frac{\sum\limits_{i=1}^{N} Z_i}{e^{-U\left(\frac{\sin\theta}{\lambda}\right)^2} \sum\limits_{i=1}^{N} f_i(0)} F(\underline{G}) \qquad (2\text{-}22)$$

where Z is the atomic number and U is the overall temperature
factor. True point scatterers with no spatial extent would
require an infinite number of data, and use of the limited
set of measurable intensities can cause the peaks to be
surrounded by large ripples; and in practice U is chosen
such that a compromise is obtained between the broad overlapping
peaks and the occurrence of large ripples. The large origin

peak is removed using:

$$I(\underline{G}) = \underline{F}(\underline{G})^2 - e^{-U\left(\frac{\sin\theta}{\lambda}\right)^2} \sum_{i=1}^{N} f_i^2(\underline{G}) . \qquad (2-23)$$

If a trial structure is not known or cannot be obtained from the Patterson function, it is possible to obtain a set of trial phases, and hence a trial structure, from the intensities alone. The methods for determining the phases of a Bragg reflection in terms of its intensity and those of the other reflections are known as direct methods.

In direct methods it is assumed that the total scattering density is the sum of the contributions from separate atomic density distributions and that it is always positive. The latter assumption is not always true in neutron diffraction. If these conditions are true, it has been shown (Sayre, 1952) that the structure factor, $\underline{F}(\underline{G})$, is related to the sum of all product pairs of structure factors, $\underline{F}(\underline{G}').\underline{F}(\underline{G}'')$, where $\underline{G}'+\underline{G}'' = \underline{G}$:

$$\underline{F}(\underline{G}) = K(\underline{G}) \sum_{\text{all } \underline{G}'+\underline{G}''=\underline{G}} \underline{F}(\underline{G}').\underline{F}(\underline{G}'') \qquad (2-24)$$

where $K(\underline{G})$ is a scaling term. If we limit ourselves to crystals whose space groups are centro-symmetric, that is, the phase factor of a reflection is either +1 or -1, we can see that if $|\underline{F}(\underline{G})|$ is large then the terms of the series must be either mostly positive or mostly negative. Thus, if a

particular product pair has large $\underline{F}$'s, then the signs, S, of
the reflections are given by the relation:

$$S(\underline{F}(\underline{G})) \sim S(\underline{F}(\underline{G}')).S(\underline{F}(\underline{G}''))$$

or

$$S(\underline{F}(\underline{G})).S(\underline{F}(\underline{G}')).S(\underline{F}(\underline{G}'')) \sim +1 \qquad (2-25)$$

where $\sim$ indicates probably equal to.

In X-ray scattering the sharp fall off in intensities
with scattering angle precludes us from extracting information
from any reflections but those at low angles. To overcome
this, instead of using the structure factors, $\underline{F}$, unitary
structure factors, $\underline{U}$, or normalized structure factors, E, are
used; these are defined as follows:

$$\underline{U}(\underline{G}) = \frac{\underline{F}_{point}(\underline{G})}{\underline{F}(0)}$$

$$= \frac{\underline{F}(\underline{G})}{e^{-U\left(\frac{\sin\theta}{\lambda}\right)^2} \sum_{i=1}^{N} f_i(0)} \qquad (2-26)$$

the $\{\underline{U}(\underline{G})\}$ have the same phase as the $\{\underline{F}(\underline{G})\}$ and $0 \leqslant |U(\underline{G})| \leqslant 1$,

$$E^2(\underline{G}) = \frac{\underline{F}(\underline{G}).\underline{F}(\underline{G})^*}{\varepsilon \sum_{i=1}^{N} f_i^2(\underline{G})} \qquad (2-27)$$

where ε is an integer which reduces all classes of Bragg

reflections to the same basis. The distribution of the E values is theoretically independent of the size, shape or contents of the unit cell but takes a different form for a non-centro-symmetric space group.

By defining an origin for the unit cell, the phases of three reflections are fixed and these are used to generate a set of probable phases using equation (2-25). The probabilities of the correctness of these phases is tested by using:

$$S(\underline{F}(\underline{G})) \sim \Sigma \ S(\underline{F}(\underline{G}')).S(\underline{F}(\underline{G}")) \qquad (2-28)$$
$$\text{all } \underline{G}'+\underline{G}"=\underline{G}$$

and are given by:

$$P_+(\underline{U}(\underline{G})) = \frac{1}{2} + \frac{1}{2}\tanh\left[\frac{\sigma_3}{\sigma_2^3} \ |\underline{U}(\underline{G})| \ \Sigma_{\text{all } \underline{G}'+\underline{G}"=\underline{G}} \ \underline{U}(\underline{G}').\underline{U}(\underline{G}")\right]$$
$$(2-29)$$

where $\sigma_3 = \sum_{i=1}^{N} n_i^3$, $\sigma_2 = \sum_{i=1}^{N} n_i^2$ and $n_i = \dfrac{f_i(\underline{G})}{\sum_{j=1}^{N} f_j(\underline{G})}$.

Usually not only the probabilities are calculated, but also the occurrence of any inconsistent phases within the trial set is noted.

With the Patterson method the positions of the heavy scatterers are determined, and a set of calculated structure factors, $\{\underline{F}_c\}$, using these atoms can be computed. The phases

of the F_c's can be used with the observed magnitudes, $\{F_o\}$, to calculate the scattering density from which the other atoms can be located. In direct methods a limited set of trial phases is determined which enable us to compute a scattering density map using a subset of the observed structure factors and thus locate the atoms.

Refinement of the Structure

Once we have determined the position of the heavy scatterers by either of the above methods, it is then necessary to locate the remaining atoms and find the best value for all the atomic positions and temperature factors. This process is called refinement.

The light scatterers can be located by using a difference synthesis, $\Delta\rho(\underline{r})$, where the phase factors, $\phi(\underline{G})$, calculated from the heavy scatterers are used with the difference in magnitudes of the observed and calculated structure factors:

$$\Delta\rho(\underline{r}) = \frac{1}{V} \sum_{\underline{G}} (|F_o(\underline{G})| - |F_c(\underline{G})|)\phi(\underline{G})e^{-2\pi i\underline{G}\cdot\underline{r}} . \quad (2\text{-}30)$$

Here we have subtracted the contribution to the scattering density of the heavy scatterer, and the peaks correspond to those atoms not located.

To test the correctness of the deduced atomic parameters, it is usual to compare the calculated and

observed structure factors. This is done by computing a residual index (R factor):

$$R = \frac{\sum\limits_{G} |\Delta F|}{\sum\limits_{G} |F_o|} = \frac{\sum\limits_{G} ||F_o| - |F_c||}{\sum\limits_{G} |F_o|} . \qquad (2-31)$$

Thus as the model parameters are improved, the value of R is reduced. If some of the observations are known with greater certainty than others, it is usual to introduce a weighting scheme, $\{w(\underline{G})\}$, which gives a greater weight to the better known reflections. Thus we define a weighted residual index:

$$R_w = \left[\frac{\sum\limits_{G} w(|F_o| - |F_c|)^2}{\sum\limits_{G} w|F_o|^2} \right]^{\frac{1}{2}} . \qquad (2-32)$$

The weights, $\{w(\underline{G})\}$, are equal to the inverse square of the estimated standard deviation of the observations, $\{\sigma(\underline{G})\}$.

Having found a set of atomic parameters which gives a reasonable agreement between the observed and calculated structure factors, it is usual to obtain the best set of parameters by the method of least-squares. That is, we attempt to find a set of parameters, $\{p_i\}$, which gives values of $F_c(\underline{G}, \{p_i\})$ such that the function:

$$D = \sum\limits_{G} w(\underline{G}) (|F_o(\underline{G})| - |F_c(\underline{G}, \{p_i\})|)^2 \qquad (2-33)$$

will be a minimum. If a better set of p_i exist, say $\{p'_i\}$, then we have to find the set of Δp_i where:

$$p'_i = p_i + \Delta p_i .\qquad\qquad (2\text{-}34)$$

Assuming that:

$$\Delta F(\underline{G}) = |F_o(\underline{G})| - |F_c(\underline{G}, \{p_i\})| \qquad (2\text{-}35)$$

and that the Δp_i are all small, then:

$$\Delta F(\underline{G}) = \sum_i \frac{\partial F(\underline{G})}{\partial p_i} \Delta p_i \qquad (2\text{-}36)$$

and it can be shown (Hamilton, 1964) that if we have many more observations, $\{F_o(\underline{G})\}$, than parameters, $\{p_i\}$, then the set of n parameters, which will minimise the function D of equation (2-33), is given by the solution of the n independent normal equation:

$$\sum_{i=1}^{n} b_{ij} \Delta p_i = a_j \qquad j=1\ldots m \qquad (2\text{-}37)$$

where there are m observations and a_j and b_{ij} are given by:

$$a_j = \sum_{\underline{G}} w(\underline{G}) \left(\frac{\partial F(\underline{G})}{\partial p_j} \right) \Delta F(\underline{G})$$

and

$$b_{ij} = \sum_{\underline{G}} w(\underline{G}) \left(\frac{\partial F(\underline{G})}{\partial p_i} \right) \left(\frac{\partial F(\underline{G})}{\partial p_j} \right) . \qquad (2\text{-}38)$$

To make the normal equations (2-37) linear in Δp_i and hence solvable, we expanded the structure factor as a Taylor series and neglected all powers of Δp_i higher than the first (equation 2-36). This approximation is good as long as the $\{\Delta p_i\}$ are small, although it may now take several cycles of the least-squares process to achieve the best set of p_i's.

We can also obtain the estimated standard deviation, $\{\sigma(p_i)\}$, from the diagonal elements of the inverse of the matrix formed from the elements b_{ij}, or more simply, the conditional estimated standard deviation given by:

$$\sigma^2(p_i) = b_{ii}^{-1} = \left| \sum_{\underline{G}} w(\underline{G}) \left[\frac{\partial F(\underline{G})}{\partial p_i} \right]^2 \right| . \qquad (2-39)$$

Thus, the method of least-squares provides us with not only the best set of parameters but a measure of the reliability of these and, consequently, is widely used for crystallographic refinement.

Corrections to the Observed Intensities

What we measure in X-ray and neutron crystallography is that fraction of the energy, $E(\underline{G})$, scattered into a counter as the crystal, which is bathed in a uniform incident beam of intensity I_0, is rotated at a uniform angular velocity ω. This is related to the integrated intensity $J(\underline{G})$ by:

$$J(\underline{G}) = \frac{E(\underline{G})\omega}{I_0} .$$

(2-40)

To obtain the structure factors from the integrated intensities, it is necessary to make a number of corrections for experimental effects; the most important of these are discussed below.

a) Absorption

The principal attenuation of the X-ray beam is the excitation of electrons to higher energy levels within the atom. The energy lost from the beam by this process is greater than that from scattering, especially for heavy atoms, since the cross-section for this process increases with atomic number. With neutrons, absorption is not generally as large as the cross-section for the absorption processes; radiative capture, fission, (n,T) reactions, do not dominate over the scattering cross-section. The absorption, $A(\underline{G})$, for either radiation is calculated by:

$$A(\underline{G}) = V^{-1} \int_{crystal} e^{-\mu(p+q)} d\underline{r}$$

(2-41)

where p and q are the incident and diffracted path lengths, and μ is the linear absorption coefficient for the particular radiation used. In our work, the linear absorption coefficients were so small that the effect of absorption was negligible.

b) Extinction

Extinction is the attenuation of the incident beam by scattering. A normal crystal can be considered to consist of a large number of small, perfect crystallites all aligned within a small angle to each other; this small spread of angles is called the mosaic spread. Attenuation within the perfect crystallite is termed primary extinction; and the reduced scattering due to the attenuated beam at another crystallite further into the crystal, and perfectly aligned with the former, is termed secondary extinction. The correction for extinction effects used in subsequent chapters was suggested by Larson(1967) where corrected values of the calculated structure factor are given by:

$$F_c^* = KF_c(1+g\beta(2\theta)F_c^2)^{-\frac{1}{2}} \qquad (2-42)$$

where K is a scale constant, g is a variable parameter in the least-squares refinement and $\beta(2\theta)$ is a calculable angular function.

Extinction is usually more of a problem in neutron diffraction as large crystals have to be used to overcome the slow counting rates resulting from the low incident flux.

c) Geometrical Corrections

There are two corrections which may have to be applied that depend upon the geometry of the experiment.

The first is the Lorentz correction which accounts for the differing times individual planes may spend in the diffracting position. The second, which only applies to X-ray diffraction, is the polarisation of the X-ray beam by Bragg reflection. Both these effects can be corrected for by means of simple analytical expressions, namely:

i. Lorentz. For an Eulerian cradle diffractometer in the equatorial setting, the integrated intensities are multiplied by L^{-1} where L is given by:

$$L = \frac{1}{\sin 2\theta}$$

(2-43)

ii. Polarisation. The polarisation correction is independent of the method of data collection (but is only applied for X-rays), and the integrated intensities are multiplied by P^{-1} where P is given by:

$$P = \frac{1+\cos^2 2\theta}{2}$$

(2-44)

In the previous sections we have shown that diffraction of both X-rays and neutrons will occur in crystals, and that from the intensity of the diffraction peaks it is possible to obtain a model of the crystal structure in terms of the atomic positional parameters and temperature factors. In the next chapter a short review of the methods of measuring the intensities will be given along with a

detailed discussion of the neutron diffractometer which

was designed and constructed by us at McMaster University.

CHAPTER III

METHODS OF INTENSITY MEASUREMENT AND A DESCRIPTION OF

THE MCMASTER NEUTRON DIFFRACTOMETER

In crystal structure analysis, it is necessary to be
able to measure the intensity of a large number of Bragg
reflections on a single crystal sample. There are two main
methods of doing this: film methods and diffractometer methods,
the former being limited to X-ray diffraction.

X-ray Methods

X-rays are generated by bombarding a target material,
which in our case was either copper or molybdenum, with
electrons. The emitted X-ray spectrum has several characteristic
lines, and one of these (Kα) is selected either by using
a suitable filter or by Bragg reflecting a collimated beam
with a single crystal set at the appropriate Bragg angle.
The angular divergence and cross-section of the beam are
governed by an exit collimator.

With film techniques the sample crystal, bathed in the
the X-ray beam, and a photographic film are moved in such a
manner that the diffraction peaks are individually recorded
on the film, the amount of blackening of the film being
proportional to the intensity of the peak. The two main types

of X-ray cameras used in crystal structure analysis are the Weissenberg camera and the Buerger Precession camera; both produce a photograph of the lattice points of a particular reciprocal lattice plane.

For the measurement of X-ray intensities, diffractometers have recently supplanted film methods. A diffractometer consists of a goniostat which can rotate the crystal so that a particular reciprocal lattice vector is in the diffracting position and also rotate an X-ray detector to measure the intensity of the diffraction peak. The diffractometers used in this work were both of the four-circle type, a three-circle Eulerian cradle goniostat with a fourth circle carrying a detector in the normal-beam equatorial geometry; this is schematically illustrated in Figure 3-1. Although each diffraction peak is observed individually, the exposure times can be extremely short as the X-ray detector efficiency is very high. In our case the X-ray diffractometer, a Syntex, was controlled by an on-line computer to make efficient use of the high counting rates.

Neutron Diffraction

Diffractometers are universally used in neutron diffraction; they are quite similar to X-ray diffractometers, differing only in the radiation source and the type of detector.

The core of a nuclear reactor is the source of neutrons

Figure 3-1.

A perspective drawing of a four-circle goniostat in the
equatorial geometry.

ω & 2θ AXIS

REFLECTED
BEAM

χ CIRCLE

φ CIRCLE

φ AXIS

EQUATORIAL
PLANE

χ AXIS

2θ CIRCLE

ω CIRCLE

INCIDENT BEAM
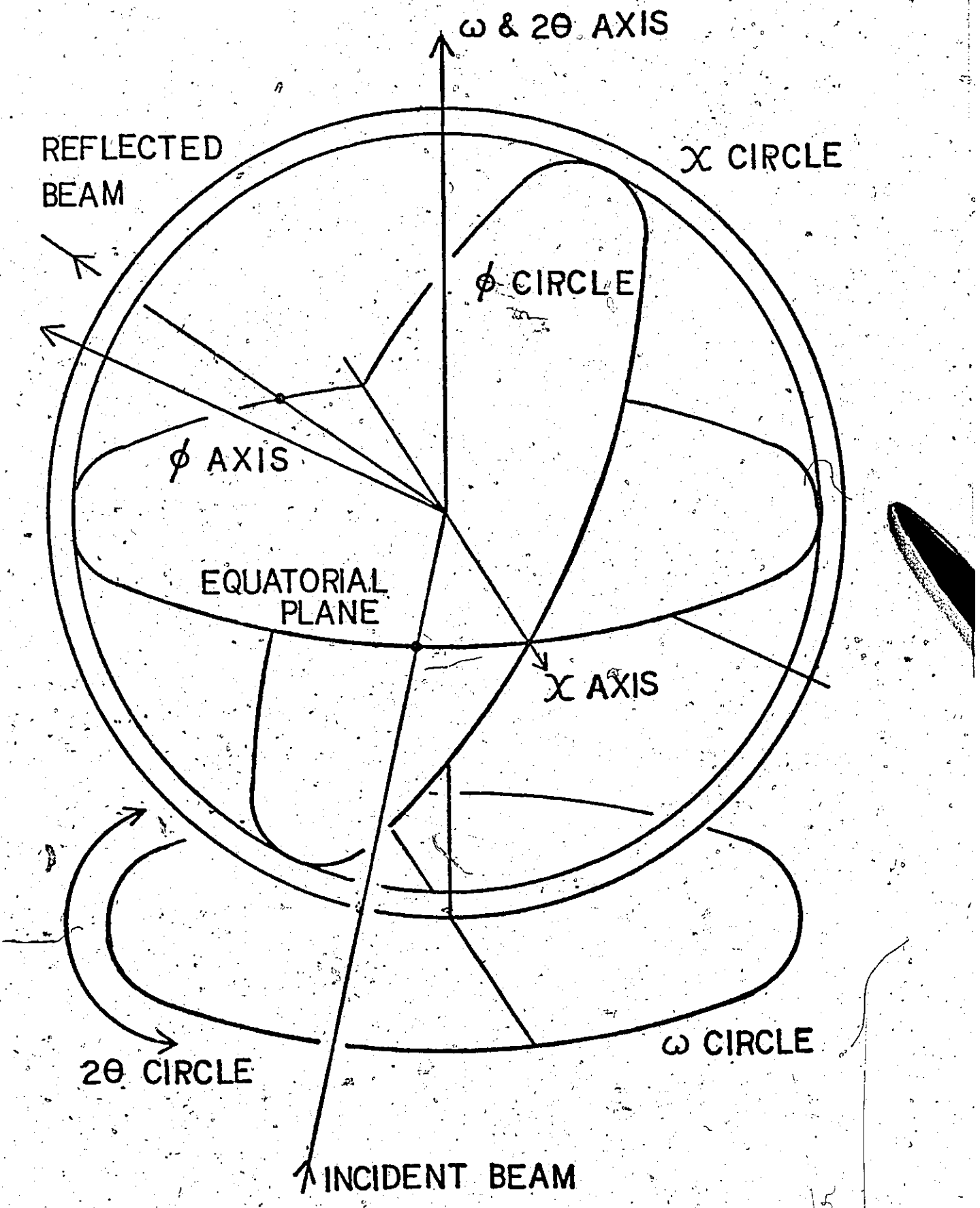
which when in equilibrium with the reactor moderator have a Maxwellian spectrum. For a moderator temperature of $293^\circ K$, the peak neutron flux is at a wavelength of 1.14 Å. A white beam of neutrons from the core passes through the reactor's biological shield in a beam tube which forms the primary collimator. A monochromatic beam is produced by Bragg reflection of the white beam from a single crystal monochromator. The monochromator selects a single wavelength at a particular angle defined by a second collimating beam tube. The angular divergence of the beam and its small wavelength-spread depend upon the mosaic spread of the crystal monochromator and the angular acceptance of the two collimators. A diagram of the experimental arrangement used at beam port #6 of the McMaster nuclear reactor is shown in Figure 3-2. The crystal monochromator in this case was a single aluminium crystal set in the transmission geometry for Bragg reflection from the (220) plane, the Bragg angle being 21.8° and the wavelength being 1.062 Å.

The neutron flux available at the sample is of the order of 10^6 neutrons $cm^{-2}s^{-1}$ which is several orders of magnitude less than that of a typical X-ray beam ($\sim 10^{10}$ X-ray quanta $cm^{-2}s^{-1}$); thus, larger cross-section beams and large samples are used in neutron diffraction. It is essential to have as efficient a detector as possible and the Helium-3 type, whose efficiencies can be very high, is now widely used; even so, the rate of observing the

Figure 3-2.

The experimental configuration of the neutron

diffractometer at beam-port #6 of the McMaster

nuclear reactor.

Reactor biological shield

pool

core

triple axis spectrometer

shielding tanks

double axis spectrometer

Neutron Diffractometer

X monochromator

B beam tube

S beam stop
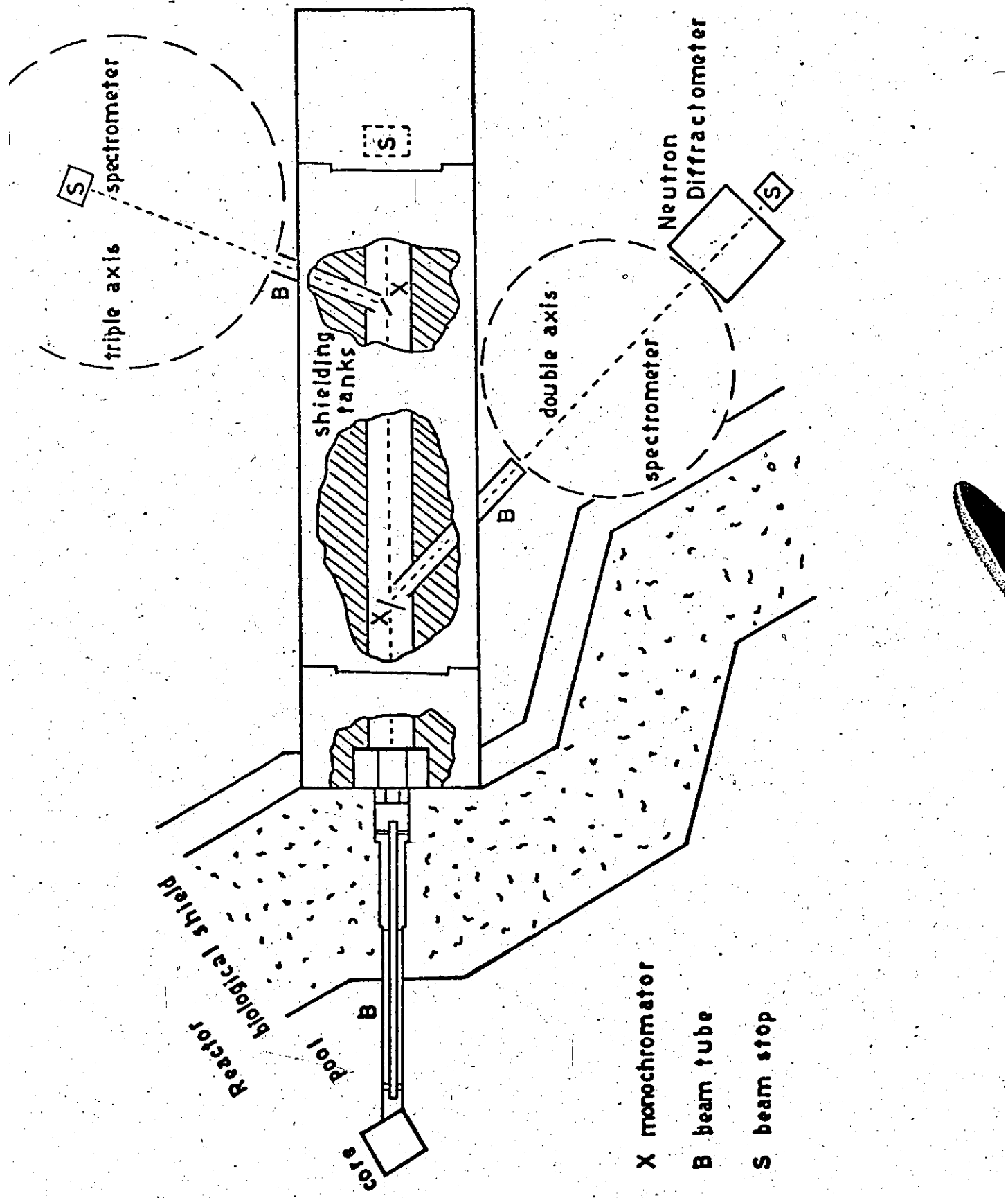
diffraction peaks is considerably slower than with an X-ray diffractometer.

A detailed description of the neutron diffractometer designed and built by us at McMaster will be given in the next section.

The McMaster Neutron Diffractometer

This neutron diffractometer is a four-circle equatorial geometry instrument (cf. Figure 3-1), and in its design there were several criteria which had to be met.

The cost was not to exceed $15,000 and, in fact, the final cost was approximately $11,000. It would have to be both compact and portable as the crystallography group did not have the exclusive use of a beam port at the reactor; and not only was the space limited at the shared beam ports, but the diffractometer had to be able to be used at any of these beam ports. The need to run the diffractometer 24 hours a day made some form of automatic control essential and, as a large number of measurements would be made, it was necessary that the ouput format be compatible with the university computing centre's CDC 6400 computer.

The cost criterion ruled out the use of a small digital computer to control the diffractometer as it would have added a further $7,000 to the cost; instead, a hard-wired logic controller which cost $1,000 was designed. Cost also made the use of a commercial four-circle goniostat impossible,

and a much cheaper one was built by ourselves (Plate 3-1).

All commercial diffractometer goniostats are primarily

designed for X-ray diffraction which uses very narrow beams

and small crystals; this requires their mechanical tolerances

to be very small. Such precision is not required with

neutron diffraction, and our low cost goniostat has been

highly successful. The choice, on the basis of cost, of

paper tape as a control and output medium was not as

successful. At the time the diffractometer was designed,

it was understood that the CDC 6400 computer would be capable

both of producing punched paper control tapes and reading the

output tapes. In fact, after a considerable delay only a

paper tape reader was installed. This meant that the control

tapes have to be punched on another computer, a situation

which is somewhat tedious. Also, most of the diffractometer's

breakdowns have occurred in the input/output Teletype,

although it is only fair to comment that the Teletype is by

far the cheapest such device available, costing about $900.

To make the diffractometer as compact and portable as

possible, a modular form of construction was used. The three

main sections (Plate 3-2) are stacked on top of one another,

the lowest section having castors for easy movement. The

diffractometer has been used at two of the reactor's six beam

ports (#5 and #6), and no major problems were encountered in

the move between these ports. The design was kept compact by

the use throughout of solid state electronics and by using

Plate 3-1.

The four-circle goniostat of the neutron diffractometer.

A. χ motor.

B. ϕ motor.

C. 2θ motor.

D. ω motor.

E. χ circle.

F. ϕ circle.

G. 2θ circle.

H. ω circle.

J. He^3 detector pre-amplifier.

K. He^3 detector and its shielding.

L. Fission chamber pre-amplifier.

M. Goniometer head.

N. Sample crystal.

O. Motor stepper and power supply.
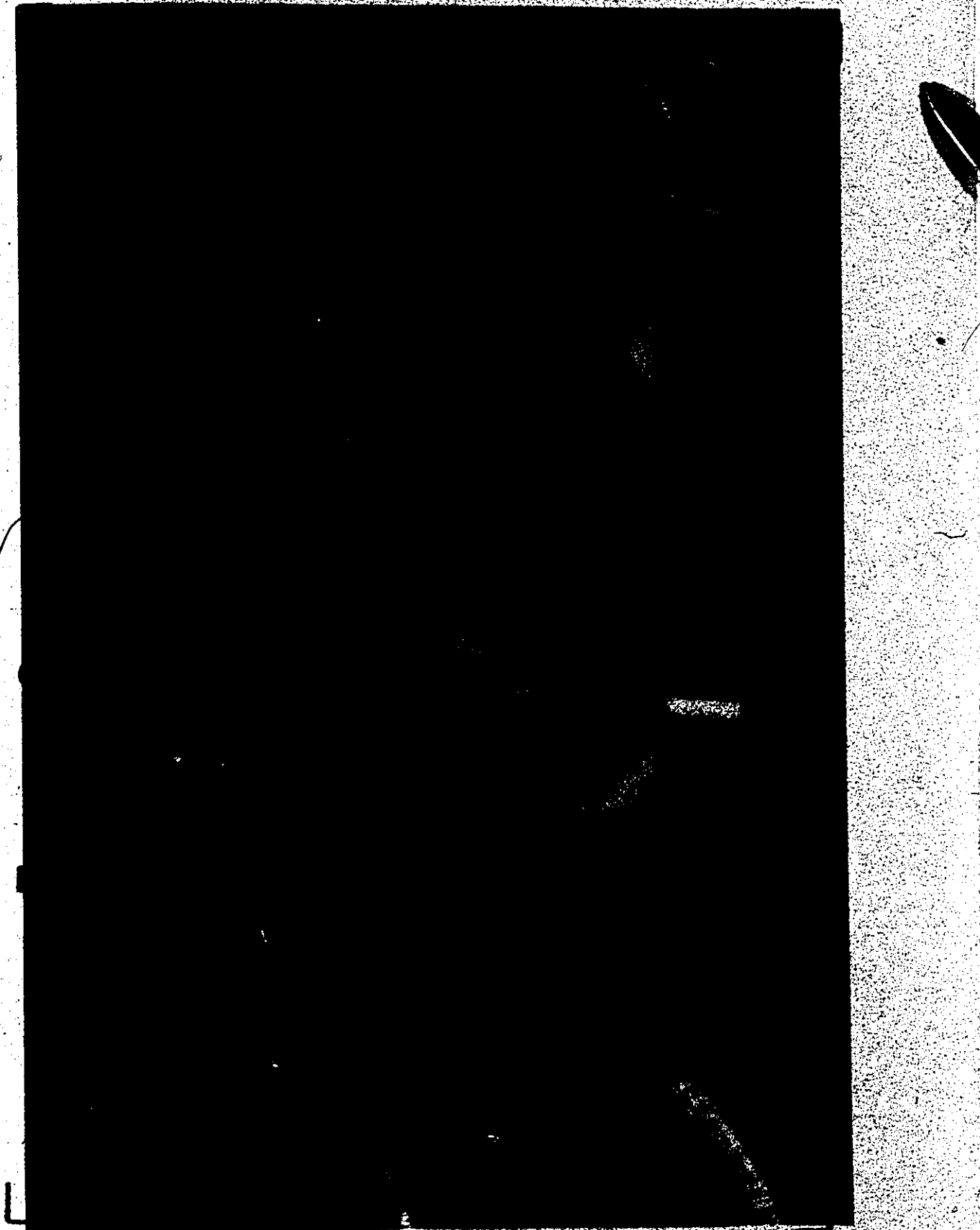
Plate 3-2.

A general view of the neutron diffractometer.

A. Control electronics.

B. High voltage power supplies.

C. Detector amplifiers.

D. Ratemeter.

E. Scaler.

F. Pre-set scaler.

G. Data scanner.

H. Beam stop.

J. Goniostat.

K. Tape reader (Teletype).

L. Teletype.

M. Motor slewing and jogging controls.

a Helium-3 (^{3}He) counter rather than the then conventional Boron trifluoride (^{10}BF$_3$) counter which requires a large amount of shielding.

The overall performance of the diffractometer has been very good, although experience has shown that a different method of control tape input would have been advisable. A detailed description of the design is given in the next sections.

The Mechanical Design

The frame of the diffractometer is made up of three sections: an interchangeable base section, a centre section containing the goniostat and a top section housing the control logic and counting electronics. All three sections can be separated from one another. The base section can be replaced by one of a different size if the height of the goniostat has to be changed, and it is fitted with castors for portability and jacks for levelling.

The goniostat is mounted on an inverted U section steel girder in the centre section of the frame. The girder and its associated structure while being rather heavy (approximately 30 kg) provide adequate stiffness to maintain the goniostat in correct alignment and provide support for the driving motors, limit switches and ancillary electrical equipment. On the mounting feet of the girder, adjustment is provided for lateral movement of the girder with respect

to the frame; this in conjunction with the jacks provides full three-dimensional adjustment.

Two nine-inch Troyke engineering rotary tables mounted coaxially on the girder, one above the other, form the basis of the ω and 2θ circles of the goniostat. These tables are readily available at low cost; they also have the necessary setting accuracy (within 1' over 360° rotation of the table). The upper table (2θ) has an aluminium bracket holding the detector tube, its shielding and the detector pre-amplifier; the bracket has provision for small adjustment ($\pm$ 2.5 cm) of both height and of the radius at which the counter is situated. A nominal sample to detector radius of 28 cm is used which with a 1 cm^2 aperture at the detector gives an adequate angular acceptance (approximately 2°) with all modes of scanning. A shaft passing through the centre hole of the 2θ table is attached at its lower end to the ω table by means of a tapered shank and plate; this allows it to be removed and recentred if required. Attached to the top end of the shaft is a 10 cm diameter disk onto which an Electronics and Alloys's χ and ϕ circles are bolted.

The motors driving the 2θ and ω circles are Slo-Syn stepping motors of 45 oz-in torque rating; each step being 5° which, driving through the 90:1 worm reduction gear of the tables, results in a rotation of $1/18^\circ$ per step about these axes. The χ and ϕ motors which are similar to the 2θ and ω motors, but with a reduced torque rating of 25 oz-in, are

mounted on their respective circles. They drive through gear trains resulting in the same degree of rotation per step as those of ω and 2θ. A motor is made to step by applying an electrical pulse to a translator board (manufactured by Slo-Syn) consisting of an electronic switch tail ring counter providing a series of pulses which drive the motor through one step. These translator cards, one for each motor, are mounted on a motor power supply chassis which also has circuitry for slewing and jogging the motors during setting-up procedures. This chassis is bolted to the centre section frame.

A fission counter used for monitoring the incident beam and its associated pre-amplifier are mounted on a bracket which can be bolted onto either side of the frame so that incident neutron beams in either direction can be used. The counting and control electronics are mounted in the top section of the frame which may be removed and placed away from the goniostat so that cryostats, etc., can be mounted around the sample.

Detection and Counting Electronics

A beam monitor counter is used to control the diffracted beam counter. This is an A.E.C.L. type 5 fission counter on loan from A.E.C.L.. It contains fissionable ^{235}U in the form of uranium oxide (90% ^{235}U) coated on a central 25 mm diameter portion of the two 0.5 mm thick aluminium

windows. The output signal is amplified by a Canberra Industries (C.I.) type 806 pre-amplifier and a type 816 amplifier; bias voltage for the detector is provided by a Hewlett-Packard 6516A high voltage power supply. A Texas-Nuclear Texlium Helium-3 detector tube is used for the diffracted beam detector. This detector contains ^{3}He at four atmospheres pressure and krypton, for quenching, at one atmosphere. The bias supply, pre-amplifier and amplifier are the same as for the monitor counter.

The amplifier output of the ^{3}He counter feeds both a linear ratemeter (C.I. type 1480) and a printing scaler (C.I. type 1473). Output of the fission counter amplifier feeds a printing timer/scaler (C.I. type 1492). The latter module operates in its master mode slaving the 1473 scaler. The scalers are scanned by a data scanner (C.I. type 1488) which prints out the contents of both scalers on a modified model A.S.R. 33 Teletype.

The Canberra electronics units are mounted in a standard bin and power supply unit (C.I. type 1400), the two Hewlett-Packard high voltage power supplies being mounted directly above this unit in the top frame section. A block diagram of the counting electronics and the control electronics is in Figure 3-3.

Control Electronics

The control instructions are read from punched paper

Figure 3-3.

A block diagram of the counting electronics and the control electronics.

CONTROL UNIT

HIGH VOLTAGE POWER SUPPLY #6516A

HIGH VOLTAGE POWER SUPPLY #6516A

AMP. #816 | AMP. #816 | RATEMETER #1480 | SCALER #1473 | PRE SET SCALER #1492 | DATA SCANNER #1488

PRE-AMP. #806

PRE-AMP. #806

TELETYPE

ASR 33

TAPE READER

He^3 DETECTOR

FISSION CHAMBER

MOTOR STEPPER & POWER SUPPLY

MOTORS → 2θ   ω   X   φ
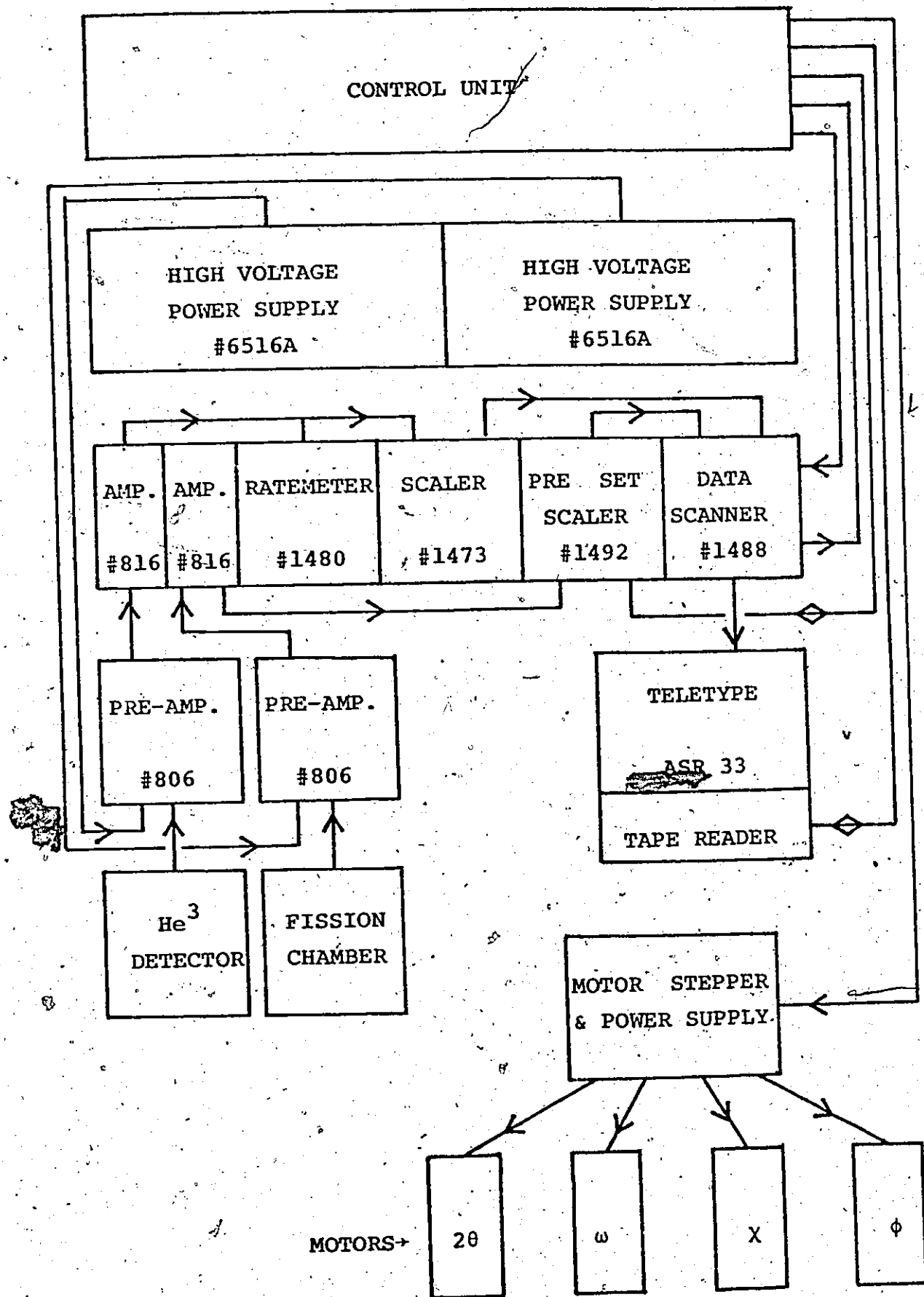
tape on the tape reader of the teletype. The output data is written on punched tape and the page printer of the same teletype which is used in the duplex mode (cf. Figure 3-3).

Characters are read from the input tape, and each character when decoded moves one of the motors one step, either forward or backward, or at the end of a sequence of motor moves will start the count cycle. When the count cycle starts, the reader is automatically switched off, and the teletype is left ready to print the results accumulated by the data scanner. After printing the results of the count cycle, the teletype automatically starts to read the input tape again; this process continues until the end of the tape is reached where the tape sensor on the teletype switches the system off.

The reader output signal is electro-mechanically converted from parallel to serial format within the teletype. This serial output is decoded by a hard-wired logic unit which is built up with Digital Equipment Corporation's flip-chip modules. The logic unit electronically reconverts the serial signal to parallel format and then decodes it from a five-bit binary form to a 32 valued decimal form. Only nine of the possible 32 binary characters are used; these correspond to forward and reverse of each motor and the start of the count cycle signal (Table 3-1). The electronic control for gating the teletype reader and printer is also built of flip-chip modules and is mounted on the same panel.

Table 3-1. Table of characters recognized by the control unit logic and their functions

Function	Teletype character	8-bit ASCII code	5-bit binary character
Increase 2θ by 1/18°	return	101-10001	11000
Decrease 2θ by 1/18°	T	001-01011	10101
Increase ω by 1/18°	delete	111-11111	11111
Decrease ω by 1/18°	;	110-10111	01011
Increase χ by 1/18°	↑	011-11011	11101
Decrease χ by 1/18°	?	111-11100	11110
Increase φ by 1/18°	&	011-00101	10010
Decrease φ by 1/18°	/	111-10101	11010
Start count cycle	A	100-00010	00001
No action	blank	000-00000	00000

The Scan Control Paper Tape

From the cell dimensions, lattice type, principal axes orientation and wavelength, the setting angles of the four circles for the Bragg reflections are calculated. This is done using the programme DIFSET of the XRAY 71 programme library. The programme DIFPCH is used to punch out a set of cards, one for each reflection, containing the Miller indices and the setting angles. A group of about 20 of these cards is chosen and, using the FORTRAN programme MACDIF, the sequence of commands needed to set the angles on the goniostat and to scan the reflections is written on a magnetic tape. This tape is read by either the PDP 9 or PDP 15 computer in the Tandem Van de Graaff Accelerator Laboratory using the MACRO programme ASTIG, and the commands are punched out on a paper tape which can be read by the diffractometer Teletype. The conversion from cards to paper tape via magnetic tape is necessary as the University Computing Centre's CDC 6400 computer does not have a paper tape punch, and magnetic tape is the only compatible transfer medium between the CDC 6400 and the PDP 9/15 for large quantities of information.

The paper tape is prepared for an ω step scan mode; that is, the 2θ, χ and ϕ values are set, and the crystal is then rotated in steps ($1/18^{\circ}$) through a small angle about its ω value. After each step of ω, a count of the diffracted beam is recorded and punched onto a paper tape. This diffractometer output paper tape is read by the CDC 6400

computer using the FORTRAN programme DIFDAT. The values of the diffracted beam count are summed for each reflection, and those counts due to background are subtracted; thus, the integrated intensities of the reflections are obtained.

In the previous sections we have described how the integrated intensities of the Bragg reflections can be measured. In our work to be described in the following chapters, all the intensity measurements were made using diffractometers, both X-ray and neutron. X-ray film methods were confined to space group analysis and the alignment of crystals used for the neutron diffraction experiments.

CHAPTER IV

ANOMALOUS NEUTRON SCATTERING AND THE QUESTION OF

FERROELECTRICITY IN LITHIUM HYDRAZINIUM SULPHATE

The apparent ferroelectric nature of lithium

hydrazinium sulphate, $Li(N_2H_5)SO_4$, was reported by Pepinsky,

Vedam, Okaya and Hoshino (1958). Their measurements were

made using a ferroelectric hysteresis bridge, and they

observed well-formed hysteresis loops from about $258^{O}K$ up to

$353^{O}K$ from which they concluded that the crystal was

ferroelectric. Above $353^{O}K$, high electrical conductivity

which increases with temperature prevented good measurements

and below $258^{O}K$, the loops became distorted and difficult to

saturate. They found no evidence of a phase transition either

from dielectric measurements in the range $77^{O}K$ to $313^{O}K$ or

from specific-heat measurements in the range $153^{O}K$ to $478^{O}K$.

At room temperature they reported a value of $0.30\mu Ccm^{-2}$ for

the spontaneous polarisation and $320Vcm^{-1}$ for the coercive

field.

The crystal structure has been investigated several

times. Three X-ray determinations were published in 1964:

Niizeki & Koizumi, 1964; Brown, 1964; and Van den Hende &

Boutin, 1964. The former was only a projection, and neither

the lithium nor the hydrogen positions were located. Of the

latter two, which were based on three-dimensional measurements, neither located the hydrogen positions, but Brown correctly located the lithium position. In the next chapter of this work, an X-ray redetermination of the structure in which all the hydrogen atoms were located is given. A neutron diffraction determination of a normal sample based on measurements of three orthogonal projections was made by Padmanabhan & Balasubramanian (1967), and a recent more complete determination using a deuterated sample was made by Ross (1970). The crystals are orthorhombic, space group $Pna2_1$ (C_{2v}^9), with lattice parameters $\underline{a} = 9.929(5)$, $\underline{b} = 8.973(3)$, $\underline{c} = 5.181(2)$ Å and four molecules in the unit cell. The permanent dipole lies along the $\underline{c}$ direction. The structure is composed of an $LiSO_4^-$ framework of corner-sharing oxygen tetrahedra with channels which run along the $\underline{c}$ direction and contain the hydrazinium ions (cf. Figures 5-1 and 5-2). The NH_3^+ group of the hydrazinium ion forms hydrogen bonds to the framework, and the NH_2 group forms one hydrogen bond to the framework and one to the NH_2 group related by the $\underline{c}$ screw axis to give an ordered N-H....N-H chain directed along the negative $\underline{c}$ direction (cf. Figure 4-1).

Several nuclear magnetic resonance studies (Cuthbert & Petch, 1963; MacClement, Pintar & Petch, 1967; Knispel & Petch, 1970; Parker & Schmidt, 1971; and Howell & Schmidt, 1969) of both normal and deuterated material have explained

the motion of the hydrazinium ion. These are reviewed in a paper on the nuclear quadrupole resonance of ^{14}N in the NH_2 group by Hastings & Oja (1972). The conclusion of these works is that below 50°K there is some oscillation of the NH_2 group about the N-N axis; this oscillation increases linearly with temperature. There is also some oscillation of the NH_3 group below 100°K, but above this temperature the group begins hindered rotation. At about 150°K, proton exchange in the N-H-N plane of the NH_2 group begins, and this also increases linearly with temperature to around 320°K where both the proton exchange and the oscillation around the N-N axis increase rapidly with temperature, the exchange process dominating. Above 480°K, the point which Cuthbert and Petch ascribed to a second order structural phase transition, motion of the whole N_2H_5 ion is observed.

Vanderkooy, Cuthbert & Petch (1964) showed that the D.C. conductivity was anisotropic, the conductivity in the $\underline{c}$ direction being more than two orders of magnitude greater than in the $\underline{a}$ or $\underline{b}$ directions, and that the current in the $\underline{c}$ direction was carried by protons.

The supposed ferroelectric switching in $Li(N_2H_5)SO_4$ was thought to result from one of two mechanisms. The first involves only the reorientation of the hydrogen bonds from the negative to the positive $\underline{c}$ direction (Figure 4-1). Such a realignment would produce a change in polarisation of the right order of magnitude. As the $LiSO_4^-$ framework is

Figure 4-1.

A possible ferroelectric switching mechanism in

Li$(N_2H_5)SO_4$ whereby the direction of spontaneous

polarisation is governed by the direction of the

hydrogen bonds which link the hydrazinium ions into

chains.
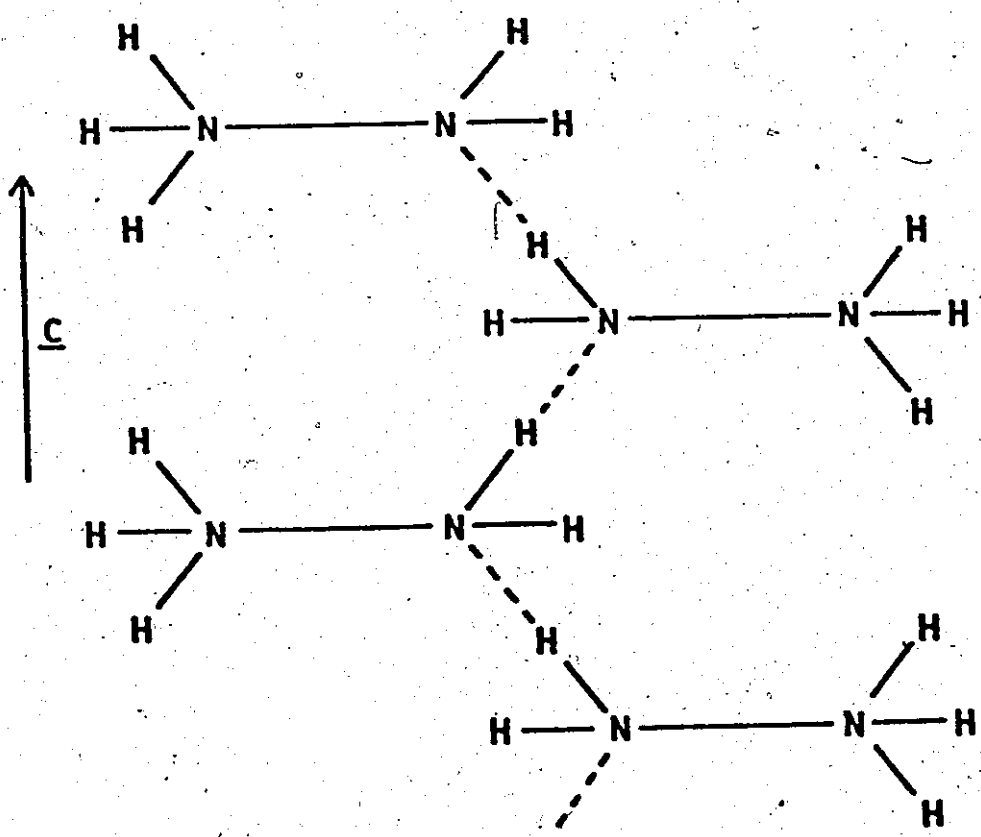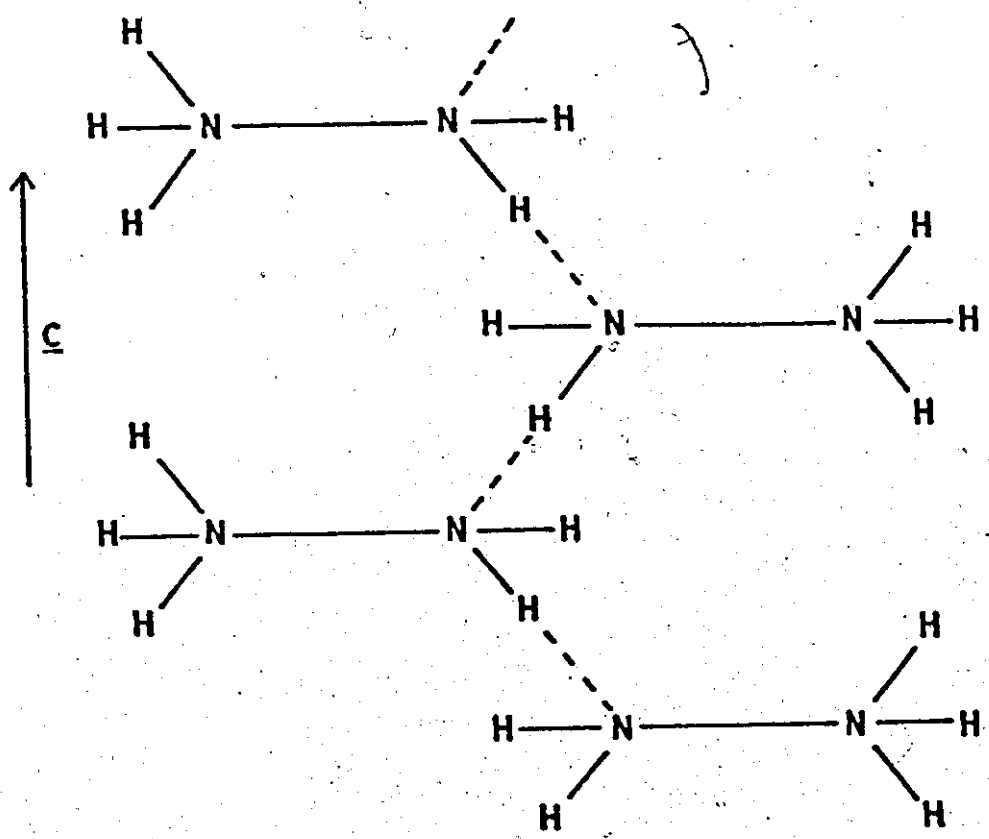
non-centro-symmetric, oppositely switched domains would have crystallographically distinct structures. In the second mechanism the hydrogen bonds reorient, and in addition the framework changes from a right-handed to a left-handed form. The resulting structure is the enantiomorph of the original structure, but the two are otherwise crystallographically equivalent. Using a crystal made with ^{6}Li, which is an anomalous scatterer of neutrons, we hoped to distinguish between these two mechanisms by examining the changes which would occur in the neutron structure factors of Bijvoet pairs during ferroelectric switching.

Theory

In X-ray diffraction the breakdown of Friedel's law, which states that $I(\underline{G}) \equiv I(-\underline{G})$, is well known in non-centro-symmetric crystals containing atoms with complex scattering amplitudes (Coster, Knol & Prims, 1930). A similar effect occurs in neutron diffraction when an atom has a high absorption and hence a complex scattering amplitude. We can write the neutron scattering amplitude, b, for such an atom as a complex number:

$$b = b' + ib'' \tag{4-1}$$

where b' and b" are the real and imaginary components.

Using the relation for a complex number:

$$re^{i\theta} = r\cos\theta + ir\sin\theta \tag{4-2}$$

we can rewrite the structure factor expression (equation 2-11) as:

$$\underline{F}(\underline{G}) = \sum_{i=1}^{N} b_i T_i(\underline{G}) \cos 2\pi(\underline{G} \cdot \underline{r}_i) + i \sum_{i=1}^{N} b_i T_i(\underline{G}) \sin 2\pi(\underline{G} \cdot \underline{r}_i)$$

(4-3)

Substituting equation (4-1) in equation (4-3) and separating those terms arising from the real and imaginary parts of b, we have:

$$\underline{F}(\underline{G}) = \sum_{i=1}^{N} b'_i T_i(\underline{G}) \cos 2\pi(\underline{G} \cdot \underline{r}_i) + i \sum_{i=1}^{N} b'_i T_i(\underline{G}) \sin 2\pi(\underline{G} \cdot \underline{r}_i)$$

$$- \sum_{i=1}^{N} b''_i T_i(\underline{G}) \sin 2\pi(\underline{G} \cdot \underline{r}_i) + i \sum_{i=1}^{N} b''_i T_i(\underline{G}) \cos 2\pi(\underline{G} \cdot \underline{r}_i)$$

(4-4)

or more simply:

$$\underline{F}(\underline{G}) = A + iB - C + iD$$

$$= (A-C) + i(B+D)$$

(4-5)

where

$$A = \sum_{i=1}^{N} b'_i T_i(\underline{G}) \cos 2\pi(\underline{G} \cdot \underline{r}_i)$$

$$B = \sum_{i=1}^{N} b'_i T_i(\underline{G}) \sin 2\pi(\underline{G} \cdot \underline{r}_i)$$

$$C = \sum_{i=1}^{N} b''_i T_i(\underline{G}) \sin 2\pi(\underline{G} \cdot \underline{r}_i)$$

$$D = \sum_{i=1}^{N} b''_i T_i(\underline{G}) \cos 2\pi (\underline{G} \cdot \underline{r}_i).$$

Similarly, we can write $\underline{F}(-\underline{G})$ using equation (4-4) and the relationships $\cos(-\theta) = \cos(\theta)$ and $\sin(-\theta) = -\sin(\theta)$:

$$\underline{F}(-\underline{G}) = A - iB + C + iD$$

$$= (A+C) + i(D-B) \qquad (4-6)$$

Now $I(\underline{G}) \propto \underline{F}(\underline{G}) \cdot \underline{F}^*(\underline{G}) = \left[(A-C) + i(B+D)\right] \cdot \left[(A-C) - i(B+D)\right]$

$$= (A-C)^2 + (B+D)^2 \qquad (4-7)$$

and similarly

$$I(-\underline{G}) \propto \underline{F}(-\underline{G}) \cdot \underline{F}^*(-\underline{G}) = \left[(A+C) + i(D-B)\right] \cdot \left[(A+C) - i(D+B)\right]$$

$$= (A+C)^2 + (D-B)^2 . \qquad (4-8)$$

Therefore: $$I(\underline{G}) \neq I(-\underline{G}) \qquad (4-9)$$

when there are atoms present which scatter anomalously.

It should be noted that in a centro-symmetric space group--that is, if there is an atom at $\underline{r}$, there will be an atom of the same type at $-\underline{r}$--a closer examination of equation (4-4) is needed. The terms which are summations of the sine terms are zero as for every term, $b_i T_i(\underline{G}) \sin 2\pi (\underline{G} \cdot \underline{r}_i)$, there is a term, $b_i T_i(\underline{G}) \sin 2\pi (\underline{G} \cdot -\underline{r}_i) \equiv -b_i T_i(\underline{G}) \sin 2\pi (\underline{G} \cdot \underline{r}_i)$. Thus, the F's reduce to:

$$\underline{F}(\underline{G}) = A + iD$$

and

$$\underline{F}(-\underline{G}) = A + iD$$

hence in a centro-symmetric space group:

$$I(\underline{G}) = I(-\underline{G})$$

whether or not anomalous scatterers are present. It is only in a non-centro-symmetric structure with anomalous scatterers present that Friedel's law breaks down, that is:

$$I(\underline{G}) \neq I(-\underline{G})$$

This effect can be used in $Li(N_2H_5)SO_4$ since the structure is non-centro-symmetric and ^6Li has a comparatively high neutron absorption cross-section and hence a complex scattering length. In this experiment we compared the ratio, $I(\underline{G})/I(-\underline{G}) = (x/y)$ of a set of reflections with the ratio for these reflections when the crystal had been poled[*] in the opposite sense. After poling, the ratio would be y/x if the structure inverts. If poling only reorients the hydrogen bond, then a different structure results and the individual intensities will change to give a ratio in general different from either y/x or x/y.

---

[*]The verb "pole" is used to indicate the process by which the crystal is placed for a short period in an electric field greater than the coercive field. Such a field should be sufficient to produce a single domain in the crystal if it is ferroelectric.

Although the predicted effect is small and would normally be masked by experimental errors arising from absorption and extinction, it is possible to measure the ratio to much higher accuracy by making the measurements on the same reflection both before and after domain reversal. The ratio of the structure factors is:

$$R_0 = \frac{|\underline{F}|}{|\underline{F}'|} \tag{4-10}$$

where $(\underline{F})$ and $(\underline{F}')$ are the structure factors before and after the application of a reversing field. The constant of proportionality relating $\underline{F} \cdot \underline{F}^*$ to I is identical for both measurements since both are made on the same reflection, under identical conditions. Hence:

$$R_0 = \left(\frac{I}{I'}\right)^{\frac{1}{2}} \tag{4-11}$$

If the structure inverts on switching by a reversal of the $\underline{c}$ direction, the reflection $(\underline{G})$, which we shall now denote by its Miller indices $hk\ell$, becomes the $hk\bar{\ell}$ reflection; and since $|F_{hk\bar{\ell}}| \equiv |F_{\overline{hk}\bar{\ell}}|$ in the space group $Pna2_1$ even with the presence of anomalous scatterers:

$$R_0^2 = \frac{I}{I'} = \frac{I_{hk\ell}}{I_{hk\bar{\ell}}} \equiv \frac{I_{hk\ell}}{I_{\overline{hk}\bar{\ell}}} \tag{4-12}$$

The values of x/y (= $R_c{}^2$(b)) and y/x (= $R_c{}^2$(c)) can be calculated from the known structure and compared with the observed values $R_o{}^2$. Values of $R_c{}^2$ can also be calculated for a mechanism in which only the hydrogen atoms move along the chain by calculating values of I from the coordinates of Padmanabhan & Balasubramanian (1967) and values of I' from a similar model in which H(2) is moved to the opposite end of its hydrogen bond. A third possibility is that no change occurs in the crystal, and in this case $R_c{}^2$(a) $\equiv$ 1 for all reflections.

Experimental

^{6}Li(N$_2$H$_5$)SO$_4$ single crystals were prepared by evaporation from an aqueous solution of isotope separated ^{6}LiCO$_3$ (atomic % ^{6}Li 95.54) and (N$_2$H$_6$)SO$_4$. The crystal used for the final experiment measured approximately 4 × 7 × 8 mm and was mounted on a goniometer head with poling electrodes on its (001) faces. This crystal was coated with per-fluoro-kerosene to prevent slow decomposition in the very humid atmosphere around the reactor, the fluorine compound being used to prevent a high background caused by incoherent scattering from the hydrogen in conventional oils and spray-on plastic films. Intensity measurements were made on the McMaster neutron diffractometer at beam-port #6 using an ω scan at a wavelength of 1.062 Å. The reflections observed had 2θ values in the range $20° < 2θ < 40°$ and there were

27 steps ($1/18^\circ$) in each scan. The first and last three steps of each scan were used to estimate the background level. The approximate duration of an individual step was thirty minutes at a reactor power of 1.5 MW and was timed by a count of 10^5 on the fission counter which monitored the main beam.

Values of $F_c(\underline{G})$ and $F_c(-\underline{G})$ were calculated using the scattering lengths given by the Neutron Diffraction Commission (1969) ($b'=0.18$, $b''=0.025\times10^{-12}$cm) and the coordinates of Padmanabhan & Balasubramanian (1967). From these a set of reflections was chosen which showed significant Friedel inequalities. The crystal was poled by applying a field (630Vcm^{-1}) in excess of the coercive field (320Vcm^{-1}) and the intensity of the Bragg reflection, I, measured. The crystal was then poled in the opposite sense and the new intensity, I', measured. This was repeated on a set of ten reflections. From these intensities, the ratios $R_0 (= \underline{F}_0/\underline{F}'_0 = (I/I')^{\frac{1}{2}})$ were calculated.

Results and Discussion

The ratio R_0 of the observed structure factors and the error σ in R_0 arising from counting statistics are shown in Table 4-1. Also shown are calculated values of the ratio R_c for several cases: a) no structural change; b) inversion of the cell, hkℓ to hk$\bar{\ell}$; c) inversion of the cell, hk$\bar{\ell}$ to hkℓ; d) reorientation of the hydrogen bond from $-\underline{c}$ to $+\underline{c}$;

Table 4-1. The observed and calculated values of the ratio

of the structure factors

hkℓ	R_O	σ	R_C(a)	R_C(b)	R_C(c)	R_C(d)	R_C(e)
031	1.015	0.025	1.000	1.062	0.942	1.376	1.396
0$\bar{3}$1	0.980	0.033	1.000	1.062	0.942	1.376	1.396
151	0.976	0.024	1.000	0.959	1.043	1.064	1.065
1$\bar{5}$1	0.981	0.027	1.000	0.959	1.043	1.064	1.065
1$\bar{5}$1	1.021	0.025	1.000	0.959	1.043	1.064	1.065
$\bar{1}\bar{5}$1	1.040	0.030	1.000	0.959	1.043	1.064	1.065
113	1.010	0.062	1.000	1.051	0.952	0.985	0.984
113	1.088	0.046	1.000	1.051	0.952	0.985	0.984
1$\bar{1}$3	0.997	0.044	1.000	1.051	0.952	0.985	0.984
1$\bar{1}$3	0.962	0.038	1.000	1.051	0.952	0.985	0.984
$\bar{1}$13	1.060	0.063	1.000	1.051	0.952	0.985	0.984
$\bar{1}\bar{1}$3	1.002	0.053	1.000	1.051	0.952	0.985	0.984
$\bar{1}\bar{1}$3	0.909	0.071	1.000	1.051	0.952	0.985	0.984

Table 4-2. The values of χ^2 and probability for each model

Model	χ^2	Probability
(a)	11.19	59%
(b)	36.53	< 1%
(c)	37.67	< 1%
(d)	376.73	<< 1%
(e)	414.72	<< 1%

e) reorientation of the hydrogen bond from $+c$ to $-c$.

The correctness of each model was tested using a x^2 test:

$$\chi^2 = \sum_{i=1}^{N} \frac{\left[R_{o_i} - R_{c_i}\right]^2}{\sigma^2} \qquad (4-13)$$

where the sum was performed over the 13 independent measurements. Table 4-2 shows the values of χ^2 and the probability that a second experiment would have a larger value of χ^2 if the model is correct.

It is evident that model a is overwhelmingly more probable and that no structural change occurs on reversal of the poling field. Schmidt, Drumheller & Howell (1971) have extensively investigated the dielectric properties of $Li(N_2H_5)SO_4$ and have proposed a model in which the protonic conduction along the c direction is partially blocked by extrinsic barriers along the N-H....N-H chain. Using this model they can predict the dielectric properties quite well and conclude that $Li(N_2H_5)SO_4$ is not ferroelectric. Our failure to observe any permanent alteration in the molecular structure of the crystal as a result of poling is in agreement with their results and confirms the fact that it is impossible to reverse the permanent dipole moment of $Li(N_2H_5)SO_4$.

A paper on the work described in this chapter has been published by Anderson and Brown (1972).

CHAPTER V

AN ACCURATE REDETERMINATION OF THE CRYSTAL STRUCTURE OF
LITHIUM HYDRAZINIUM SULPHATE BY X-RAY DIFFRACTION

There have been several X-ray investigations of the
crystal structure of lithium hydrazinium sulphate, $Li(N_2H_5)SO_4$.
None of those yet published gives all the atomic positions to
a suitable accuracy for a study of the hydrogen bonding
system as there are large discrepancies in the sulphur-oxygen
bond lengths. This work is an accurate refinement of the
structure, and comparison is made with the recent neutron
diffraction redetermination (Ross, 1970) using a deuterated
sample, $Li(N_2D_5)SO_4$.

Experimental

Single crystals of $Li(N_2H_5)SO_4$ were prepared by
evaporation from an aqueous solution of $LiCO_3$ and $(N_2H_6)SO_4$.
All diffraction measurements were made at room temperature on
a crystal with dimensions $0.2 \times 0.2 \times 0.3$ mm on the Syntex
four-circle X-ray diffractometer using MoKα radiation
($\lambda=0.71069$ Å) monochromated by reflection from a graphite
crystal. The lattice parameters are given in Table 5-1 and
were refined by the method of least-squares from the 2θ
settings of fifteen reflections (Table 5-2). Intensities of

65

Table 5-1. Crystallographic data for Li(N$_2$H$_5$)SO$_4$

Crystal system	Orthorhombic
Space group	Pna2$_1$ (C$_{2v}^9$)
a (Å)	9.929(5)*
b (Å)	8.973(3)
c (Å)	5.181(2)
Z	4
Cell volume (Å^3)	461.6(3)
D$_{calc}$ (g/cm^3)	1.958
Absorption coefficient for MoKα (mm^{-1})	0.603
Crystal size (mm)	0.2 × 0.2 × 0.3
Wavelength MoKα (Å)	0.71069
Systematic absences	Okℓ k+ℓ = 2n+1
	h0ℓ h = 2n+1

*Throughout this work, the estimated standard deviations are enclosed in parentheses.

Table 5-2. Reflections used in the least-squares refinement
of the lattice parameters of $Li(N_2H_5)SO_4$

Reflection			$2\theta_{obs}$ (°)	$2\theta_{calc}$ (°)
h	k	ℓ		
1	2	0	9.96	9.97
1	3	0	14.26	14.25
1	2	1	12.70	12.71
0	0	2	15.77	15.77
0	1	1	9.07	9.08
-2	3	-1	17.82	17.81
1	1	0	6.09	6.12
-1	2	1	12.71	12.71
-1	3	1	16.30	16.30
2	4	1	21.54	21.54
3	1	2	20.58	20.58
-3	1	0	13.16	13.14
2	0	1	11.37	11.38
2	3	0	15.95	15.94
-1	1	0	6.12	6.12

911 independent reflections with $\sin\theta/\lambda < 0.76$ were measured and corrected for Lorentz and polarisation effects. No correction was made for absorption as this was considered to be negligible ($\mu = 0.603$ mm^{-1}).

Refinement of the Structure

The non-hydrogen atomic positions of Brown (1964) were used as a basis for the refinement. After initial refinement of the positional and isotropic thermal parameters of these atoms with the full matrix least-squares programme CRYLSQ of the XRAY 71 programme library system, all the hydrogen atoms were located with a three-dimensional difference electron density map. Further refinement with anisotropic temperature factors for all non-hydrogen atoms and isotropic temperature factors for the hydrogen atoms gave a residual index, R (cf. equation 2-31), of 0.022. During the latter cycles of refinement, the temperature factor of H(3) refined to a negative, and hence unphysical value, and was set at a typical value of 0.04 and not refined further. The final cycles included an extinction correction where the corrected values of F_c, given by:

$$F_c^{*} = KF_c\left[1 + 0.94 \times 10^{-3} \times \beta(2\theta)F_c^{2}\right]^{-\frac{1}{2}} , \qquad (5-1)$$

and a Cruickshank weighting scheme with weights given by:

$$w = (0.250 - 0.032|F_o| + 0.0016|F_o|^2)^{-1} \qquad (5-2)$$

were used. This gave a final weighted residual index, R_w (cf. equation 2-32), of 0.027. The final atomic positions and temperature factors are given in Table 5-3.

Description of the Structure

Views of the structure along the a and c directions are given in Figures 5-1 and 5-2. The framework of LiO_4 and SO_4 tetrahedra has average Li-O and S-O distances of 1.937(18) Å and 1.473(9) Å respectively. The S-O(1) distance is 1.487(2) Å, almost midway between the previously reported X-ray diffraction values of 1.45(3) Å (Brown, 1964) and 1.557 Å (Van den Hende & Boutin, 1964) and agrees well with the recent neutron diffraction value of 1.484 Å. Bond lengths and angles are given in Table 5-4.

Table 5-5 gives details of the hydrogen bonds. N(1), the nitrogen atom of the $-NH_2$ group, is involved in three single hydrogen bonds, twice as a donor and once as an acceptor. The $-NH_3^+$ group forms three hydrogen bonds, one of which (H(5)) is bifurcated. A staggered configuration exists between the $-NH_3^+$ group and the $-NH_2$ group and its lone pair; the dihedral angles are given in Table 5-6.

A bond-strength summation using the method of Brown and Shannon (1973) was calculated (Table 5-7). The cation

Table 5-3. Parameters derived from the final least-squares refinement of X-ray data for Li(N$_2$H$_5$)SO$_4$

Atom	Positional coordinates				Temperature factors*				
	x	y	z	U or U$_{11}$	U$_{22}$	U$_{33}$	U$_{12}$	U$_{13}$	U$_{23}$
Li	0.3312(3)	0.4333(3)	0.2533(12)	21(1)	19(1)	18(1)	-1(1)	-1(2)	-2(2)
S	0.1580(1)	0.1285(1)	0.2500(†)	11.0(1)	12.4(1)	11.7(1)	-1.4(1)	-0.9(2)	0.1(2)
O(1)	0.1909(2)	0.1052(2)	0.5271(3)	26.6(7)	24.3(7)	12.7(6)	-2.5(5)	-5.3(5)	2.2(5)
O(2)	0.0115(1)	0.1540(2)	0.2282(5)	11.5(4)	31.7(7)	28.1(8)	-0.5(4)	-1.3(7)	6.1(8)
O(3)	0.2299(1)	0.2593(2)	0.1533(4)	21.9(6)	20.2(7)	24.2(7)	-8.9(5)	2.2(6)	3.9(6)
O(4)	0.3040(2)	0.4957(2)	0.6023(3)	32.0(7)	19.4(7)	22.0(7)	-6.2(6)	4.8(6)	-8.7(6)
N(1)	0.0235(2)	0.4157(2)	0.7488(7)	30.8(8)	27.6(8)	35.3(9)	-8.6(6)	-1.0(13)	3.5(13)
N(2)	0.4400(2)	0.2136(2)	0.7381(6)	22.1(6)	23.5(6)	21.8(7)	1.6(5)	1.5(10)	-0.1(10)
H(1)	0.103(4)	0.392(4)	0.776(9)	16(9)					
H(2)	0.026(7)	0.445(6)	0.582(15)	65(20)					
H(3)	0.358(4)	0.192(6)	0.680(11)	40(5)					
H(4)	0.446(6)	0.234(8)	0.895(17)	69(26)					
H(5)	0.462(3)	0.282(4)	0.616(8)	8(8)					

*Expressions used for the temperature factors are:

$$\exp[-2\pi^2 \times 10^{-3} \ (U_{11}h^2a*^2 + U_{22}k^2b*^2 + U_{33}\ell^2c*^2 + 2U_{12}hka*b* + 2U_{13}h\ell a*c* + 2U_{23}k\ell b*c*)] \ \text{and}$$

$$\exp[-2\pi^2 \times 10^{-3} \ U(\frac{2\sin\theta}{\lambda})^2].$$

†This parameter was used to define the origin and was not refined.

§Not refined.

Table 5-3. Parameters derived from the final least-squares refinement of X-ray data for Li(N$_2$H$_5$)SO$_4$

Atom	Positional coordinates			Temperature factors*					
	x	y	z	U or U_{11}	U_{22}	U_{33}	U_{12}	U_{13}	U_{23}
Li	0.3312(3)	0.4333(3)	0.2533(12)	21(1)	19(1)	18(1)	-1(1)	-1(2)	-2(2)
S	0.1580(1)	0.1285(1)	0.2500(†)	11.0(1)	12.4(1)	11.7(1)	-1.4(1)	-0.9(2)	0.1(2)
O(1)	0.1909(2)	0.1052(2)	0.5271(3)	26.6(7)	24.3(7)	12.7(6)	-2.5(5)	-5.3(5)	2.2(5)
O(2)	0.0115(1)	0.1540(2)	0.2282(5)	11.5(4)	31.7(7)	28.1(8)	-0.5(4)	-1.3(7)	6.1(8)
O(3)	0.2299(1)	0.2593(2)	0.1533(4)	21.9(6)	20.2(7)	24.2(7)	-8.9(5)	2.2(6)	3.9(6)
O(4)	0.3040(2)	0.4957(2)	0.6023(3)	32.0(7)	19.4(7)	22.0(7)	-6.2(6)	4.8(6)	-8.7(6)
N(1)	0.0235(2)	0.4157(2)	0.7488(7)	30.8(8)	27.6(8)	35.3(9)	-8.6(6)	-1.0(13)	3.5(13)
N(2)	0.4400(2)	0.2136(2)	0.7381(6)	22.1(6)	23.5(6)	21.8(7)	1.6(5)	1.5(10)	-0.1(10)
H(1)	0.103(4)	0.392(4)	0.776(9)	16(9)					
H(2)	0.026(7)	0.445(6)	0.582(15)	65(20)					
H(3)	0.358(4)	0.192(6)	0.680(11)	40(5)§					
H(4)	0.446(6)	0.234(8)	0.895(17)	69(26)					
H(5)	0.462(3)	0.282(4)	0.616(8)	8(8)					

* Expressions used for the temperature factors are:

$$\exp\left[-2\pi^2 \times 10^{-3}\left(U_{11}h^2a^{*2} + U_{22}k^2b^{*2} + U_{33}\ell^2c^{*2} + 2U_{12}hka^*b^* + 2U_{13}h\ell a^*c^* + 2U_{23}k\ell b^*c^*\right)\right]$$ and

$$\exp\left[-2\pi^2 \times 10^{-3}\, U\left(\frac{2\sin\theta}{\lambda}\right)^2\right].$$

†This parameter was used to define the origin and was not refined.

§Not refined.

Figure 5-1.

The crystal structure of $Li(N_2H_5)SO_4$ viewed along the $\underline{a}$ direction.
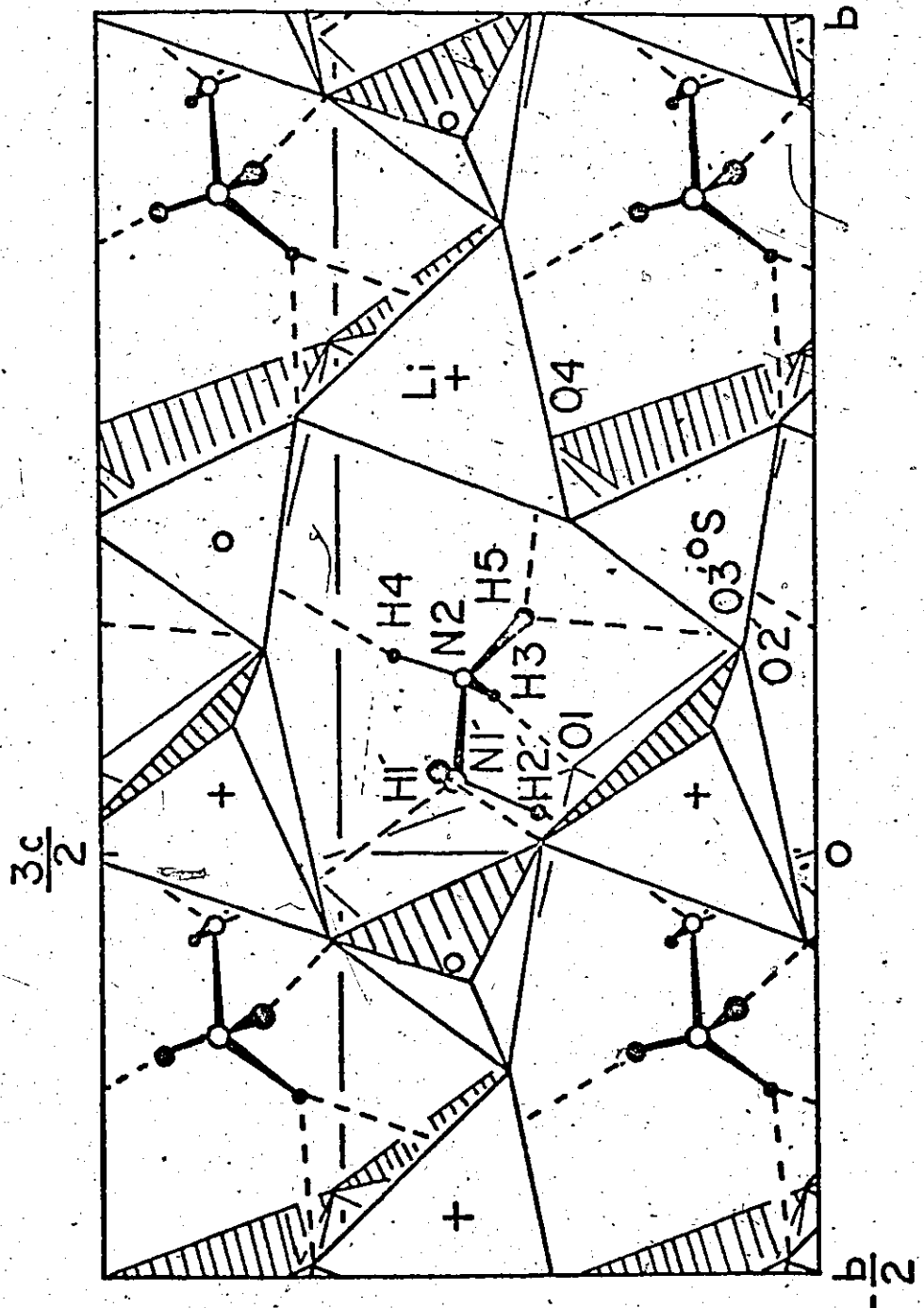
Figure 5-2.

The crystal structure of $Li(N_2H_5)SO_4$ viewed along the $\underline{c}$ direction.

$\frac{a}{2}$
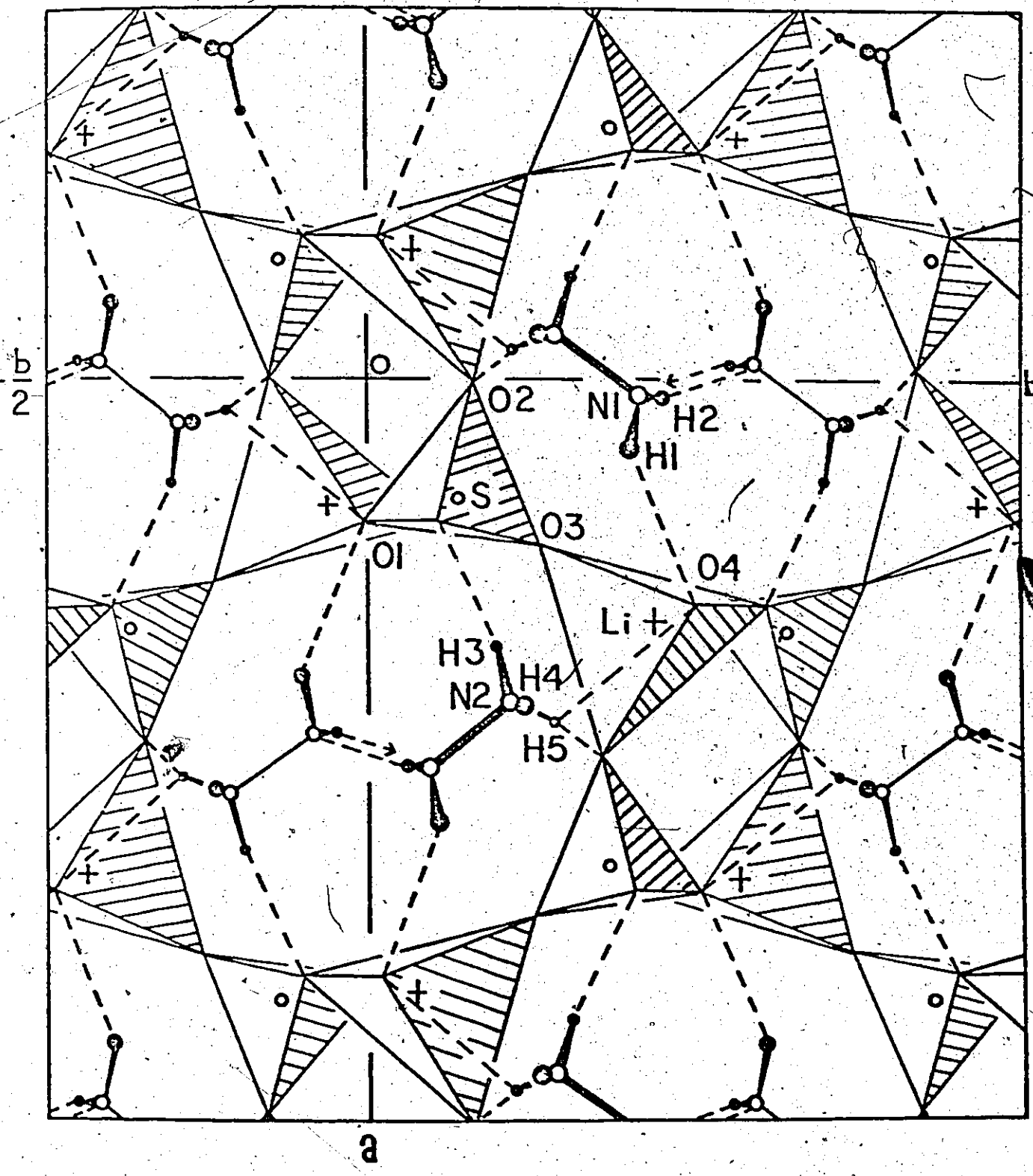
$\frac{b}{2}$ — b

O2 N1 H2
H1

S O3
O1 O4

Li +

H3 H4
N2
H5

a

Table 5-4. Bond distances and angles in Li(N$_2$H$_5$)SO$_4$ as determined by X-ray diffraction compared with those in Li(N$_2$D$_5$)SO$_4$ as determined by neutron diffraction (Ross, 1970)

LiO$_4$ tetrahedron

	X-ray (Å)	Neutron (Å)		X-ray (°)	Neutron (°)
Li – O(1)	1.950(5)	1.940	O(1) – Li – O(2)	112.3(2)	112.2
Li – O(2)	1.959(3)	1.976	O(1) – Li – O(3)	114.9(3)	115.2
Li – O(3)	1.928(4)	1.940	O(1) – Li – O(4)	108.7(2)	109.3
Li – O(4)	1.912(6)	1.914	O(2) – Li – O(3)	97.8(2)	97.3
			O(2) – Li – O(4)	108.0(3)	107.4
			O(3) – Li – O(4)	114.7(2)	114.7

SO$_4$ tetrahedron

	X-ray (Å)	Neutron (Å)		X-ray (°)	Neutron (°)
S – O(1)	1.487(2)	1.480	O(1) – S – O(2)	108.2(1)	108.6
S – O(2)	1.477(1)	1.472	O(1) – S – O(3)	109.7(1)	110.1
S – O(3)	1.462(2)	1.463	O(1) – S – O(4)	109.5(1)	109.1
S – O(4)	1.465(2)	1.473	O(2) – S – O(3)	109.3(1)	109.2
			O(2) – S – O(4)	109.8(1)	109.9
			O(3) – S – O(4)	110.4(1)	109.9

Table 5-4. Bond distances and angles in Li(N$_2$H$_5$)SO$_4$ as determined by X-ray diffraction compared with those in Li(N$_2$D$_5$)SO$_4$ as determined by neutron diffraction (Ross, 1970) (Continued).

(N$_2$H$_5$) ion

	X-ray (Å)	Neutron (Å)		X-ray (°)	Neutron (°)
N(1) - N(2)	1.427(3)	1.421	N(2) - N(1) - H(1)	111(2)	107
N(1) - H(1)	0.83(4)	1.011	N(2) - N(1) - H(2)	102(4)	106
N(1) - H(2)	0.91(8)	1.025	N(2) - N(1) - H(2')	111(2)	111
N(1) - H(2') *	2.18(7)	2.034	H(1) - N(1) - H(2)	102(5)	107
			H(1) - N(1) - H(2')	103(4)	105
			H(2) - N(1) - H(2')	126(4)	121

	X-ray (Å)	Neutron (Å)		X-ray (°)	Neutron (°)
N(2) - H(3)	0.89(5)	1.011	N(1) - N(2) - H(3)	111(4)	110
N(2) - H(4)	0.84(9)	1.020	N(1) - N(2) - H(4)	96(5)	108
N(2) - H(5)	0.91(4)	1.019	N(1) - N(2) - H(5)	116(2)	114
			H(3) - N(2) - H(4)	116(6)	110
			H(3) - N(2) - H(5)	98(4)	106
			H(4) - N(2) - H(5)	121(6)	109

*Throughout this work, an atom which is primed is related by symmetry to the equivalent atom in the asymmetric unit.

Table 5-5. Hydrogen bond lengths and angles in Li(N$_2$H$_5$)SO$_4$

For each bond, the X-ray result is given in the first line and the neutron result of Ross (1970) in the second.

D-H....A			D-H (Å)	H...A (Å)	D-A (Å)	<D-H...A (°)
N(1)	H(1)	O(4)	0.83(4) 1.011	2.38(4) 2.300	2.975(3) 2.980	129(3) 124
N(1)	H(2)	N(1')	0.91(8) 1.025	2.18(7) 2.034	3.043(3) 3.040	156(5) 166
N(2)	H(3)	O(1)	0.89(5) 1.011	2.00(7) 1.891	2.874(3) 2.882	169(5) 166
N(2)	H(4)	O(2)	0.84(9) 1.020	2.10(8) 1.922	2.892(4) 2.896	158(7) 159
N(2)	H(5)	O(2)	0.91(4) 1.019	2.15(5) 2.060	2.982(4) 2.978	153(3) 149
N(2)	H(5)	O(4)		2.48(4) 2.473	2.954(3) 2.956	113(3) 108

Table 5-6. Dihedral angles of the (N_2H_5) ion (X-ray)
compared with those of the (N_2D_5) ion (neutron)

Plane defined by atoms			Plane defined by atoms			Dihedral angle	
						X-ray ($^{\circ}$)	Neutron ($^{\circ}$)
N(1)	N(2)	H(1)	N(1)	N(2)	H(2)	108	114
N(1)	N(2)	H(1)	N(1)	N(2)	H(2')	-114	-114
N(1)	N(2)	H(1)	N(1)	N(2)	H(3)	170	172
N(1)	N(2)	H(3)	N(1)	N(2)	H(4)	121	120
N(1)	N(2)	H(3)	N(1)	N(2)	H(5)	-111	-119

Table 5-7. Bond-strengths in $Li(N_2H_5)SO_4$ calculated from bond lengths determined by X-ray diffraction

Bond-strengths in valence units and bond lengths in Å (in brackets) for bonds between O and Li, S and H.

	Li	S	H(1)	H(3)	H(4)	H(5)	Sums around anions
O(1)	0.24 (1.950)	1.45 (1.487)		0.16* (2.00)			1.86
O(2)	0.24 (1.959)	1.49 (1.477)			0.14* (2.10)	0.14* (2.15)	2.02
O(3)	0.26 (1.928)	1.56 (1.462)					1.82
O(4)	0.26 (1.912)	1.55 (1.465)	0.11* (2.375)			0.10* (2.48)	2.02
Sums around cations	1.00	6.06					

Bond-strengths (s) are calculated from the expression $s = (R/R_0)^{-N}$ where R is the bond length and

	H-O	Li-O	S-O
R_0	0.86*	1.378	1.622
N	2.17*	4.065	4.290

*The parameters for H apply to bonds determined by neutron diffraction and will tend to underestimate the bond-strength in this case.

sums were satisfactory, but the anion sums at O(1) and O(3) are significantly low at 1.86(1) and 1.82(1) valence units respectively. Both O(1) and O(3) are bonded to one sulphur atom and one lithium atom, and O(1) accepts one hydrogen bond; there are no other possible hydrogen bonds to either oxygen atom. Use of the X-ray determined hydrogen positions would tend to underestimate the hydrogen bond strengths, and the calculation was repeated using the neutron positions of Ross (Table 5-8). There was some improvement of the sum at O(1), but the non-hydrogen bonded O(3) was even lower at 1.81(1) valence units.

Table 5-8. Bond-strengths in Li(N$_2$D$_5$)SO$_4$ calculated for the bond lengths determined from the neutron diffraction results of Ross (1970)

Bond-strengths in valence units and bond lengths in Å (in brackets) for bonds between O and Li, S and D.

	Li	S	D(1)	D(3)	D(4)	D(5)	Sums around anions
O(1)	0.25 (1.940)	1.48 (1.480)		0.18 (1.891)			1.91
O(2)	0.23 (1.976)	1.52 (1.472)			0.18 (1.922)	0.15 (2.060)	2.07
O(3)	0.25 (1.940)	1.56 (1.463)					1.81
O(4)	0.26 (1.914)	1.51 (1.473)	0.12 (2.300)			0.10 (2.473)	1.99
Sums around cations	0.99	6.07					

Bond-strengths (s) are calculated from the expression $s = (R/R_0)^{-N}$ where R is the bond length and

	D-O	Li-O	S-O
R$_0$	0.86	1.378	1.622
N	2.17	4.065	4.290

CHAPTER VI

DETERMINATION OF THE CRYSTAL STRUCTURE OF LITHIUM HYDRAZINIUM FLUOROBERYLLATE BY X-RAY AND NEUTRON DIFFRACTION

The crystal structures of several hydrazinium compounds have been determined, but only one $(Li(N_2H_5)SO_4)$ has been found with chains of hydrogen bonded hydrazinium ions where the donor and acceptor of the hydrogen bonds is the $-NH_2$ group. This investigation was to determine whether the hydrazinium ions in $Li(N_2H_5)BeF_4$ also formed this type of chain and to obtain accurate details of all the hydrogen bonds in the structure.

Preparation of the Crystals

Lithium hydrazinium fluoroberyllate, $Li(N_2H_5)BeF_4$, was prepared by the reaction of lithium carbonate and hydrazonium fluoroberyllate in aqueous solution:

$$Li_2CO_3 + 2(N_2H_6)BeF_4 \rightarrow 2Li(N_2H_5)BeF_4 + H_2O + CO_2$$

$$(6-1)$$
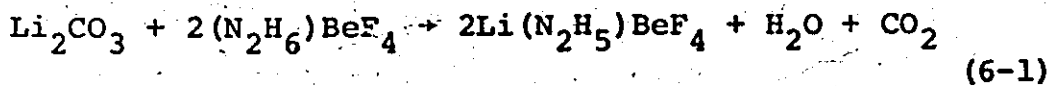
using the method of Tédenac et al. (1971). The very small $(3.4 \times 10^{-3} mm^3)$ single crystal used for the X-ray work was easily grown by evaporation from an aqueous solution of $Li(N_2H_5)BeF_4$. The large single crystals $(56mm^3)$ for the

neutron work were grown from a small seed crystal by slow

evaporation of a saturated aqueous solution.

Experimental (X-ray)

X-ray diffraction measurements were made at room

temperature on a single crystal with dimensions

$0.13 \times 0.13 \times 0.2$ mm using the Syntex diffractometer.

Graphite monochromated MoKα radiation was used,

$\lambda = 0.71069$ Å. The lattice parameters (Table 6-1) were

refined by a least-squares analysis of the 2θ settings of

fifteen reflections (Table 6-2). The space group,

$Pna2_1 (C_{2v}^9)$, was confirmed from systematic absences observed

on precession camera photographs and the successful refinement

of the structure in a non-centro-symmetric cell. The

intensities of 700 independent reflections with

$\sin\theta/\lambda < 0.704$ Å^{-1} were measured and corrected for Lorentz

and polarisation effects but not for absorption which was

negligible ($\mu=0.25$ mm^{-1}).

Experimental (Neutron)

A single crystal with dimensions $2.5 \times 2.5 \times 9.0$ mm

was used for the neutron diffraction measurements. The

singleness of the crystal was checked by comparing several

X-ray precession photographs of different parts of the

crystal. Precession photographs were also used to align the

c axis of the crystal coincident with the goniometer head

Table 6-1. Crystallographic data for Li$(N_2H_5)BeF_4$

	X-ray	Neutron
Crystal system	Orthorhombic	
Space group	Pna2$_1$ (C$_{2v}^9$)	
a (Å)	9.811(4)	
b (Å)	8.880(8)	
c (Å)	5.139(4)	
Z	4	
Cell volume (Å^3)	447.7(6)	
D$_{calc}$ (g/cm^3)	1.854	
Absorption coefficient (mm^{-1})	0.25 (MoKα)	0.039
Crystal size (mm)	0.13 × 0.13 × 0.2	2.5 × 2.5 × 9.0
Wavelength (Å)	0.71069 (MoKα)	1.091
Systematic absences	0kℓ k + ℓ = 2n+1 hoℓ h = 2n+1	

Table 6-2. Reflections used in the least-squares refinement
of the lattice parameters of Li(N$_2$H$_5$)BeF$_4$

Reflection			$2\theta_{obs}$	$2\theta_{calc}$
h	k	ℓ	(^{o})	(^{o})
3	-1	0	13.30	13.30
4	0	0	16.67	16.66
1	-2	1	12.86	12.84
1	-1	0	6.20	6.19
-1	-3	-1	16.48	16.47
-1	-2	1	12.83	12.84
5	-2	1	24.19	24.21
2	0	2	17.94	17.96
1	-2	-1	12.82	12.84
2	-1	0	9.50	9.49
2	0	-2	17.99	17.96
5	-1	0	21.38	21.38
0	-3	-1	15.92	15.93
4	-1	0	17.30	17.29
3	-2	1	17.43	17.44

axis. To avoid possible decomposition caused by the high humidity around the reactor, the crystal was coated with per-fluoro-kerosene.

The diffraction measurements were made using the neutron diffractometer described in Chapter III at beam port #5 of the McMaster nuclear reactor. The neutron beam, monochromated by reflection from the (111) plane of a single copper crystal, had a wavelength of 1.091 Å. The intensities of 470 independent reflections with $\sin\theta/\lambda < 0.65$ were measured using the ω step scanning technique. The number of steps in the scan varied from 27, for reflections whose 2θ value was $< 20°$, to 45 steps, for those reflections in the 2θ range $80° \leqslant 2\theta < 100°$, each step being $1/18°$. The first 1/9th and last 1/9th of the steps in each scan were used to determine the background. The duration of each step was controlled by a fission counter which monitored the main beam. A monitor count of 10^4 for each step was used, and the approximate time for a step was one minute at a reactor power of 5 MW. The measured intensities were corrected for Lorentz effects using the FORTRAN programme DIFDAT.

Solution and Refinement of the Structure (X-ray)

Lithium hydrazinium fluoroberyllate was assumed to be isostructural with lithium hydrazinium sulphate, and the coordinates of Padmanabhan & Balasubramanian (1967) were used as a basis for the refinement. Initial refinement of the

positions and isotropic temperature factors of the heavy atoms, using the X-ray measurements with the full matrix least-squares programme ORFLS of the XRAY 67 programme library system, gave a residual index, R_x (cf. equation 2-31), of 0.076. A three-dimensional difference electron density map was used to locate the hydrogen atoms and, after further refinement with isotropic temperature factors for the hydrogen atoms and anisotropic temperatures for all other atoms, R_x was reduced to 0.040. Three reflections showed significant effects of extinction, and the final cycles of refinement of the X-ray data used the local least-squares programme CUDLS in which extinction corrected values of F_c, given by:

$$F_c^* = K_x F_c [1+0.88 \times 10^{-6} \times \beta_x (2\theta) F_c^2]^{-\frac{1}{2}} \qquad (6-2)$$

were used (cf. equation 2-42). The final weighted residual index, R_{wx} (cf. equation 2-32), was 0.039 where the weights were given by:

$$w = (0.26-0.018|F_o|+0.00059|F_o|^2)^{-1} \qquad (6-3)$$

and unobserved reflections were given zero weight if $|F_c| < |F_o|$. The final atomic parameters and temperature factors are given in Table 6-3. The observed and calculated

Table 6-3. Parameters derived from the final least-squares refinement of X-ray data for $Li(N_2H_5)BeF_4$

Atom	Positional coordinates			Temperature factors*					
	x	y	z	U or U_{11}	U_{22}	U_{33}	U_{12}	U_{13}	U_{23}
Li	0.322(1)	0.436(1)	0.251(2)	19(2)	23(3)	21(3)	1(2)	−4(3)†	−2(3)
N(1)	0.0225(4)	0.4116(4)	0.7455(†)	33(2)	28(2)	34(2)	−7(1)	0(2)	4(2)
N(2)	0.4422(3)	0.2228(4)	0.742(1)	27(1)	26(1)	26(2)	2(1)	1(2)	4(2)
Be	0.1584(4)	0.1270(5)	0.248(1)	15(1)	20(2)	16(2)	−1(1)	−2(2)	−1(2)
F(1)	0.1958(2)	0.1051(2)	0.540(1)	35(1)	25(1)	18(1)	−3(1)	−4(1)	2(1)
F(2)	0.0002(2)	0.1433(3)	0.231(1)	16(1)	40(1)	31(1)	−3(1)	−1(1)	6(1)
F(3)	0.2249(2)	0.2701(2)	0.141(1)	29(1)	23(1)	26(1)	−10(1)	0(1)	3(1)
F(4)	0.2983(2)	0.4881(2)	0.591(1)	36(1)	25(1)	22(1)	−6(1)	4(1)	−8(1)
H(1)	0.097(6)	0.389(6)	0.803(17)	49(19)					
H(2)	0.011(5)	0.463(5)	0.598(11)	13(12)					
H(3)	0.362(4)	0.192(5)	0.690(12)	18(13)					
H(4)	0.450(7)	0.259(8)	0.908(15)	33(20)					
H(5)	0.472(6)	0.296(7)	0.614(16)	25(19)					

*Expressions used for the temperature factors are:

$$\exp\left[-2\pi^2 \times 10^{-3} \cdot (U_{11}h^2a^{*2} + U_{22}k^2b^{*2} + U_{33}\ell^2c^{*2} + 2U_{12}hka^*b^* + 2U_{13}h\ell a^*c^* + 2U_{23}k\ell b^*c^*)\right] \text{ and}$$

$$\exp\left[-2\pi^2 \times 10^{-3} \cdot U\left(\frac{2\sin\theta}{\lambda}\right)^2\right].$$

†This parameter was used to define the origin and was not refined.

X-ray structure factors are given in Appendix A.

Refinement of the Structure (Neutron)

The atomic positions of the X-ray work were used for the initial refinement of the structure with the neutron measurements. The coherent neutron scattering lengths reported by Bacon (1972) were used (Li, -0.214; N, 0.94; H, -0.374; Be, 0.774; F, 0.56×10^{-12} cm). Refinement of the atomic positions and isotropic temperature factors of all atoms, using the full matrix least-squares programme CRYLSQ of the XRAY 71 programme library system, gave a residual index, R_N, of 0.122. Further refinement with anisotropic temperature factors reduced the residual index, although the temperature factor for the lithium atom refined to a non-positive definite value and had to be refined isotropically. Several of the strong reflections showed evidence of extinction effects, and an isotropic extinction parameter was included in the refinement. The corrected values of F_c were given by:

$$F_c^* = K_N F_c [1 + 0.46 \times 10^{-2} \times \beta_N (2\theta) F_c^2]^{-\frac{1}{2}} . \qquad (6-4)$$

The final stages of the least-squares refinement used the local programme CUDLS. The temperature factor of the lithium atom still could not be refined anisotropically. A refinement of the scattering length of lithium changed its value from

-0.214×10^{-12} cm to -0.195×10^{-12} cm indicating that there could be a higher percentage of ^{6}Li (scattering length 0.18×10^{-12} cm) in this sample than the 7.42% ^{6}Li in naturally occurring lithium. Even so, this did not enable an anisotropic temperature factor to be used for this atom, and in the subsequent stages of the refinement the scattering length was reset to its original value of -0.214×10^{-12} cm, and an isotropic temperature factor was used. A weighting scheme was used during the final cycles of least-squares refinement, the weights being given by:

$$ w = \frac{1}{\sigma_{F_{o}}^{2}} \qquad (6-5) $$

where $\sigma_{F_{o}}$ is the standard deviation of F_{o} estimated from the counting statistics of the measurements. The final weighted residual index, R_{wN}, was 0.044, and the final atomic parameters and temperature factors are given in Table 6-4. The observed and calculated neutron structure factors are given in Appendix A.

Description of the Structure

Li(N$_2$H$_5$)BeF$_4$ is isostructural with Li(N$_2$H$_5$)SO$_4$ (cf. Chapter V) but with differences in the hydrogen bonding arrangement. Views of the structure along the <u>a</u> and <u>c</u> directions are given in Figures 6-1 and 6-2.

Table 6-4. Parameters derived from the final least-squares refinement
of neutron diffraction data for $Li(N_2H_5)BeF_4$*

| Atom | Positional coordinates | | | Temperature factors* | | | | | |
	x	y	z	U or U_{11}	U_{22}	U_{33}	U_{12}	U_{13}	U_{23}
Li	0.3213(18)	0.4353(20)	0.2766(86)	33(5)					
N(1)	0.0228(6)	0.4107(7)	0.7455(†)	31(3)	36(3)	61(9)	-7(2)	2(6)	0(5)
N(2)	0.4418(6)	0.2219(6)	0.7397(39)	26(3)	31(3)	48(6)	2(2)	2(6)	-6(6)
Be	0.1585(4)	0.1260(5)	0.2468(36)	15(2)	23(2)	31(5)	-1(2)	-1(5)	9(5)
F(1)	0.1963(8)	0.1058(9)	0.5505(37)	31(4)	25(4)	49(9)	-5(3)	-7(5)	10(5)
F(2)	0.0001(6)	0.1416(8)	0.2305(41)	14(3)	38(3)	36(6)	-4(2)	4(6)	-12(7)
F(3)	0.2263(7)	0.2704(7)	0.1447(30)	28(3)	26(4)	32(9)	-8(3)	-2(4)	5(4)
F(4)	0.2985(8)	0.4877(8)	0.5980(37)	30(4)	28(4)	53(8)	-7(3)	-3(5)	-17(5)
H(1)	0.116(1)	0.384(2)	0.791(7)	33(7)	84(10)	86(25)	-15(8)	-13(16)	-13(17)
H(2)	0.019(2)	0.451(3)	0.572(7)	88(16)	69(15)	28(21)	-28(12)	12(16)	1(12)
H(3)	0.347(1)	0.195(2)	0.710(9)	30(7)	84(11)	145(29)	10(8)	-25(15)	14(19)
H(4)	0.445(3)	0.275(3)	0.926(8)	89(20)	68(13)	83(29)	48(14)	11(18)	-15(15)
H(5)	0.472(2)	0.292(4)	0.613(6)	50(10)	111(17)	14(14)	7(12)	13(10)	24(13)

*Expressions used for the temperature factors are:

$$\exp\left[-2\pi^2 \times 10^{-3}\left(U_{11}h^2a^{*2} + U_{22}k^2b^{*2} + U_{33}\ell^2c^{*2} + 2U_{12}hka^*b^* + 2U_{13}h\ell a^*c^* + 2U_{23}k\ell b^*c^*\right)\right]$$ and

$$\exp\left[-2\pi^2 \times 10^{-3} \, U\left(\frac{2\sin\theta}{\lambda}\right)^2\right].$$

†Not refined.

Figure 6-1.

The crystal structure of $Li(N_2H_5)BeF_4$ viewed along the $\underline{a}$ direction.
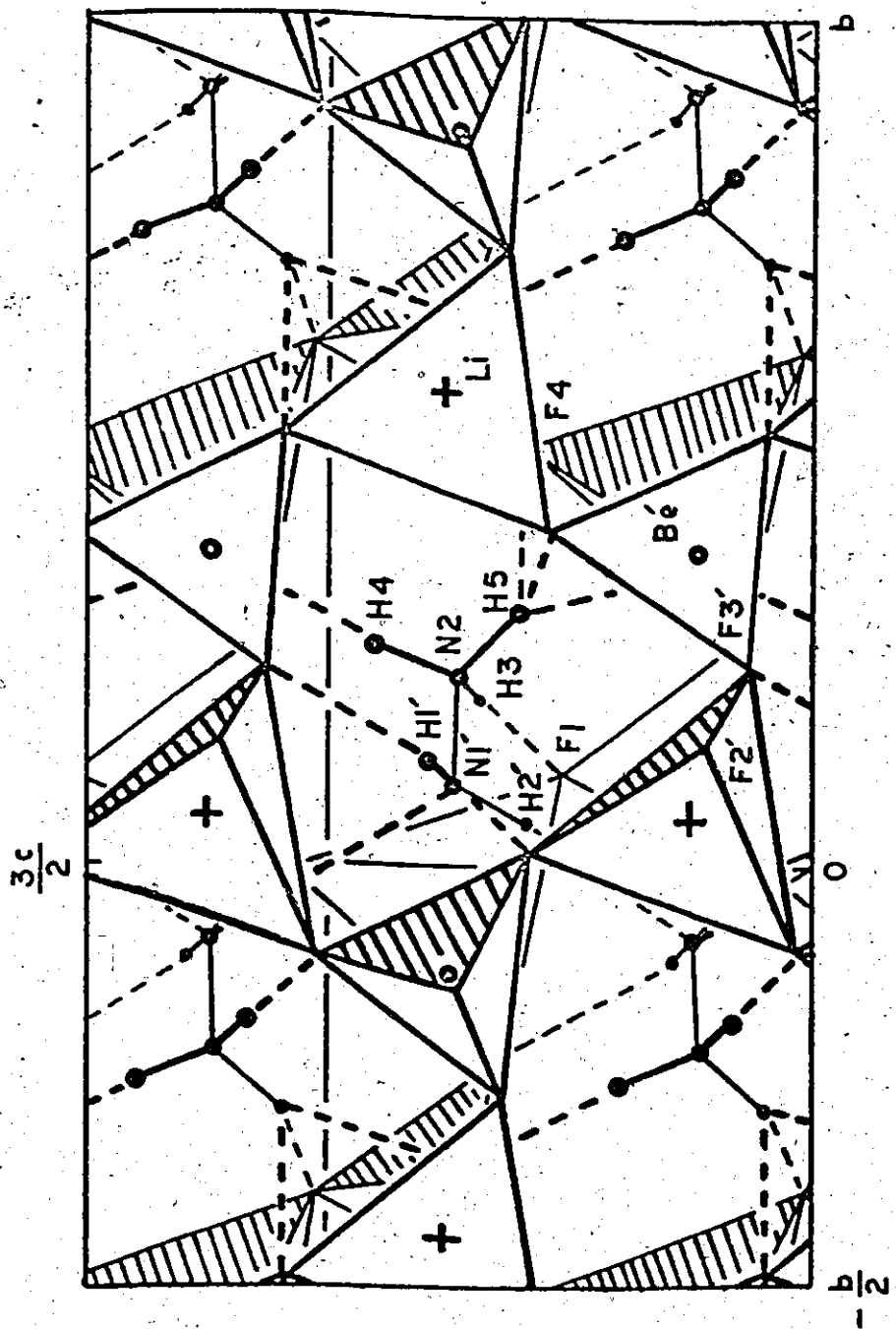
Figure 6-2.

The crystal structure of $Li(N_2H_5)BeF_4$ viewed along the $\underline{c}$ direction.
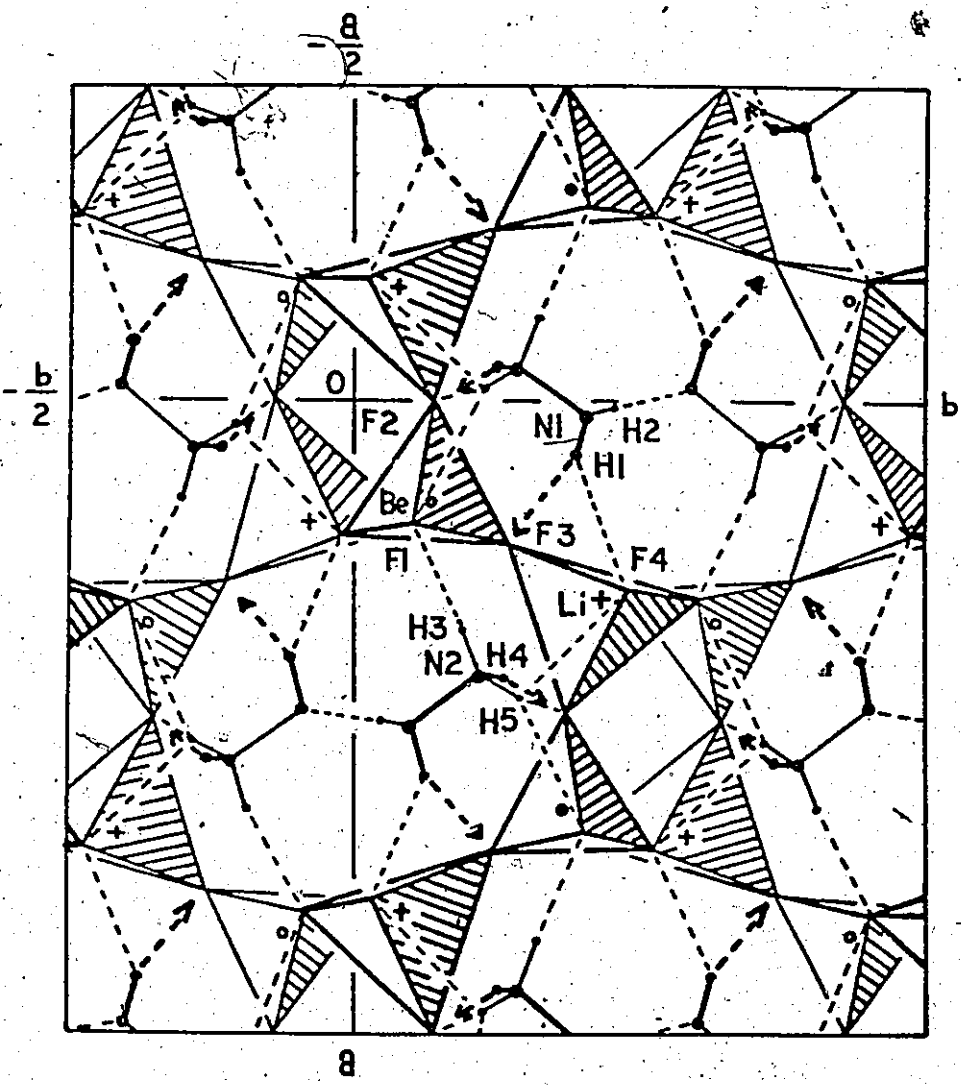
Table 6-5 gives the bond lengths and angles. The BeF_4 and LiF_4 tetrahedra are nearly regular with mean Be-F and Li-F bond lengths of 1.546(13) Å and 1.853(20) Å respectively. The N-N distance is 1.431(5) Å, and the N-H bonds of the neutron diffraction work are systematically longer with a mean length of 0.98(3) Å compared to the X-ray diffraction value of 0.89(4) Å. Table 6-6 gives details of the hydrogen bonding, and Table 6-7 gives the dihedral angles of the (N_2H_5) ion. The hydrogen bond formed by H(1) is bifurcated and that of H(5) is trifurcated, although the arrangement is similar to that in $Li(N_2H_5)SO_4$.

A fuller discussion of the comparison between the X-ray and neutron diffraction results, the hydrazinium ion and the hydrogen bonding of this and other structures will be given in Chapters IX and X.

Table 6-5. Bond distances and angles for $Li(N_2H_5)BeF_4$

LiF_4 tetrahedron

	X-ray (Å)	Neutron (Å)		X-ray (°)	Neutron (°)
Li – F(1)	1.861(8)	1.917(33)	F(1) – Li – F(2)	110.8(4)	107(2)
Li – F(2)	1.886(6)	1.897(20)	F(1) – Li – F(3)	114.8(5)	111(2)
Li – F(3)	1.842(7)	1.863(25)	F(1) – Li – F(4)	109.8(4)	111(1)
Li – F(4)	1.825(10)	1.730(46)	F(2) – Li – F(3)	99.6(3)	98(1)
			F(2) – Li – F(4)	105.5(4)	110(2)
			F(3) – Li – F(4)	115.6(4)	120(2)

BeF_4 tetrahedron

	X-ray (Å)	Neutron (Å)		X-ray (°)	Neutron (°)
Be – F(1)	1.557(9)	1.614(26)	F(1) – Be – F(2)	107.6(4)	106.9(12)
Be – F(2)	1.561(4)	1.563(7)	F(1) – Be – F(3)	110.5(4)	108.9(9)
Be – F(3)	1.532(5)	1.537(11)	F(1) – Be – F(4)	109.9(3)	109.6(9)
Be – F(4)	1.534(6)	1.508(16)	F(2) – Be – F(3)	109.0(3)	109.8(7)
			F(2) – Be – F(4)	108.6(3)	108.9(8)
			F(3) – Be – F(4)	111.1(4)	112.7(11)

Table 6-5. Bond distances and angles for Li(N₂H₅)BeF₄ (Continued)

(N₂H₅) ion

	X-ray (Å)	Neutron (Å)		X-ray (°)	Neutron (°)
N(1) – N(2)	1.431(5)	1.421(8)	N(2) – N(1) – H(1)	107(4)	108(1)
N(1) – H(1)	0.81(6)	0.97(2)	N(2) – N(1) – H(2)	110(3)	105(2)
N(1) – H(2)	0.89(5)	0.96(3)	N(2) – N(1) – H(2')	111(1)	112(1)
N(1) – H(2')	2.15(5)	2.12(3)	H(1) – N(1) – H(2)	123(6)	110(3)
			H(1) – N(1) – H(2')	92(6)	97(2)
			H(2) – N(1) – H(2')	115(4)	120(2)

	X-ray (Å)	Neutron (Å)		X-ray (°)	Neutron (°)
N(2) – H(3)	0.87(5)	0.97(2)	N(1) – N(2) – H(3)	104(3)	109(1)
N(2) – H(4)	0.91(8)	1.07(4)	N(1) – N(2) – H(4)	104(4)	109(2)
N(2) – H(5)	0.97(7)	0.95(3)	N(1) – N(2) – H(5)	114(4)	112(2)
			H(3) – N(2) – H(4)	118(6)	106(3)
			H(3) – N(2) – H(5)	105(5)	110(3)
			H(4) – N(2) – H(5)	112(6)	108(3)

Table 6-6. Hydrogen bond lengths and angles in Li(N₂H₅)BeF₄

For each bond, the X-ray result is given in the first line and the neutron result in the second.

D-H....A			D-H (Å)	H....A (Å)	D-A (Å)	<D-H....A (°)
N(1)	H(1)	F(3)	0.81(6)	2.39(7)	3.103(5)	148(6)
			0.97(2)	2.34(3)	3.122(13)	137(2)
N(1)	H(1)	F(4)	0.89(5)	2.42(6)	2.902(5)	119(6)
			0.96(3)	2.25(2)	2.892(11)	123(2)
N(1)	H(2)	N(1')	0.87(5)	2.15(5)	3.044(3)	178(5)
			0.97(2)	2.12(3)	3.052(5)	163(2)
N(2)	H(3)	F(1)	0.91(8)	1.96(5)	2.832(5)	172(6)
			1.07(4)	1.87(3)	2.794(13)	158(3)
N(2)	H(4)	F(2)		1.93(7)	2.834(8)	168(5)
				1.81(4)	2.856(26)	165(3)
N(2)	H(5)	F(4)		2.41(6)	2.855(5)	107(4)
				2.43(3)	2.842(12)	106(2)
N(2)	H(5)	F(2)	0.97(7)	2.06(8)	2.941(8)	150(6)
			0.95(3)	2.07(4)	2.939(26)	152(3)
N(2)	H(5)	F(1)		2.40(6)	3.099(5)	129(5)
				2.41(3)	3.086(12)	128(2)

Table 6-7. Dihedral angles of the (N_2H_5) ion

Plane defined by atoms			Plane defined by atoms			Dihedral angle	
						X-ray (^{o})	Neutron (^{o})
N(1)	N(2)	H(1)	N(1)	N(2)	H(2)	136	119
N(1)	N(2)	H(1)	N(1)	N(2)	H(2')	-94	-108
N(1)	N(2)	H(1)	N(1)	N(2)	H(3)	176	186
N(1)	N(2)	H(3)	N(1)	N(2)	H(4)	125	116
N(1)	N(2)	H(3)	N(1)	N(2)	H(5)	-114	-124

CHAPTER VII

THE CRYSTAL STRUCTURE OF LITHIUM HYDROXYLAMMONIUM SULPHATE

This work describes the solution and refinement of the crystal structure of lithium hydroxylammonium sulphate, $Li(NH_3OH)SO_4$, from X-ray diffraction measurements. The positions of all atoms were accurately determined and their correctness confirmed by a bond-strength summation.

Experimental

Single crystals of $Li(NH_3OH)SO_4$ were grown by slow evaporation from an aqueous solution of $(NH_3OH)_2SO_4$ and Li_2SO_4 in stoichiometric quantities. Very thin hexagonal crystals were formed, but recrystallisation improved the thickness to a size suitable for X-ray work.

The space group, Pbca (D_{2h}^{15}), was deduced from systematic absences on Weissenberg photographs. For accurate measurement of the lattice parameters and determination of the structure, a single crystal measuring $0.1 \times 0.1 \times 0.4$ mm was selected. All of these measurements were made at room temperature on a Syntex four-circle X-ray diffractometer using MoKα radiation ($\lambda = 0.71069$ Å) monochromated by reflection from a graphite crystal. The lattice parameters (Table 7-1) were refined by a least-squares

Table 7-1. Crystallographic data for Li(NH$_3$OH)SO$_4$

Crystal system	Orthorhombic
Space group	Pbca (D$_{2h}^{15}$)
$\underline{a}$(Å)	18.461(5)
$\underline{b}$(Å)	7.267(3)
$\underline{c}$(Å)	6.695(2)
Z	8
Cell volume (Å^3)	898.2(5)
D$_{calc}$ (g/cm^3)	2.027
Absorption coefficient for MoKα (mm^{-1})	0.63
Crystal size (mm)	0.1 × 0.1 × 0.4
Wavelength MoKα (Å)	0.71069
Systematic absences	0kℓ k = 2n + 1 h0ℓ ℓ = 2n + 1 hk0 h = 2n + 1

analysis of the 2θ settings of fifteen reflections (Table 7-2).

Intensities of 1574 independent reflections with sin θ/λ<0.705

were measured and corrected for Lorentz and polarisation

effects but not for absorption which was negligible

$(\mu = 0.63 \text{ mm}^{-1})$.

Solution and Refinement of the Structure

The structure was solved from a three-dimensional

Patterson synthesis. The hydrogen atom positions were found

from a three-dimensional difference electron density map.

The atomic parameters and temperature factors were refined

by the full matrix least-squares programme CRYLSQ of the

XRAY 71 programme library system. With anisotropic

temperature factors for all non-hydrogen atoms, the residual

index, R (cf. equation 2-31), was 0.034. The final weighted

residual index, R_w (cf. equation 2-32), was 0.027, where the

weights were given by:

$$w = (0.1146 - 0.0044|F_o| + 0.00004|F_o|^2)^{-1}. \quad (7-1)$$

Final atomic positions and temperature factors are given in

Table 7-3. The observed and calculated structure factors are

given in Appendix A.

Description of the Structure

Views of the structure projected along the a and c

directions are shown in Figures 7-1 and 7-2.

Table 7-2.   Reflections used in the least-squares refinement of the lattice parameters of Li(NH$_3$OH)SO$_4$

Reflection			$2\theta_{obs}$ (°)	$2\theta_{calc}$ (°)
h	k	ℓ		
-2	-1	1	9.40	9.39
-1	-2	3	21.67	21.68
-3	-1	1	10.61	10.62
-4	-1	1	12.12	12.13
2	-1	1	9.39	9.39
3	-1	1	10.62	10.61
-8	0	0	17.71	17.72
3	-1	2	14.99	14.99
-2	-1	2	14.14	14.15
-3	2	1	14.38	14.39
4	-1	1	12.13	12.12
2	1	1	9.38	9.38
1	-2	1	12.98	12.98
-4	-1	-1	12.11	12.11
-3	-2	1	14.42	14.42

Table 7-3. Parameters derived from the final least-squares refinement

Atom	Positional coordinates			Temperature factors*					
	x	y	z	U or U_{11}	U_{22}	U_{33}	U_{12}	U_{13}	U_{23}
Li	0.2612(2)	0.2535(8)	0.4122(8)	24(2)	21(2)	20(2)	-2(3)	0(2)	4(2)
S	0.1559(1)	0.0520(1)	0.1577(1)	12.7(2)	12.8(2)	13.8(2)	0.0(3)	0.3(3)	0.5(3)
O(1)	0.3348(1)	0.4390(3)	0.3394(3)	22(1)	25(1)	21(1)	-4(1)	-2(1)	11(1)
O(2)	0.3289(1)	0.0586(3)	0.4777(3)	25(1)	24(1)	18(1)	5(1)	1(1)	7(1)
O(3)	0.2076(1)	0.2075(2)	0.1649(3)	24(1)	20(1)	20(1)	-9(1)	-2(1)	2(1)
O(4)	0.0810(1)	0.1213(3)	0.1458(4)	15(1)	21(1)	29(1)	5(1)	2(1)	2(1)
O(5)	0.4468(1)	0.1444(3)	0.0716(3)	34(1)	34(1)	36(1)	-1(1)	1(1)	9(1)
N	0.4446(1)	0.0037(4)	0.2142(4)	31(1)	28(1)	28(1)	-3(1)	6(1)	-0(1)
H(1)	0.404(2)	0.017(5)	0.326(6)	11(9)					
H(2)	0.429(2)	-0.109(5)	0.146(5)	12(9)					
H(3)	0.493(2)	0.005(7)	0.263(7)	25(11)					
H(4)	0.400(3)	0.085(9)	0.001(10)	87(20)					

* Expressions used for the temperature factors are:

$$\exp\left[-2\pi^2 \times 10^{-3}\,(U_{11}h^2a^{*2} + U_{22}k^2b^{*2} + U_{33}\ell^2c^{*2} + 2U_{12}hka^*b^* + 2U_{13}h\ell a^*c^* + 2U_{23}k\ell b^*c^*)\right] \text{ and}$$

$$\exp\left[-2\pi^2 \times 10^{-3}\,U\left(\frac{2\sin\theta}{\lambda}\right)^2\right].$$

Figure 7-1.

The crystal structure of $Li(NH_3OH)SO_4$ viewed along the $\underline{a}$ direction.
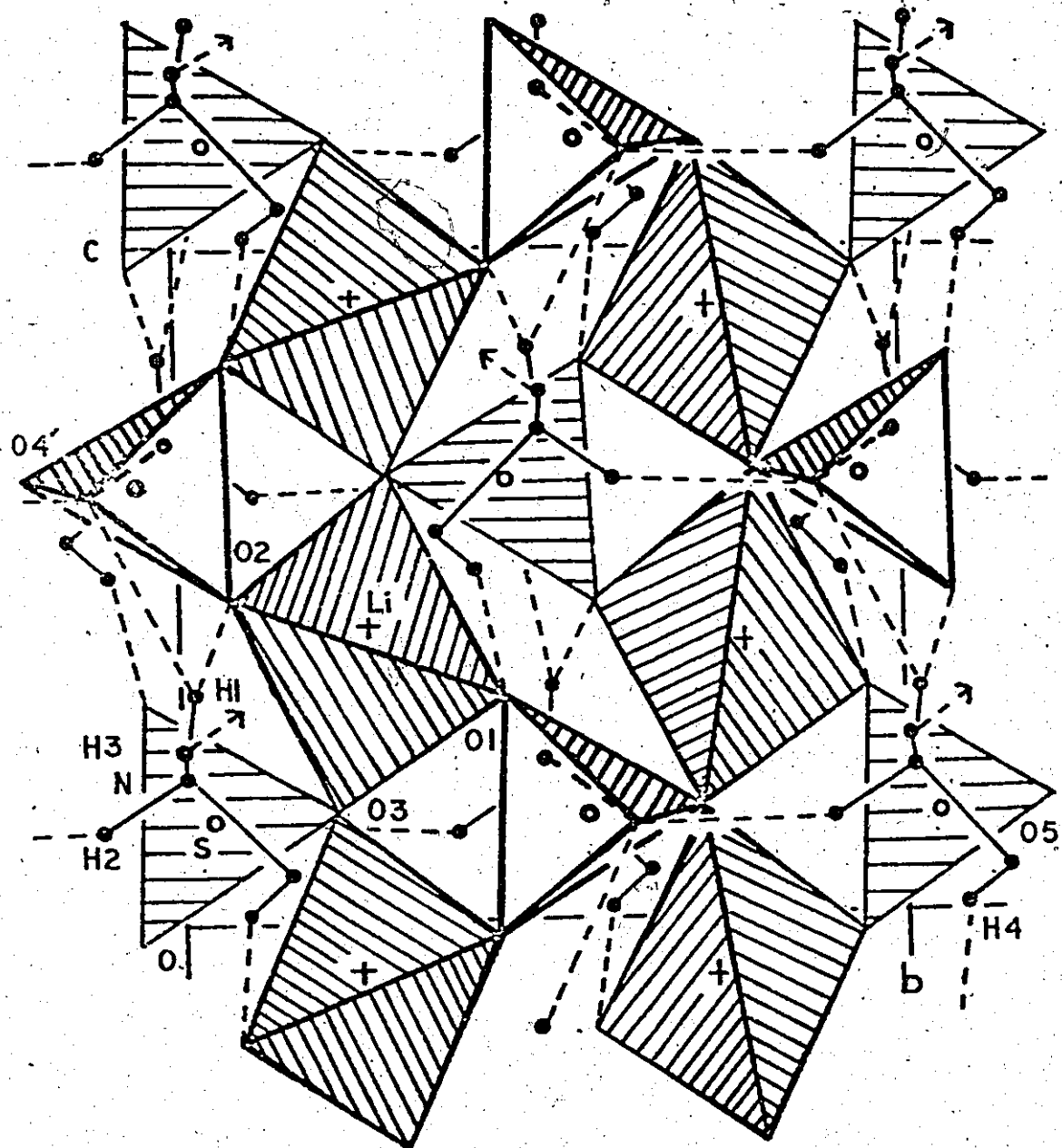
Figure 7-2.

The crystal structure of $Li(NH_3OH)SO_4$ viewed along the $\underline{c}$ direction.
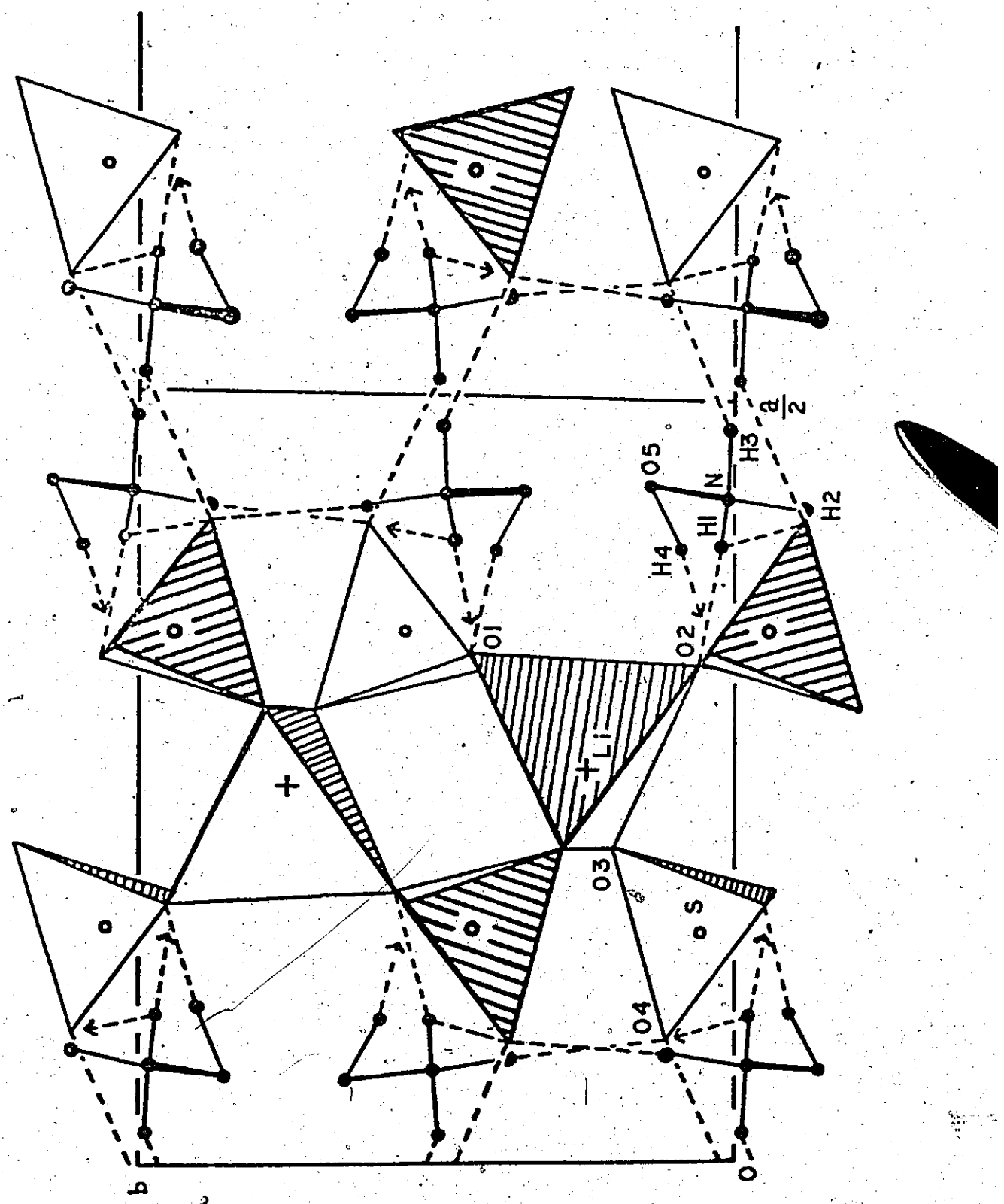
Crystals of $Li(NH_3OH)SO_4$ are composed of sheets of $LiSO_4$ which are held together by hydrogen bonds from the hydroxylammonium ions. This structure is quite different from the stuffed tetrahedral framework structures of the isoelectronic $Li(N_2H_5)SO_4$ and $Li(N_2H_5)BeF_4$ or the compounds of the form $LiMSO_4$ and $LiMBeF_4$ (M = K, Rb, Cs, NH_4) discussed by Chung and Hahn (1972).

The bond lengths and bond angles are given in Table 7-4.

The lithium and sulphur atoms are at the centres of oxygen tetrahedra which share corners to form the $LiSO_4$ sheets normal to the a direction. Effectively, there are three layers within the sheets, a layer of LiO_4 tetrahedra at $\frac{2n + 1}{4}a$ and two layers of SO_4 tetrahedra at $\frac{4n + 1}{8}a$ and $\frac{4n + 3}{8}a$ (cf. Figure 7-2). The average Li-O and S-O bond lengths are 1.963(15)Å and 1.477(2)Å respectively, compared to 1.937(17)Å and 1.473(9)Å for these bonds in $Li(N_2H_5)SO_4$.

The hydroxylammonium ions are not midway between the sheets but lie in hollows in the surface SO_4 layers (cf. Figure 7-1). The $-NH_3$ group of the (NH_3OH) ion forms a single hydrogen bond (H(2)) and a bifurcated hydrogen bond (H(1)) to oxygen atoms of the nearest sheet. The -OH group also forms a single hydrogen bond to this sheet. H(3) of the NH_3 group forms a single hydrogen bond in an oxygen atom (O(4)) of the SO_4 tetrahedron pointing out of the next sheet. Details of the hydrogen bonds are given in Table 7-5.

Table 7-4. Bond distances and angles for $Li(NH_3OH)SO_4$

SO_4 tetrahedron

	(Å)		(°)
S - O(1)	1.478(2)	O(1) - S - O(2)	110.3(1)
S - O(2)	1.476(2)	O(1) - S - O(3)	108.8(1)
S - O(3)	1.480(2)	O(1) - S - O(4)	110.1(1)
S - O(4)	1.473(2)	O(2) - S - O(3)	108.6(1)
		O(2) - S - O(4)	108.7(1)
		O(3) - S - O(4)	110.2(1)

LiO_4 tetrahedron

	(Å)		(°)
Li - O(1)	1.975(5)	O(1) - Li - O(2)	96.4(2)
Li - O(2)	1.939(6)	O(1) - Li - O(3)	104.8(3)
Li - O(3)	1.957(5)	O(1) - Li - O(3')	117.2(3)
Li - O(3')	1.981(5)	O(2) - Li - O(3)	113.1(3)
		O(2) - Li - O(3')	103.5(3)
		O(3) - Li - O(3')	119.7(2)

NH_3OH ion

	(Å)		(°)
N - O(5)	1.400(4)	O(5) - N - H(1)	116(2)
N - H(1)	1.06(3)	O(5) - N - H(2)	107(2)
N - H(2)	0.98(4)	O(5) - N - H(3)	101(3)
N - H(3)	0.96(4)	H(1) - N - H(2)	102(3)
		H(1) - N - H(3)	115(3)
O(5) - H(4)	1.08(6)	H(2) - N - H(3)	116(3)
		N - O(5) - H(4)	89(3)

Table 7-5. Hydrogen bond lengths and angles of the (NH_3OH) ion

D-H....A			D-H (Å)	H....A (Å)	D-A (Å)	<D-H....A (°)
N	H(1)	O(2)	1.06(3)	1.75(3)	2.799(3)	170(3)
N	H(1)	O(4)		2.38(4)	3.066(4)	121(2)
N	H(2)	O(4)	0.98(4)	1.97(4)	2.856(3)	149(3)
N	H(3)	O(4)	0.96(4)	1.93(4)	2.820(3)	155(4)
O(5)	H(4)	O(1)	1.08(6)	1.62(6)	2.656(3)	158(6)

The O-N distance of the ion is 1.400(4)Å and the average
N-H distance is 1.00(4)Å and O-H distance is 1.08(6)Å.
The O-H bond is staggered with respect to H(1) and H(2) of
the $-NH_3$ group, and the dihedral angles are given in Table 7-6.

The strengths of the bonds formed by the oxygen
atoms, calculated from the bond lengths using the method
of Brown and Shannon (1973), are given in Table 7-7. Each
oxygen atom of the sheet forms one strong bond (1.5 valence
units) with a sulphur atom. The equivalence of the Li-O
and H....O bonds in terms of their strengths is seen in the
way O(1) and O(2) complete threefold coordination by forming
one bond to each Li and H while O(3) forms two bonds to
Li and, O(4) accepts three rather weak hydrogen bonds. The
R.M.S. deviation of the sums of the bond-strengths from the
valence is 0.04 valence units.

Table 7-6. Dihedral angles of the (NH_3OH) ion

Plane defined by atoms	Plane defined by atoms	Dihedral angle (^{o})
O(5) – N – H(1)	O(5) – N – H(2)	-112
O(5) – N – H(1)	O(5) – N – H(3)	125
O(5) – N – H(1)	O(5) – N – H(4)	-76

Table 7-7. Bond-strengths in Li(NH$_3$OH)SO$_4$

Bond-strengths in valence units and bond lengths in Å (in brackets) for bonds between O and Li, S and H.

	Li	S	H(1)	H(2)	H(3)	H(4)	Sums around anions
O(1)	0.23 (1.975)	1.49 (1.478)				0.25* (1.62)	1.97
O(2)	0.25 (1.939)	1.50 (1.476)	0.21* (1.75)				1.96
O(3)	0.24 (1.957) 0.23 (1.981)	1.48 (1.480)					1.95
O(4)		1.51 (1.473)	0.11* (2.38)	0.17* (1.97)	0.17* (1.93)		1.96
Sums around cations	0.95	5.98					

Bond-strengths (s) are calculated from the expression $s = (R/R_0)^{-N}$ where R is the bond length and
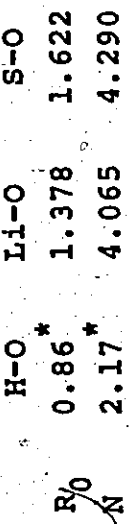
	H-O	Li-O	S-O
R_0	0.86*	1.378	1.622
N	2.17*	4.065	4.290

*The parameters for H apply to bonds determined by neutron diffraction and will tend to underestimate the bond-strength in this case.

CHAPTER VIII

THE CRYSTAL STRUCTURE OF HYDRAZONIUM FLUOROBERYLLATE

This work involves the solution and refinement of the crystal structure of hydrazonium fluoroberyllate, $(N_2H_6)BeF_4$, by X-ray diffraction methods. The compound was first reported and studied by Tédenac et al. (1971) who reported only the lattice parameters and space group. In this work we determined all the atomic positions and were able to determine the hydrogen bonding scheme.

Experimental

Crystals of hydrazonium fluoroberyllate, $(N_2H_6)BeF_4$, were prepared by the action of hydrofluoric acid on a mixture of $N_2H_4 \cdot H_2O$ and $Be(OH)_2$ in aqueous solution (Tédenac et al., 1971):

$$N_2H_4 \cdot H_2O + 4HF + Be(OH)_2 \rightarrow (N_2H_6)BeF_4 + 3H_2O . \qquad (8-1)$$
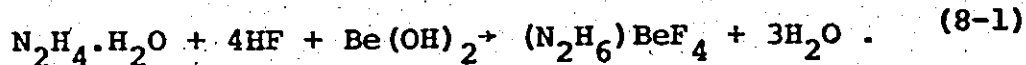
The crystals were washed with water and dried by warming under vacuum before sealing in dried quartz capillaries. This was necessary since previous attempts to make measurements on unsealed crystals were unsuccessful as they underwent severe surface decomposition. The space group, $P2_1/c$ (C_{2h}^5), was confirmed from the systematic absences observed on precession photographs. All X-ray diffraction

110

measurements were made at room temperature on the Syntex

four-circle diffractometer using MoKα radiation ($\lambda = 0.71069$Å)

monochromated by reflection from a graphite crystal. The

lattice parameters (Table 8-1) were refined by a least-squares

analysis of the 2θ measurements of fifteen reflections

(Table 8-2). The intensities of 770 independent reflections

with sin $\theta/\lambda < 0.60$ were measured and corrected for Lorentz

and polarisation effects. No absorption correction was made,

the maximum error in F introduced by its neglect being much

less than one per cent.

Solution and Refinement of the Structure

Attempts to solve the structure from a

three-dimensional Patterson synthesis failed. Sharpening

the Patterson did not reduce the overlapping of peaks

sufficiently for a solution to be found, and direct methods

had to be used.

The normalised structure factors (cf. equation 2-27)

were calculated, and all triple-products of the phase factors

were calculated (cf. equation 2-28) for the 100 reflections

with the highest E values. Three reflections ((235), (510)

and (252)) were chosen to define the origin, and the phases

of eighteen further reflections were assigned from the

triple-product relationships where probability of correctness

was $\geqslant 0.98$. These eighteen phases were then checked against

a larger group of 73 products, and no discrepancies were

Table 8-1. Crystallographic Data for $(N_2H_6)BeF_4$

Crystal system	Monoclinic
Space group	$P2_1/c$ (C_{2h}^5)
$\underline{a}$ (Å)	5.568(2)
$\underline{b}$ (Å)	7.305(2)
$\underline{c}$ (Å)	9.910(4)
β (°)	98.25(3)
Z	4
Cell volume (Å^3)	398.9(2)
D_{calc} (g/cm^3)	1.983
Absorption coefficient for MoKα (mm^{-1})	0.28
Crystal size (mm)	0.1 × 0.1 × 0.15
Wavelength MoKα (Å)	0.71069
Systematic absences	h0ℓ ℓ = 2n+1
	0k0 k = 2n+1

Table 8-2. Reflections used in the least-squares refinement
of the lattice parameters of $(N_2H_6)BeF_4$

Reflection h k ℓ	$2\theta_{obs}$ (°)	$2\theta_{calc}$ (°)
0 2 0	11.17	11.17
1 2 1	14.35	14.35
0 2 -3	16.77	16.79
-2 1 1	15.84	15.84
2 1 -1	15.83	15.83
0 0 -4	16.68	16.67
-1 3 1	18.57	18.59
-1 2 -1	14.34	14.36
-2 1 -2	18.90	18.90
-1 0 -2	11.92	11.90
-1 0 2	10.31	10.31
1 3 1	19.06	19.06
0 3 -1	17.29	17.30
2 1 2	18.89	18.89
-1 0 -4	19.21	19.21

found. This process was repeated, and 69 more phases were determined. The programmes used were NORMSF, SINGEN and PHASE of the XRAY 71 programme library system.

A three-dimensional electron density synthesis using these 90 phased reflections was made, and all non-hydrogen atoms were located. After a least-squares refinement of the positional and anisotropic thermal parameters of these atoms, using the programme CRYLSQ, all hydrogen atoms were located from difference electron density maps. In the refinement of the hydrogen atom temperature factors two of them, H(5) and H(6), refined to negative values; these were reset to typical values (0.025) and not refined further. Further refinement led to a residual index, R (cf. equation 2-31), of 0.044. There was no apparent extinction, and a final refinement gave a weighted residual index, R_w (cf. equation 2-32), of 0.043 where the weights, w, were given by:

$$w = (1.14 - 0.073|F_o| + 0.0014|F_o|^2)^{-1}. \qquad (8\text{-}2)$$

Final atomic positions and temperature factors are given in Table 8-3, and the table of observed and calculated structure factors is given in Appendix A.

Description of the Structure

Views of the structure projected down the <u>a</u> and <u>b</u> directions are given in Figures 8-1 and 8-2.

Table 8-3. Parameters derived from the final least-squares refinement

Atom	Positional coordinates			Temperature factors*					
	x	y	z	U or U_{11}	U_{22}	U_{33}	U_{12}	U_{13}	U_{23}
Be	0.7545(11)	0.2993(8)	0.0634(6)	16(3)	19(3)	18(3)	2(3)	5(2)	2(3)
F(1)	0.5276(4)	0.1835(4)	0.0835(3)	25(1)	27(2)	25(2)	-9(1)	4(1)	-1(1)
F(2)	-0.0182(5)	0.1752(4)	0.0943(3)	31(2)	23(2)	21(1)	8(1)	3(1)	2(1)
F(3)	0.7825(5)	0.4541(3)	0.1701(3)	29(1)	17(1)	29(2)	1(1)	0(1)	-3(1)
F(4)	0.7247(5)	0.1372(4)	0.4137(3)	27(1)	34(2)	23(1)	1(1)	2(1)	-7(1)
N(1)	0.3593(9)	0.3602(7)	0.2982(5)	26(2)	32(3)	29(3)	7(2)	12(2)	10(2)
N(2)	0.1510(8)	0.3097(7)	0.3566(5)	21(2)	25(2)	30(2)	3(2)	8(2)	8(2)
H(1)	0.419(11)	0.483(10)	0.330(7)	24(19)					
H(2)	0.486(11)	0.300(8)	0.324(6)	13(16)					
H(3)	0.294(11)	0.374(9)	0.206(7)	28(18)					
H(4)	0.032(11)	0.360(9)	0.315(6)	17(18)					
H(5)	0.142(11)	0.187(10)	0.350(7)	25†					
H(6)	0.179(11)	0.332(9)	0.443(7)	25†					

*Expressions used for the temperature factors are:

$$\exp\left[-2\pi^2 \times 10^{-3}\,(U_{11}h^2a^{*2} + U_{22}k^2b^{*2} + U_{33}\ell^2c^{*2} + 2U_{12}hka^*b^* + 2U_{13}h\ell a^*c^* + 2U_{23}k\ell b^*c^*)\right]\ \text{and}$$

$$\exp\left[-2\pi^2 \times 10^{-3}\,U\left(\frac{2\sin\theta}{\lambda}\right)^2\right].$$

†Not refined.

Figure 8-1.

The crystal structure of $(N_2H_6)BeF_4$ viewed along the $\underline{a}$ direction.
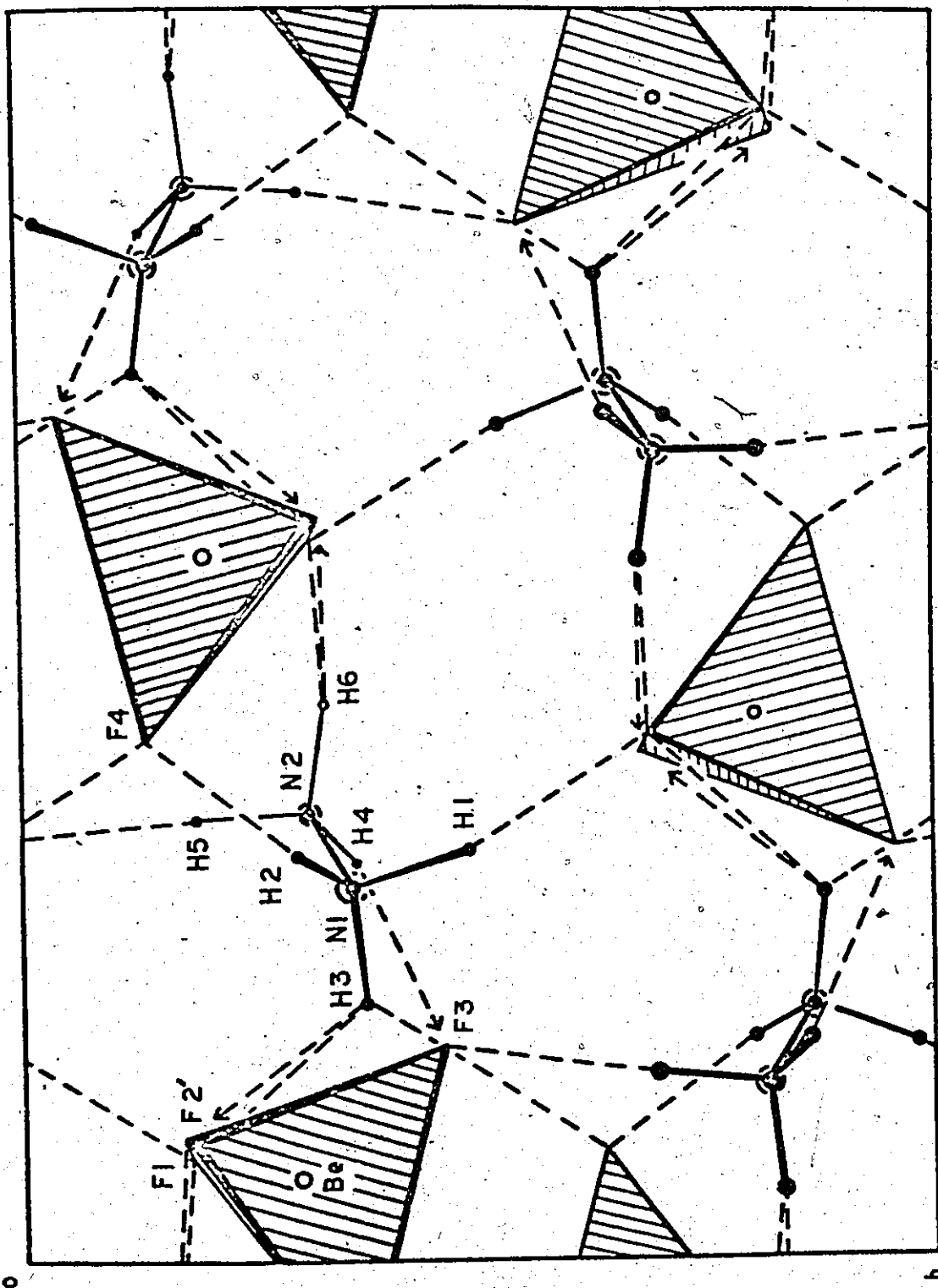
Figure 8-2.

The crystal structure of $(N_2H_6)BeF_4$ viewed along the $\underline{b}$ direction.
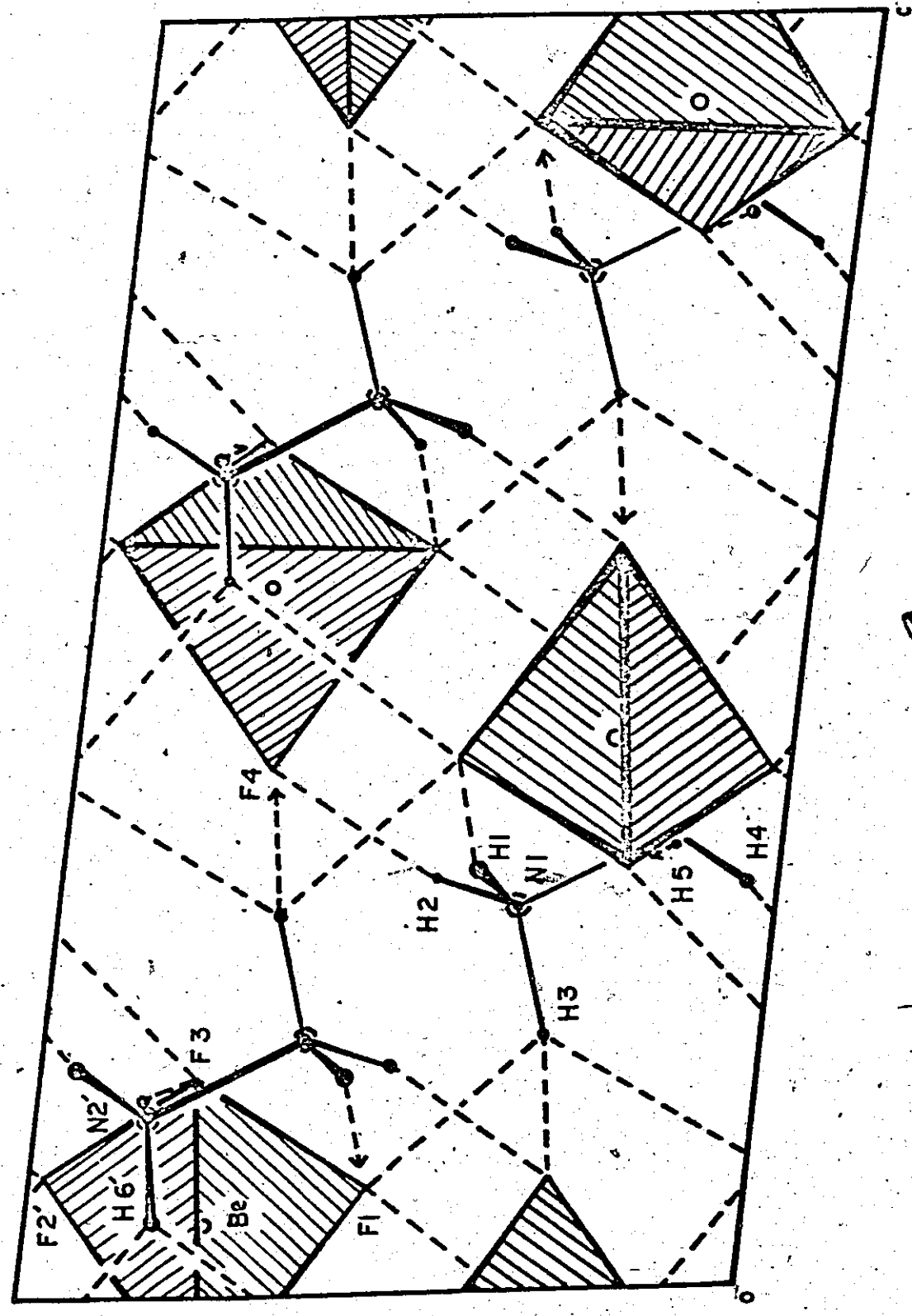
The crystal contains nearly regular BeF_4^{2-} tetrahedra and $N_2H_6^{2+}$ ions held together by a three-dimensional system of hydrogen bonds. Table 8-4 gives the bond lengths and angles, and Table 8-5 gives details of the hydrogen bonds.

The $-N(1)H_3$ group of the hydrazonium ion forms two strong single hydrogen bonds (H(1) and H(2)) and a weak trifurcated hydrogen bond (H(3)). The five fluorine atoms which are the acceptors of these bonds are all on different tetrahedra. The $-N(2)H_3$ group forms two strong single hydrogen bonds (H(4) and H(5)) and one bifurcated hydrogen bond (H(6)). These bonds are also to fluorine atoms on different tetrahedra. Thus, three fluorine atoms (F(2), F(3) and F(4)) are involved in two hydrogen bonds and one bond to Be (Average Be-F = 1.544(5)Å) and one (F(1)) in three hydrogen bonds and a rather longer bond to Be (Be-F(1) = 1.557(8)Å). The overall average Be-F bond length is 1.547(7)Å compared to 1.546(13)Å for the Be-F bonds in $Li(N_2H_5)BeF_4$.

The $N_2H_6^{2+}$ ion has a staggered configuration; the dihedral angles are give in Table 8-6. The N-N distance is 1.417(16)Å, and the average N-H distance is 0.89(6)Å.

Table 8-4. Bond distances and angles for $(N_2H_6)BeF_4$

BeF_4 tetrahedron

	(Å)			(°)
Be – F(1)	1.557(8)	F(1) – Be – F(2)		108.1(4)
Be – F(2)	1.552(10)	F(1) – Be – F(3)		108.4(4)
Be – F(3)	1.540(7)	F(1) – Be – F(4)		108.0(4)
Be – F(4)	1.540(8)	F(2) – Be – F(3)		107.1(4)
		F(2) – Be – F(4)		109.8(4)
		F(3) – Be – F(4)		115.3(4)

N_2H_6 ion

	(Å)		(°)
N(1) – N(2)	1.417(16)	N(2) – N(1) – H(1)	111(4)
N(1) – H(1)	1.00(7)	N(2) – N(1) – H(2)	116(4)
N(1) – H(2)	0.84(6)	N(2) – N(1) – H(3)	102(4)
N(1) – H(3)	0.94(7)	H(1) – N(1) – H(2)	98(5)
		H(1) – N(1) – H(3)	106(5)
		H(2) – N(1) – H(3)	123(6)
N(2) – H(4)	0.81(6)	N(1) – N(2) – H(4)	109(5)
N(2) – H(5)	0.90(7)	N(1) – N(2) – H(5)	106(4)
N(2) – H(6)	0.86(7)	N(1) – N(2) – H(6)	108(4)
		H(4) – N(2) – H(5)	112(6)
		H(4) – N(2) – H(6)	116(5)
		H(5) – N(2) – H(6)	105(6)

Table 8-5. Hydrogen bond lengths and angles of the (N_2H_6) ion

D-H....A			D-H (Å)	H...A (Å)	D-A (Å)	<D-H...A (°)
N(1)	H(1)	F(1)	1.00(7)	1.70(7)	2.67(1)	165(6)
N(1)	H(2)	F(4)	0.84(6)	1.91(6)	2.73(3)	165(6)
N(1)	H(3)	F(1)		2.35(7)	2.77(2)	106(5)
N(1)	H(3)	F(2)	0.94(7)	2.41(7)	3.02(4)	122(5)
N(1)	H(3)	F(4)		2.25(7)	2.91(1)	126(5)
N(2)	H(4)	F(3)	0.81(6)	1.97(7)	2.77(4)	164(6)
N(2)	H(5)	F(3)	0.90(7)	1.77(7)	2.64(1)	163(6)
N(2)	H(6)	F(1)		2.23(7)	2.85(5)	129(6)
N(2)	H(6)	F(2)	0.86(7)	1.98(8)	2.66(3)	135(6)

Table 8-6.   Dihedral angles of the (N_2H_6) ion

Plane defined by atoms			Plane defined by atoms			Dihedral angle (^{0})
N(1)	N(2)	H(1)	N(1)	N(2)	H(2)	-112
N(1)	N(2)	H(1)	N(1)	N(2)	H(3)	113
N(1)	N(2)	H(1)	N(1)	N(2)	H(5)	201
N(1)	N(2)	H(4)	N(1)	N(2)	H(5)	121
N(1)	N(2)	H(4)	N(1)	N(2)	H(6)	-127

CHAPTER IX

ON THE CRYSTAL STRUCTURES OF $Li(N_2H_5)SO_4$ AND $Li(N_2H_5)BeF_4$

$Li(N_2H_5)SO_4$ and $Li(N_2H_5)BeF_4$ are isostructural, both having the space group $Pna2_1$. This is a distortion of the six-membered ring tridymite-derivative structure which has the ideal space group $Icmm$ (cf. Figure 1-1). The configuration of the six-membered rings can easily be seen in Figures 5-1 and 6-1. To obtain a measure of the distortion of the ring, it is necessary to compare the angle subtended at the anion by the lithium and beryllium or sulphur atoms with the similar compounds of $LiCsBeF_4$, $Li(NH_4)BeF_4$, $Li(NH_4)SO_4$ and those expected in the ideal space group (Table 9-1). The bridging angles at $X(1)$, $X(3)$ and $X(4)$ $(X = O$ or $F)$ are those within the ring and are all in the ranges $125-133^\circ$, $140-153^\circ$ and $125-133^\circ$ compared with the respective ideal values of 140°, 180° and 140°. The bridging angles at $X(2)$, which is the bridging anion between the planes of rings, are very low in the hydrazinium compounds at $152.0(3)^\circ$ and $146.4(1)^\circ$ for $Li(N_2H_5)BeF_4$ and $Li(N_2H_5)SO_4$ respectively. The other compounds are in the range $173-179^\circ$, close to the ideal value of 180°.

The replacement of the hydrazinium ion with the hydroxylammonium ion in the sulphate produces a radically

Table 9-1. Bond angle distortions from the ideal values in the space group Icmm

T1 = Li, T2 = Be or S, X = F or O and, M = Cs, NH$_4$ or N$_2$H$_5$ in T1(M)T2X$_4$.

Angle between atoms		Icmm (°)	Li(N$_2$H$_5$)BeF$_4$ (°)	Li(N$_2$H$_5$)SO$_4$ (°)	LiCsBeF$_4$ (°)	LiNH$_4$BeF$_4$ (°)	LiNH$_4$SO$_4$ (°)
T1	X(1)	T2	140	129.7(3)	131.8(2)	133(1)	125(1)	129(1)
T1	X(2)	T2	180	152.0(3)	146.4(1)	179(1)	177(1)	173(2)
T1	X(3)	T2	180	140.6(5)	144.3(2)	153(1)	140(1)	142(1)
T1	X(4)	T2	140	132.4(4)	134.1(1)	130(1)	126(1)	129(1)

different structure (cf. Chapter VII). This raises the question that if the distortion is a result of the cation size, why should the structure of $Li(NH_3OH)SO_4$ not be of the tridymite-derivative form as at first sight the NH_3OH^+ ion would appear smaller than the $N_2H_5^+$ ion? A possible explanation of this is that by hydrogen bonding the effective radius of the ion is reduced as two atoms which are hydrogen bonded can approach each other more closely than the sum of their ionic radii. The hydrazinium ions are hydrogen bonded into chains which run between the planes of six-membered rings. Each hydrazinium ion takes part in six hydrogen bonds, five as a donor and one as an acceptor. This sixfold coordination of the hydrazinium ion by its hydrogen bonds reduces its effective size considerably. If we compare this with the hydroxylammonium ions we see that although the $-NH_3^+$ groups will be equivalent, the four coordinated $-NH_2$ groups of the hydrazinium ion chain are likely to be smaller than the two coordinated hydroxyl groups, even though the ionic radius of nitrogen (1.71 Å) is greater than that of oxygen (1.32 Å).

Table 9-2 shows the space groups, unit cell volume and cation radius for the whole series of compounds. There appears to be an anomaly in the case of the NH_4^+ compounds whose ionic radius would place them with the tridymite-like ($P6_3$) compounds. This is probably caused by an underestimation of the ionic radius when the ion is highly coordinated and loosely bound; the coordination number of the ion is nine in $Li(NH_4)BeF_4$ and

Table 9-2. Space groups, cell volumes and cation ionic radii of stuffed tetrahedral framework compounds and $Li(NH_3OH)SO_4$

Compound	Space group	Cell volume ($Å^3$)	Cation ionic radius (Å)	Ideal space group
$LiKBeF_4$	$P6_3$	372.3	1.33	
$LiKSO_4$	$P6_3$	395.5	1.33	$P6_3/mmc$
$LiRbBeF_4$	$P6_3$	407.4	1.47	
$LiRbSO_4$	$P2_1/n$	420.3	1.47	
$Li(NH_4)BeF_4$	$Pc2_1n$	411.5	1.43	
$Li(NH_4)SO_4$	$Pc2_1n$	423.1	1.43	
$LiCsBeF_4$	$P2_1/n$	436.5	1.67	Icmm
$LiCsSO_4$	$Pc2_1n$	453.5	1.67	
$Li(N_2H_5)BeF_4$	$Pna2_1$	447.7		
$Li(N_2H_5)SO_4$	$Pna2_1$	461.6		
$Li(NH_3OH)SO_4$	Pbca	2×449.1		

eight in $Li(NH_4)SO_4$ with mean N-F and N-O bond lengths of 3.05 Å and 3.12 Å respectively.

Comparison of X-ray and Neutron Diffraction Results

Before making any comparisons among our results, it is very important to re-examine the differences between X-ray and neutron diffraction and what differences we would expect between crystal structures determined by both methods.

First of all, let us state briefly what we do in a crystal structure determination. We measure a set of structure factors $\{|F|\}$, F being the Fourier transform of the scattering density contained by a unit cell (cf. equation (2-8)). Then we try to obtain agreement between our measured set and a calculated set, which represents the expected set of values $\{F\}$ for a model which is the sum of the contributions for each atom in the cell (cf. equation (2-11)).

It can be seen from equation (2-11) that the model is described in terms of: $f_i(\underline{G})$, the Fourier transform of the scattering density of the atom at rest; $T_i(\underline{G})$, the Fourier transform of the probability density function of the centroid of the scattering density around its mean position; and $\underline{r}_i$, the set of coordinates describing the mean atomic positions.

The fundamental difference between X-ray and neutron diffraction is that in the former it is the atomic electrons which are the scatterers while for the latter the nuclei are the scatterers. Thus in the X-ray case, $f_i(\underline{G})$ (cf. equation

(2-14)) is a spherically symmetric function based on the free atom electron wave function; while in the neutron case, $f_i(\underline{G})$ is the Fourier transform of the nuclear scattering density which is taken to be a point scatterer in real space; hence, its Fourier transform in reciprocal space is a constant, b_i. The temperature factor in both cases is either spherically symmetric (isotropic) as in equation (2-10) or, more generally, the centro-symmetric ellipsoidal (anisotropic) probability distribution function given by:

$$T_i(\underline{G}) = \exp\left[-2\pi^2(U_{11}h^2a^{*2}+U_{22}k^2b^{*2}+U_{33}\ell^2c^{*2}\right.$$
$$\left.+2U_{12}hka^*b^*+2U_{13}h\ell a^*c^*+2U_{23}k\ell b^*c^*)\right]$$

$$(9-1)$$

where U_{ij} are the components of the symmetric thermal tensor of the ith atom.

It is relevant to ask how well the above representations of the scattering density and temperature factors agree with reality. The spherically symmetric form of the electron scattering density makes no allowance for distortion of the outer valence electrons by bonding effects. This distortion of the electron density into the bonding region will be about 0.5 electrons/$\AA^3$ compared to a total density of greater than 10^2 electrons/$\AA^3$ for first row atoms undergoing thermal motion or 10^3 electrons/$\AA^3$ for these atoms at rest (Lipscomb, 1972). Clearly, one would only expect to see any sizeable effect of

the bonding electron density on the mean atomic position in the case of hydrogen. In this case, the centroid of the electron density is displaced by 0.1-0.2 Å into the bond as determined from the nuclear positions. With the heavier atoms the effect of bonding electrons on their positional parameters is negligible, although it may show up as a distortion to the true thermal motion of the atoms.

To observe this latter effect, a difference synthesis is computed where $\{F_c\}$ are calculated using neutron positional and thermal parameters with X-ray form factors, and $\{F_o\}$ are the observed X-ray diffraction structure factors. Coppens (1970) has pointed out that this is of use mainly in centro-symmetric structures where there are no changes in phase factors (± 1) between F_X and F_N, but must be used with caution in a non-centro-symmetric structure where a difference in phase angles between F_X and F_N may exist.

Not only bonding effects but other inadequacies of the free atom form factor will be reflected in the X-ray temperature factors. Typically, one finds that the X-ray diffraction temperature factors will be systematically larger than those determined by neutron diffraction.

We have discussed what the effect will be of inadequacies of the X-ray form factors on the positional parameters and temperature factors where the temperature factors themselves are a harmonic approximation to the true motions of the atoms. This approximation is very good,

although corrections are sometimes applied to bond lengths to account for anharmonic thermal motion, and several workers (Dawson, 1970; Willis, 1970; Johnson, 1970) have described the use of anharmonic temperature factors in structure analysis. In this work we have not considered any anharmonic effects.

A Comparison of the Crystal Structure of $Li(N_2H_5)SO_4$ as Determined by X-ray Diffraction with that of $Li(N_2D_5)SO_4$ as Determined by Neutron Diffraction (Ross, 1970)

The crystal structure of $Li(N_2H_5)SO_4$ was described in Chapter IV, and the X-ray and neutron diffraction experimental results are given in Chapter V.

As expected, there are no significant shifts in the atomic positions of the heavy atoms. The SO_4 tetrahedron is regular with a mean S-O bond distance of 1.473(9) $\overset{o}{A}$ and mean tetrahedral angle of 109.5(5)^o. There is a slight distortion of the LiO_4 tetrahedron which has a mean Li-O bond distance of 1.937(17) $\overset{o}{A}$, the bonds to O(2) being significantly larger than the mean and that to O(4) being shorter (cf. Table 5-4). The bond lengths and angular distortions are similar in both works with a mean tetrahedral angle of 109(5)^o and the greatest angular distortion being that of O(2)-Li-O(3) at 97.8(2)^o. The N-N bond length in the hydrazinium ion is 1.427(3) $\overset{o}{A}$ which is typical for this ion.

There is a significant shift in the atomic positions

of the hydrogen atoms; as expected, the effect of bonding electrons has reduced the X-ray N-H bond distance by 0.15 Å compared to the neutron bond distance; these bond distances are 0.87(4) Å and 1.022(4) Å respectively. This can be clearly seen in Figure 9-1 which is a plane of an X-N difference map containing both nitrogen atoms. H(1) is just above the plane, and H(3) below; other atoms are shown in projection. There is a pronounced shift in the electron density into the bonding regions and into the lone pair position at N(1).

The heavy atom temperature factors are systematically larger in the X-ray work, an expected result caused by inadequacy of the free atom form factor. This can be seen (Table 9-3) in the comparison of the R.M.S. displacements on the principal axes of the thermal ellipsoids. Figure 9-2 is the plane of the X-N difference map containing the lithium and sulphur atoms; O(2) is just beneath the plane; as before, the other atoms are shown in projection. Both the lithium and sulphur atoms are at the centre of highly negative regions surrounded by a positive ripple. What is remarkable is that the positive ripple is greatest in the regions of the Li-O and S-O bonds. The oxygen atoms also have a positive ripple, but it is not as large or as well defined as that around lithium and sulphur.

Figure 9-1.

The plane containing the nitrogen atoms of an X-N difference synthesis for $Li(N_2H_5)SO_4$. The interval between contours is .043 electrons/$\overset{o}{A}^3$.

Positive contours indicated as ————————

Negative contours indicated as ------------

Zero contour indicated as —— —— ——
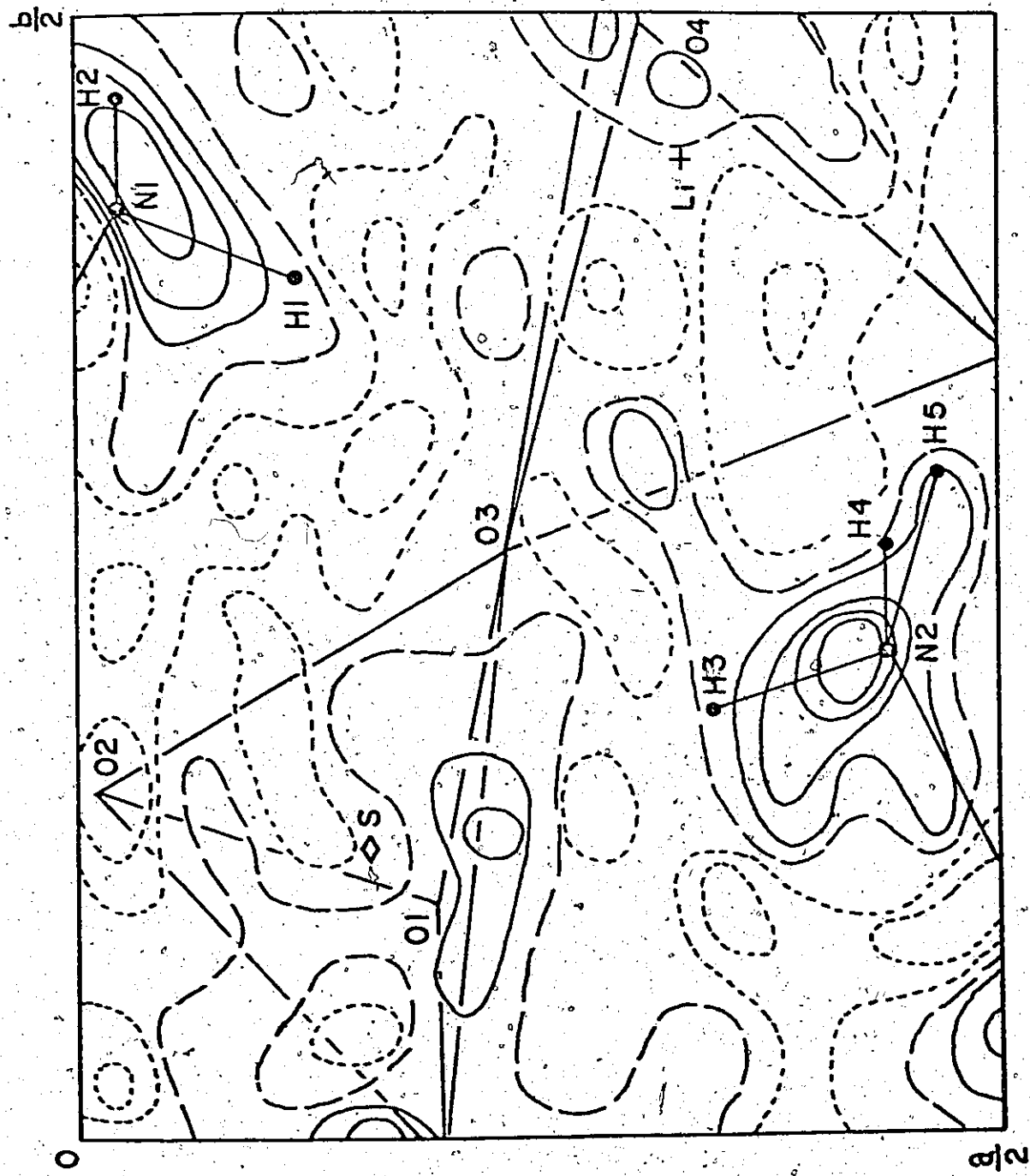
Table 9-3. A comparison between the X-ray and neutron

root-mean-square displacements along the

principal axes of the thermal ellipsoids in $Li(N_2H_5)SO_4$

The X-ray results are given in the first line and
the neutron results in the second.

Atom	R.M.S.d. axis(1) ($\overset{\circ}{A}$)	R.M.S.d. axis(2) ($\overset{\circ}{A}$)	R.M.S.d. axis(3) ($\overset{\circ}{A}$)
S	.098	.116	.109
	.062	.105	.093
Li	.127	.146	.142
	.132	.111	.061
N(1)	.142	.200	.183
	.144	.188	.172
N(2)	.141	.157	.151
	.127	.149	.154
O(1)	.104	.173	.151
	.085	.170	.141
O(2)	.107	.191	.153
	.100	.145	.171
O(3)	.104	.174	.159
	.099	.171	.142
O(4)	.196	.152	.108
	.190	.145	.104

Figure 9-2.

The plane containing the lithium and sulphur atoms of an

X-N difference synthesis for $Li(N_2H_5)SO_4$.   The interval

between contours is .043 electrons/$Å^3$.

Positive contours indicated as ———————

Negative contours indicated as ————————

Zero contour indicated as —— —— ——
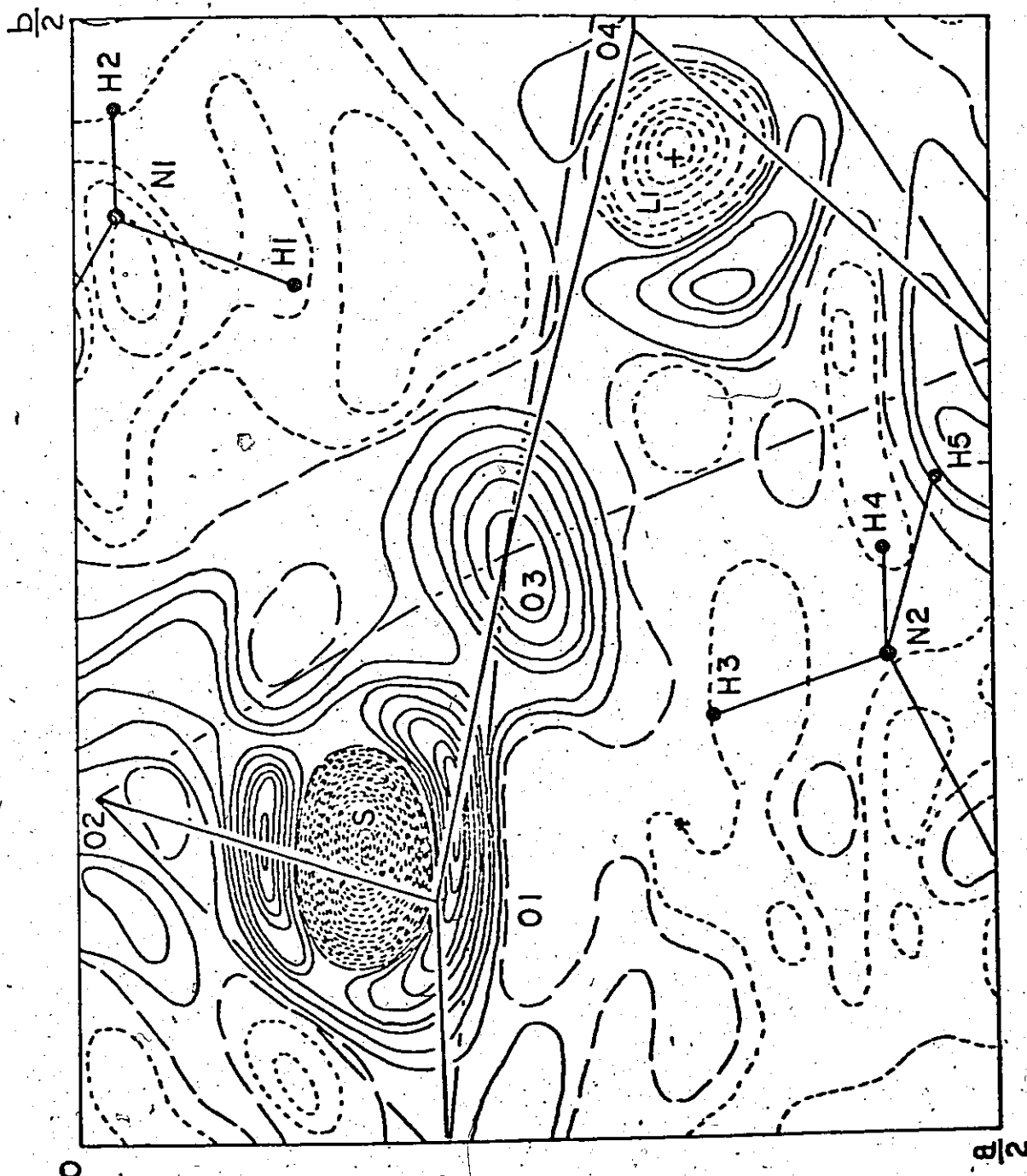
A Comparison of the Crystal Structures of $Li(N_2H_5)BeF_4$

Determined by X-ray and Neutron Diffraction

As with the isostructural sulphate, there are no significant shifts in the heavy atom positions. The BeF_4 tetrahedron was regular: mean Be-F distance 1.546(13) Å and mean tetrahedral angle 110(1)°. The LiF_4 tetrahedron showed a similar distortion to that in the LiO_4 tetrahedron, F(2) and F(4) being significantly longer and shorter respectively than the mean Li-F distance of 1.854(20) Å, and the F(2)-Li-F(3) angle being low at 99.6(3)° compared to a mean of 109(5)° (cf. Table 6-5). The N-N distance was 1.431(5) Å.

The systematic shortening of the N-H bonds by 0.11 Å occurred between the X-ray and neutron mean N-H bond lengths, these being 0.89(4) and 0.98(3) respectively; this again is typical of the 0.1-0.2 Å contraction found by other workers (Hamilton & Ibers, 1968). Figure 9-3 shows that the X-N difference map in the plane of the nitrogen atoms and H(1) has similar features to that of the sulphate. Figure 9-4 shows the corresponding map for a plane containing the lithium and beryllium atoms. Both atoms are in positive regions which are not sharply defined; this is probably caused by anomalously high temperature factors in the neutron diffraction work. There is no systematic difference between the X-ray and neutron temperature factors (Table 9-4); those in the neutron diffraction are thought to be affected by

Figure 9-3.

The plane containing the nitrogen atoms of an X-N difference synthesis for $Li(N_2H_5)BeF_4$. The interval between contours is .045 electrons/$Å^3$.

Positive contours indicated as ————————

Negative contours indicated as ––––––––––––

Zero contour indicated as —— —— ——
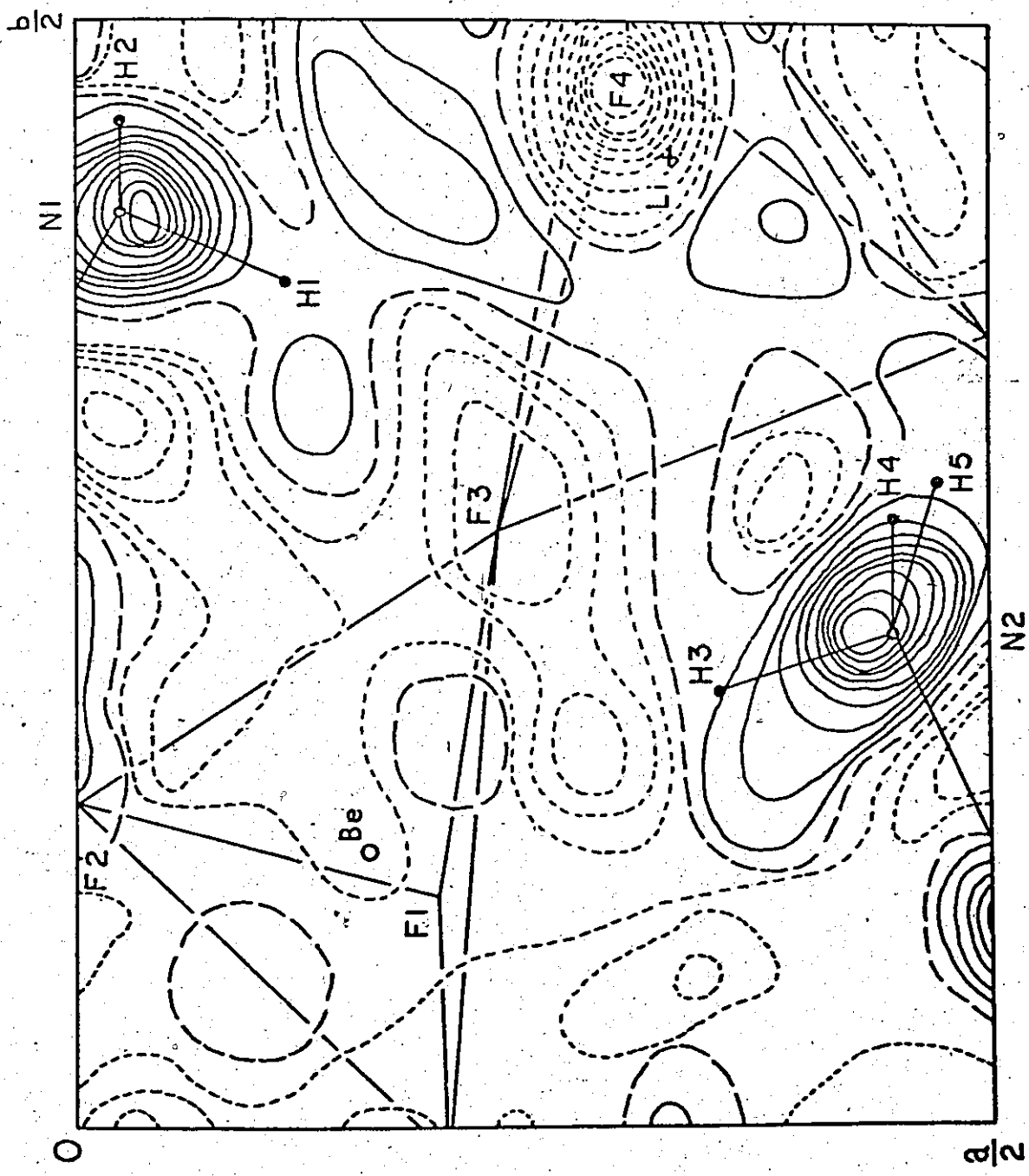
Figure 9-4.

The plane containing the lithium and beryllium atoms of

an X-N difference synthesis for $Li(N_2H_5)BeF_4$. The

interval between contours is .045 electrons/$\overset{o}{A}^3$.

Positive contours indicated as ————————

Negative contours indicated as ----------

Zero contour indicated as —— —— ——
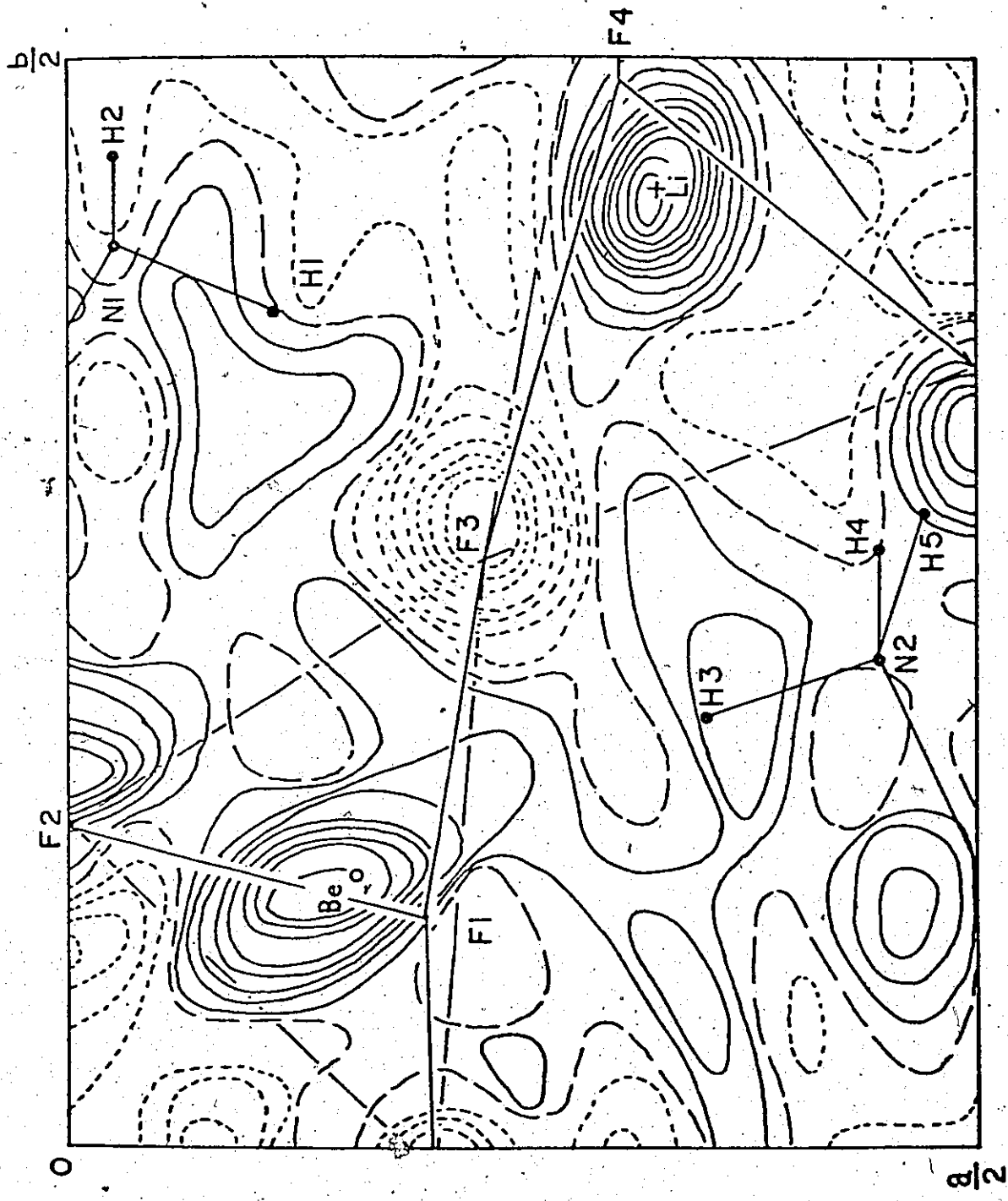
Table 9-4. A comparison between the X-ray and neutron

root-mean-square displacements along the

principal axes of the thermal ellipsoids in $Li(N_2H_5)BeF_4$

The X-ray results are given in the first line and
the neutron results in the second.

Atom	R.M.S.d. axis(1) ($\overset{\circ}{A}$)	R.M.S.d. axis(2) ($\overset{\circ}{A}$)	R.M.S.d. axis(3) ($\overset{\circ}{A}$)
Be	.142 .193	.133 .133	.113 .120
Li	.159 (.181)	.147	.128
N(1)	.198 .247	.184 .202	.147 .160
N(2)	.178 .224	.161 .175	.148 .157
F(1)	.192 .235	.157 .169	.129 .143
F(2)	.210 .225	.169 .155	.125 .113
F(3)	.194 .196	.163 .172	.124 .136
F(4)	.204 .249	.162 .185	.125 .124

absorption and anisotropic extinction caused by the large
incoherent scattering of the hydrogen atoms.

CHAPTER X

ON THE CONFIGURATION AND HYDROGEN BONDING OF

$$N_2H_6^{2+}, \quad N_2H_5^+ \text{ AND } NH_3OH^+ \text{ IONS}$$
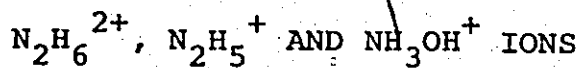
Very few of the published X-ray structures of

hydrazinium and hydrazonium compounds have reported accurate

hydrogen positions, and only the compounds $(N_2H_5)HC_2O_4$

(Nilsson, Liminga & Olovsson, 1968), $(N_2H_6)SO_4$ (Jönsson &

Hamilton, 1970) and $Li(N_2H_5)SO_4$ have been investigated by

neutron diffraction. Location of the hydrogen atoms is

essential if the hydrogen bonding is to be described

accurately, especially if weak hydrogen bonds are present.

This is the situation in the compounds we have studied

where the ions tend to form single, bifurcated and trifurcated

hydrogen bonds to the abundance of surrounding acceptor ions.

Let us first consider the nature of a hydrogen bond.

The Characterisation of a Hydrogen Bond

Pauling (1960) states that as hydrogen has only one

stable orbital (1s), it can hence form only one covalent

bond. If, however, hydrogen is coordinated in a bonding

situation with more than one atom, then the atom to which it

is covalently bonded is called the donor atom of a hydrogen

bond and the other atoms are called acceptors of the hydrogen

bond. The hydrogen atom forms the strong covalent bond with electronegative atoms; this causes the hydrogen to be acidic, and it forms bonds which are ionic in character to other electronegative atoms. The bond can be described schematically by: $D^- - H^+ \ldots A^-$. This is the type of hydrogen bond that we shall be discussing although there is one other main group of hydrogen bonds, symmetric hydrogen bonds, and two small groups, bridge bonds (boron hydrides) and metal-metal hydrogen bonds. The first row elements, fluorine, oxygen, nitrogen, make good donor atoms, also carbon when the group C-H is positive. Other possible donor elements are chlorine, sulphur and phosphorous. The acceptor must also be electronegative or especially have lone pair electrons, and typical good acceptors are fluorine, oxygen and nitrogen, and even better are F^-, Cl^-, Br^- and I^-. Sulphur and phosphorous can act as acceptors, but no case of carbon as an acceptor has been reported.

Above, we have set out the chemical characteristics of a hydrogen bond, but an operational definition is more useful to a crystallographer; that is, a strong hydrogen bond is said to exist when the interatomic distance of the donor and acceptor atoms is less than the sum of their van der Waals' radii. Hamilton & Ibers (1968) have pointed out that for weak hydrogen bonds, a better criterion is that the hydrogen-acceptor atom inter-nuclear distance should be less than the sum of their van der Waals' radii. Furthermore,

Baur (1972) states that even where no hydrogen-bonding

contact is made, the hydrogen atom will tend to be positioned

as close as possible to potential hydrogen bond acceptors, and

that the hydrogen bond must be viewed in its complete

environment: $(M)_n - D - H....A - (X)_m$ where the $M - D$ and

the $A - X$ bond lengths will be influenced by the hydrogen

bonding. This is exactly how the empirical bond-strength

method of Brown & Shannon (1973) detects the effects of

hydrogen bonds. In this work, we have assigned hydrogen

bonds using the definitions of Hamilton & Ibers and have

checked these by bond-strength summation.

Of course, when a bond exists there must be an

energy associated with it; Hydrogen bonds have formation

energies of 2-10 Kcal/mole; thus, spectroscopy could be

used to detect hydrogen bonding. The stretching mode

frequency of an unbonded O-H group is typically $> 3600 \text{ cm}^{-1}$

with a width of 10 cm^{-1}; and on formation of a hydrogen

bond, the antisymmetric stretch frequency lowers to

3600-1700 cm^{-1}, the frequency being related to the length

of the bond, and its width increases to about 100 cm^{-1}. The

bending mode frequency increases on formation of the bond.

In the compounds we have investigated, it would be very

difficult to resolve individual components of the spectra or

to assign any one component to a particular bond.

Neutron diffraction is the best method of determining

the position of the hydrogen atoms in a structure and, hence,

for studying the geometrical aspects of the hydrogen bonds. The electron density of the hydrogen atom in a structure is about 0.5 electrons/$Å^3$, and so X-ray diffraction is useful only when the compound is composed of reasonably light atoms. This certainly applies to the compounds we have studied, where sulphur was the heaviest atom, and no difficulty was found in locating the hydrogen atom.

The Configuration of the $N_2H_6^{2+}$, $N_2H_5^+$ and NH_3OH^+ Ions

In those hydrazinium and hydrazonium compounds where the hydrogen atoms have been located, the ions have a staggered configuration. Lundgren, Liminga & Olovsson (1968) have calculated the sum of the electrostatic energy and the van der Waals' energy for the rotation of the $-NH_3^+$ group about the N-N axis in $Li(N_2H_5)SO_4$. This shows that although there is a broad minima at the staggered position, the barrier against rotation into the eclipsed position is only 6 Kcal/mole. If such a small barrier is typical, then it is somewhat surprising that all the $N_2H_5^+$ and $N_2H_6^{2+}$ ions have a staggered configuration. The hydrogen atom of the hydroxyl group in the NH_3OH^+ ion is also staggered with respect to the $-NH_3$ group. Figure 10-1 shows Newman projections of these ions; also shown in the diagram are the mean values of the tetrahedral angles of the $-NH_3^+$ groups and that of the $-NH_2$ group and the symmetry related H(2') of the hydrogen bonded chain. It is apparent that not only is the staggered

Figure 10-1.

Newman projections of the $N_2H_5^+$, NH_3OH^+ and $N_2H_6^{2+}$ ions.
The projections are viewed down the N(1)-N(2) or N-O
direction. The mean values of the tetrahedral angle at
N(1) or N are given by X and that at N(2) by Y.

a) The $N_2H_5^+$ ion in Li$(N_2H_5)SO_4$ from the X-ray work.

b) The $N_2D_5^+$ ion in Li$(N_2D_5)SO_4$ from the neutron work.

c) The $N_2H_5^+$ ion in Li$(N_2H_5)BeF_4$ from the X-ray work.

d) The $N_2H_5^+$ ion in Li$(N_2H_5)BeF_4$ from the neutron work.

e) The NH_3OH^+ ion in Li$(NH_3OH)SO_4$.

f) The $N_2H_6^{2+}$ ion in $(N_2H_6)BeF_4$.

143

a.

Li(N₂H₅)SO₄   X-RAY

H1
H4
H3
H2
H5
128°
121°
114°
138°
59°
108°
111°

X 109(7)°   Y 110(8)°

b.   NEUTRON

D4
D1
D3
D2
D5
121°
120°
114°
132°
53°
114°
119°
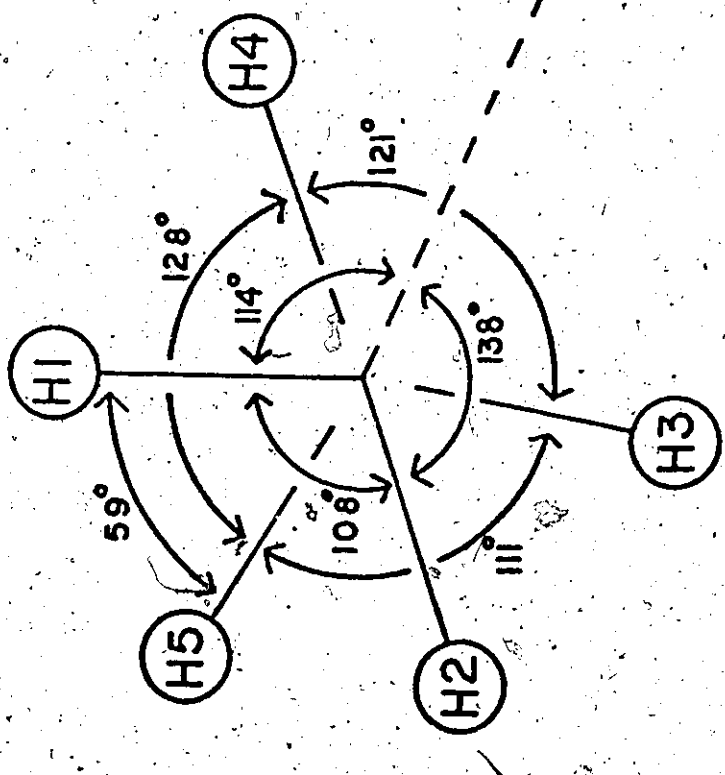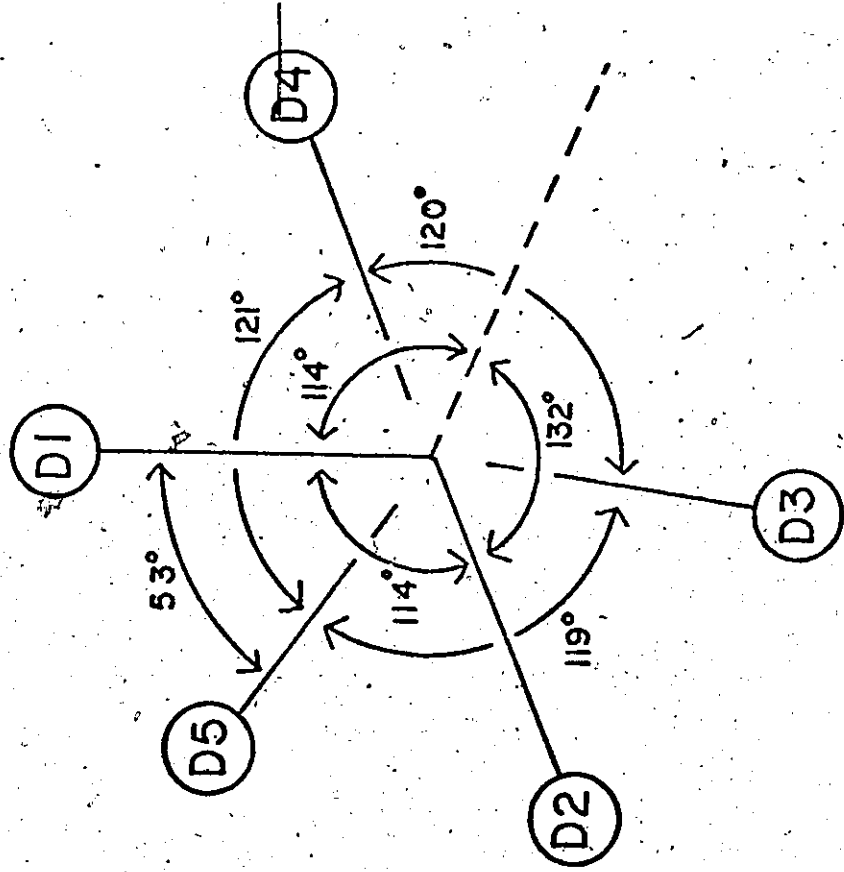
X 110(5)°   Y 110(2)°

C. Li(N₂H₅)BeF₄   X-RAY

NEUTRON

144

e.

Li(NH$_3$OH)SO$_4$

X' 110(6)°

f.

(N$_2$H$_6$)BeF$_4$

X 109(7)   Y 109(3)

145
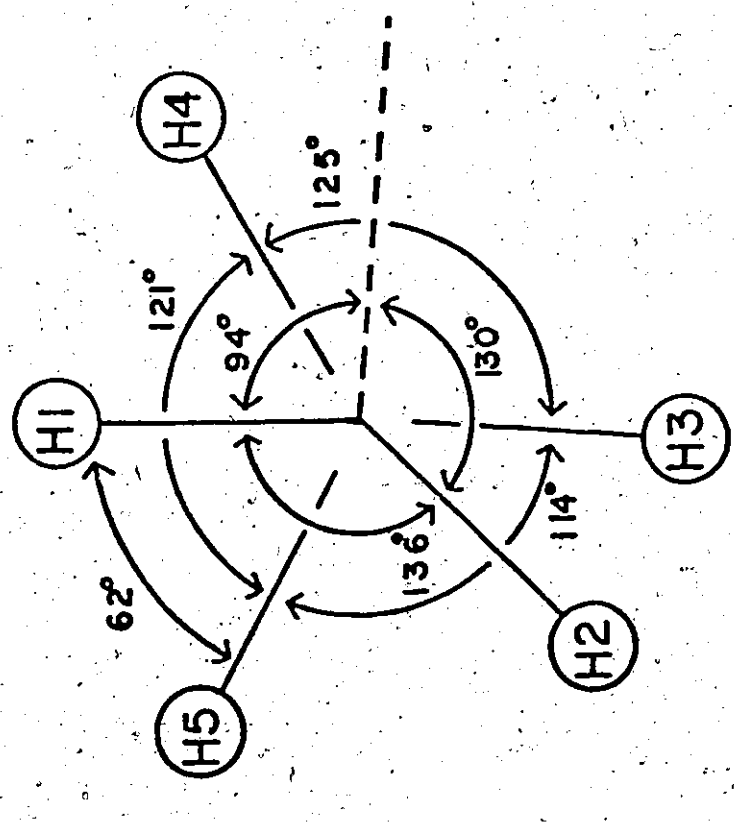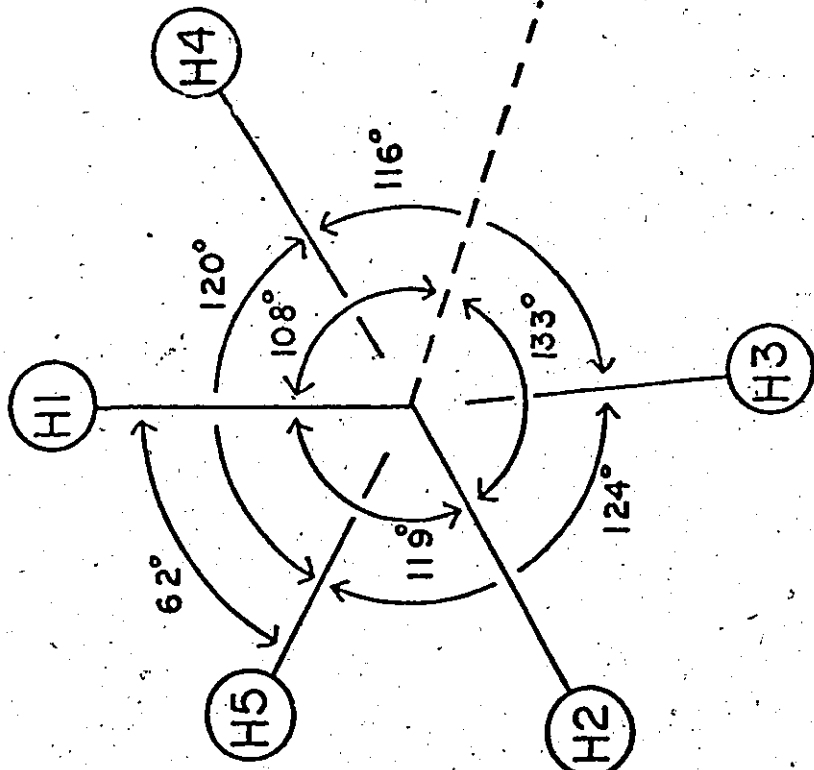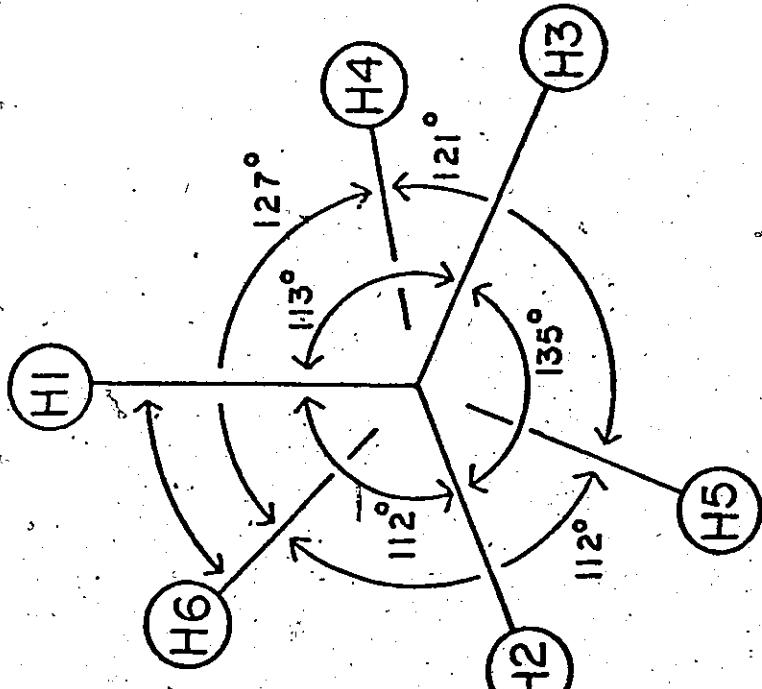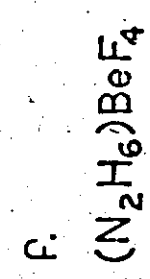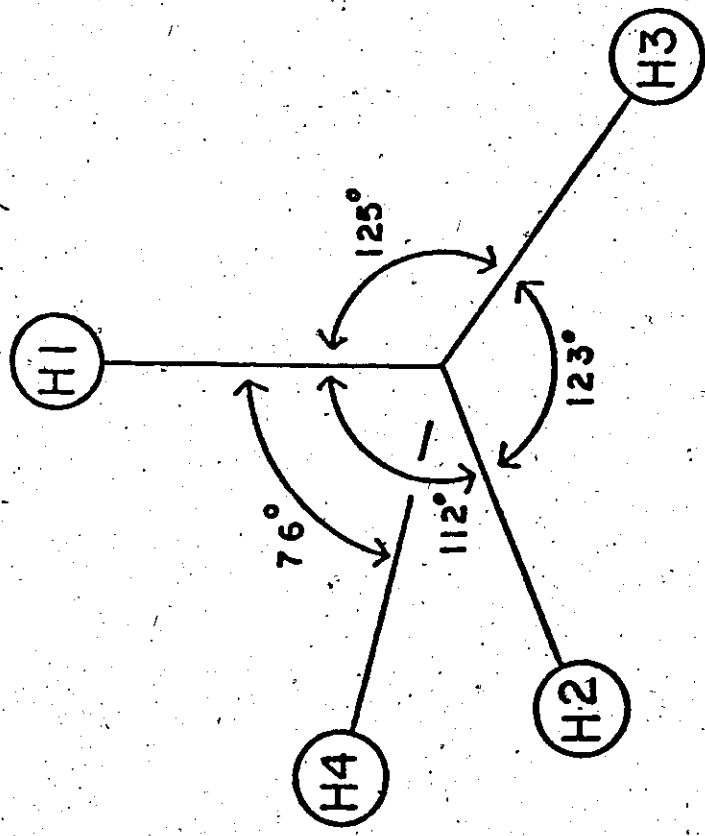
configuration almost perfect, but also the tetrahedral geometry of these groups.

Hydrogen atom temperature factors refined from X-ray diffraction measurements are notoriously inaccurate and in some cases cannot be refined (cf. Tables 5-3 and 8-3). Those for neutron diffraction are more easily refined, although the thermal motion of these atoms may be very anharmonic which would lead to an over-estimation of these parameters. The R.M.S. displacements along the principal axes of the thermal ellipsoids for the hydrogen atoms of $Li(N_2H_5)BeF_4$ are given in Table 10-1, and they show that the ellipsoids approximate oblate spheroids with their short axes lying almost along the N-H bonds (Figure 10-2). The hydrogen atoms of the $-NH_3^+$ group have slightly larger temperature factors than those of the $-NH_2$ group with their largest axes approximately in the plane of the hydrogen atoms.

The Hydrogen Bonding of the $N_2H_6^{2+}$, $N_2H_5^+$ and NH_3OH^+ Ions

In Chapters V and VII, we have used bond-strength summations to verify the assigned N-H....O hydrogen bonding scheme and have found excellent agreement with the expected ideal values except in the case of O(3) in $Li(N_2H_5)SO_4$. Using the structural determinations of NH_4F (Adrian & Feil, 1969), HF (Habuda & Gagarinsky, 1971), $Li(N_2H_5)BeF_4$ and $(N_2H_6)BeF_4$, bond-strength — bond-length curves were refined for H-F bonds determined by X-ray and neutron diffraction.

Table 10-1. The root-mean-square displacements along the principal axes of the thermal ellipsoids of the hydrogen atoms in $Li(N_2H_5)BeF_4$ and the angles these axes make with the cell axes

Atom	R.M.S.d. (Å)	Axis-a (°)	Axis-b (°)	Axis-c (°)
	0.157	22.8	73.0	75.4
H(1)	0.284	67.3	131.4	130.2
	0.313	88.8	133.8	43.8
	0.330	33.5	124.7	83.2
H(2)	0.225	121.1	143.4	107.5
	0.157	105.5	100.5	18.8
	0.148	162.9	78.4	102.5
H(3)	0.390	79.6	100.2	165.4
	0.291	76.5	15.6	97.6
	0.155	53.5	138.4	107.1
H(4)	0.356	38.9	51.1	91.1
	0.298	101.5	77.5	162.9
	0.075	104.0	101.5	18.2
H(5)	0.226	16.4	101.4	78.4
	0.344	98.5	163.8	103.8

Figure 10-2.

A thermal ellipsoid drawing of the $N_2H_5^+$ ion from the neutron diffraction investigation of $Li(N_2H_5)BeF_4$. The thermal ellipsoids include 50% probability.
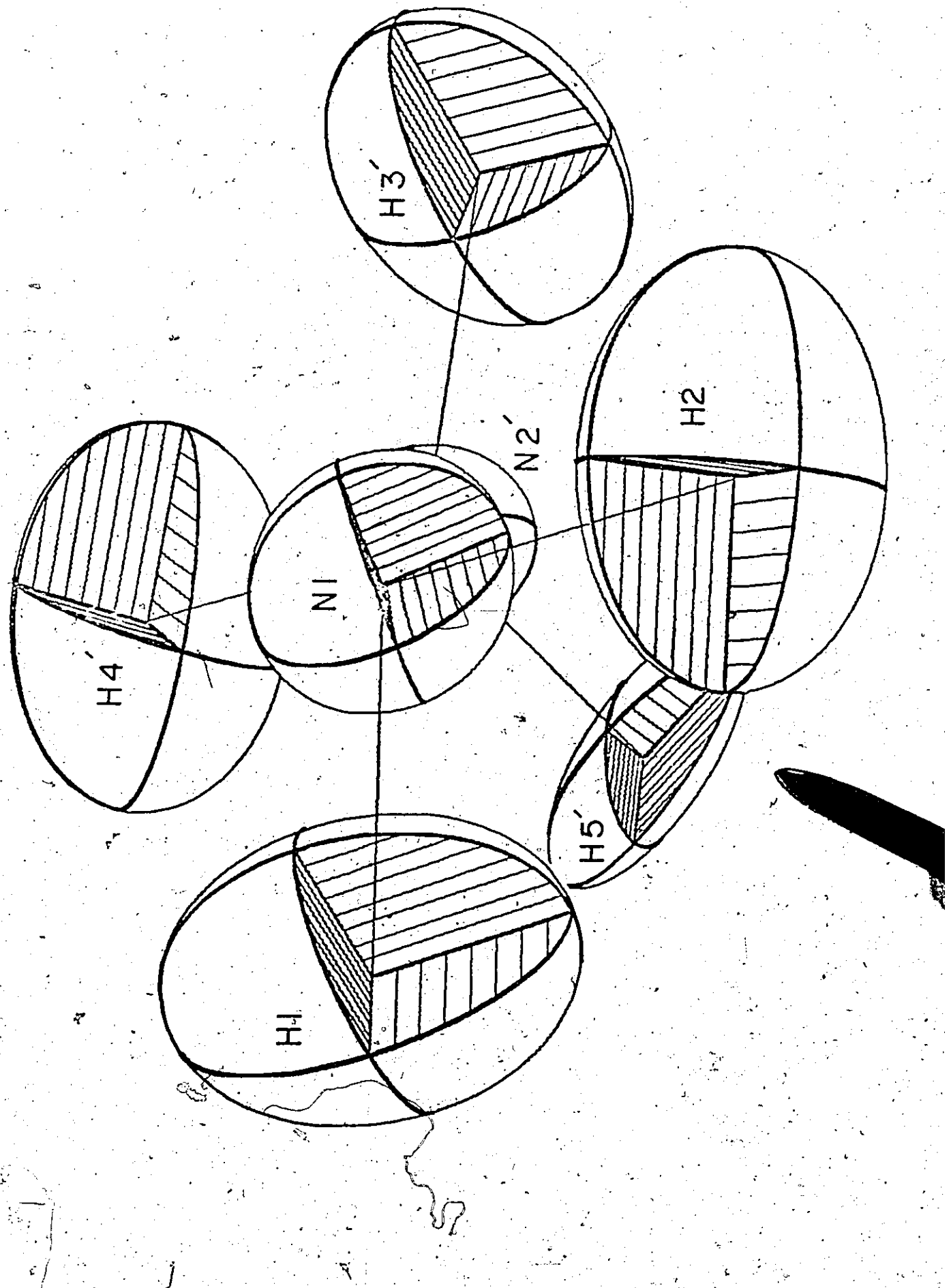
The functional form of the curves was:

$$s = (R/R_0)^{-N} \qquad (10\text{-}1)$$

where s is the bond-strength, R is the bond length and R_0 and N were parameters refined by a least-squares fit of the anion sums using the FORTRAN programme BOST. For the X-ray curve, four structures with a total of 22 H-F bonds were used giving an R.M.S. relative deviation of 8.7% while for the neutron curve, three structures with 13 H-F bonds gave an R.M.S. relative deviation of 7.6%. The parameters R_0 and N refined to respective values of 0.74 and 1.59 for the X-ray curve and 0.84 and 2.03 for the neutron curve; both curves are shown in Figure 10-3. Both the X-ray and the neutron curves should coalesce in the region of symmetric F-H-F bonds whose angles are 180°. This provides a useful check as, for such bonds, the bond-strength must be 0.5 valence units. The reported bond lengths for such bonds are 1.13 Å in both KHF_2 (Ibers, 1964) and $NaHF_2$ (McGaw & Ibers, 1963), and are in close agreement with the values predicted by the bond-strength curve.

Bond-strength summations for $Li(N_2H_5)BeF_4$ and $(N_2H_6)BeF_4$ are given in Tables 10-2, 10-3 and 10-4. For both these structures, the cation sums are very close to their ideal values. The anion sums, however, are not as good; F(3) in $Li(N_2H_5)BeF_4$, like O(3) in the sulphate, shows marked

Figure 10-3.

Bond-strength – bond-length curves for H-F bonds

determined by X-ray or neutron diffraction.

Bond strength v.u.
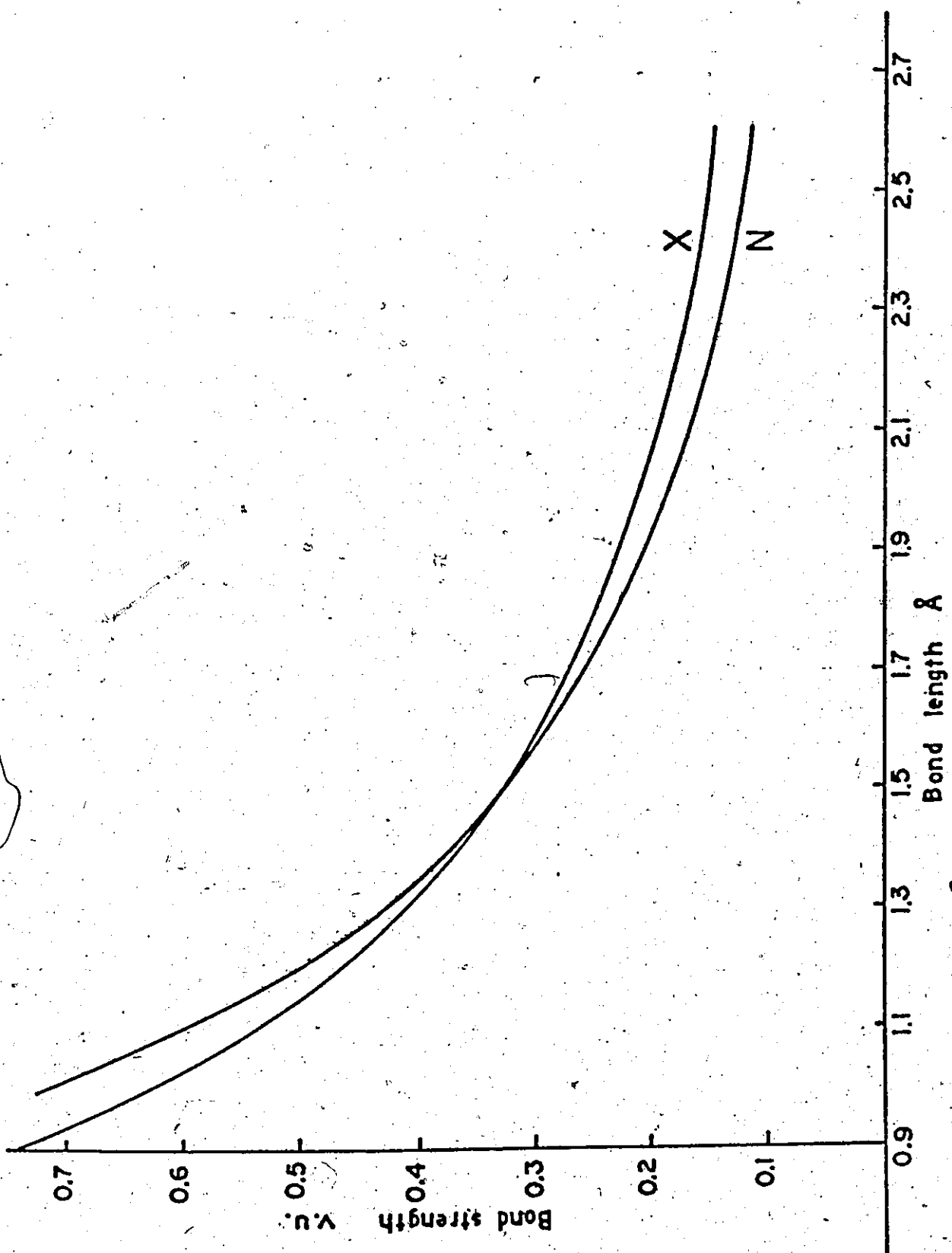
Bond length Å

Table 10-2. Bond-strengths in Li(N$_2$H$_5$)BeF$_4$ calculated from bond lengths determined by X-ray diffraction

Bond-strengths in valence units and bond lengths in Å (in brackets) for bonds between F and Li, Be and H.

	Li	Be	H(1)	H(3)	H(4)	H(5)	Sums around anions
F(1)	0.24 (1.861)	0.48 (1.557)		0.21 (1.96)		0.15 (2.40)	1.08
F(2)	0.23 (1.886)	0.47 (1.561)			0.22 (1.93)	0.20 (2.06)	1.11
F(3)	0.25 (1.842)	0.51 (1.532)	0.16 (2.39)				0.91
F(4)	0.26 (1.825)	0.51 (1.534)	0.15 (2.42)			0.15 (2.41)	1.07
Sums around cations	0.97	1.96					

Bond-strengths (s) are calculated from the expression $s = (R/R_0)^{-N}$ where R is the bond length and

	Li-F	Be-F	H-F
R$_0$	1.288	1.288	0.74
N	3.90	3.90	1.59

Table 10-3. Bond-strengths in Li(N$_2$H$_5$)BeF$_4$ calculated from bond lengths determined by neutron diffraction

Bond-strengths in valence units and bond lengths in Å (in brackets) for bonds between F and Li, Be and H.

	Li	Be	H(1)	H(3)	H(4)	H(5)	Sums around anions
F(1)	0.21 (1.917)	0.42 (1.614)		0.20 (1.87)		0.12 (2.41)	0.94
F(2)	0.22 (1.897)	0.47 (1.563)			0.21 (1.81)	0.16 (2.07)	1.06
F(3)	0.24 (1.863)	0.50 (1.537)	0.14 (2.24)				0.88
F(4)	0.32 (1.730)	0.54 (1.508)	0.14 (2.25)			0.12 (2.43)	1.11
Sums around cations	0.99	1.93					

Bond-strengths (s) are calculated from the expression $s = (R/R_0)^{-N}$ where R is the bond length and

	Li-F	Be-F	H-F
R_0	1.288	1.288	0.84
N	3.90	3.90	2.03

Table 10-4. Bond-strengths in $(N_2H_6)BeF_4$

Bond-strengths in valence units and bond lengths in Å (in brackets) for bonds between F and Be and H.

	Be	H(1)	H(2)	H(3)	H(4)	H(5)	H(6)	Sums around anions
F(1)	0.48 (1.557)	0.27 (1.70)		0.16 (2.35)			0.17 (2.23)	1.08
F(2)	0.48 (1.552)			0.15 (2.41)			0.21 (1.98)	0.85
F(3)	0.50 (1.540)				0.21 (1.97)	0.25 (1.77)		0.96
F(4)	0.50 (1.540)		0.22 (1.91)	0.17 (2.25)				0.89
Sums around cations	1.96							

Bond-strengths (s) are calculated from the expression $s = (R/R_0)^{-N}$ where R is the bond length and

	Be-F	H-F
R_0	1.288	0.74
N	3.90	1.59

deficiency for sums made with both the X-ray parameters and with the neutron parameters; and the sum at F(2) in $(N_2H_6)BeF_4$ is low. In the case of hydrogen bonds, two factors will greatly influence the accuracy of the bond-strength sums. First of all, we do not consider contributions from very weak bonds (van der Waals' contacts) where the indicated bond-strength for an H-F bond would be about 0.12-0.14 valence units; and secondly, the positional parameters of the hydrogen atoms are not as accurately known as those of the heavy atoms and, hence, the estimated error in the H-F bond lengths used in calculating the bond-strengths will be large. Although it can be argued that the predictive nature of the bond-strength summation method is not conclusive, the ability to account for bifurcated and trifurcated bonds makes it very useful.

In the type of structure we have investigated, any hydrogen positions based solely on the N-O or N-F contact distances would be incorrect as the fixed internal geometries of the hydrogen bonded cations make linear-hydrogen bonding impossible. There is no correlation of predictive value between the D-A distance and the hydrogen bond angle (Figure 10-4); however, there is a strong correlation between the H....A distance and the hydrogen bond angle for both H....F and H....O bonds (Figure 10-5). The range of hydrogen bond angles are from 106° to 172° for the N-H....F bonds and from 113° to 170° for the N-H....O

Figure 10-4.

A diagram showing the correlation between the hydrogen

bond angle and the donor-acceptor distance.
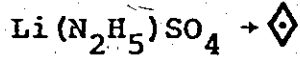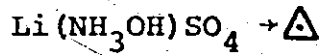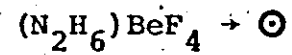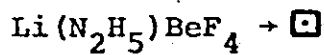
$Li(N_2H_5)BeF_4 \rightarrow$ ⊡

$(N_2H_6)BeF_4 \rightarrow$ ⊙

$Li(NH_3OH)SO_4 \rightarrow$ △

$Li(N_2H_5)SO_4 \rightarrow$ ◇

Bifurcated bonds indicated by "

Trifurcated bonds indicated by "'

N-H....N bonds indicated by §

O-H....O bond indicated by †

All bonds are those determined by X-ray diffraction.

D—H...A Angle (°)
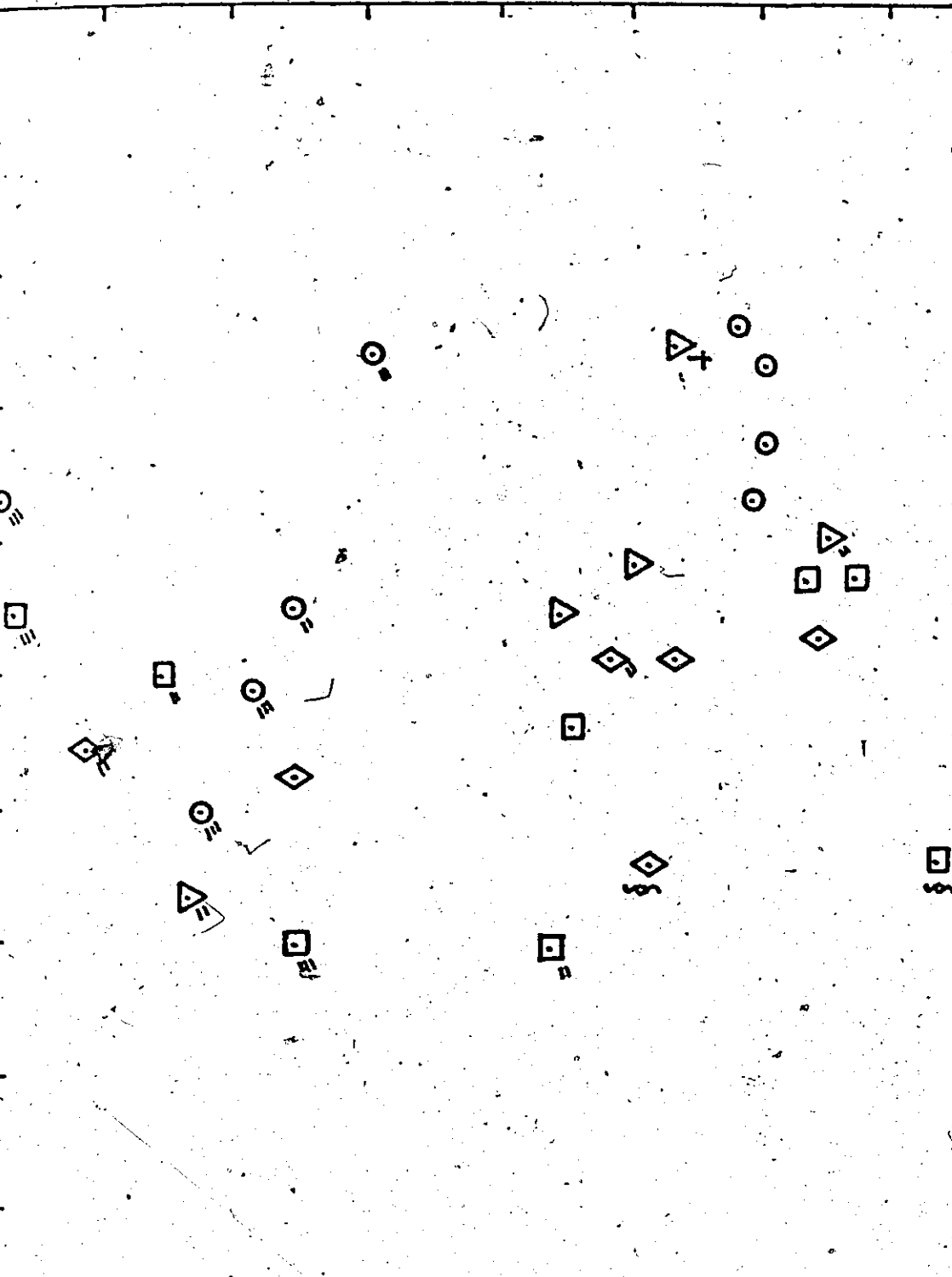
D—A Distance (Å)

Figure 10-5.

A diagram showing the correlation between the hydrogen

bond angle and the hydrogen-acceptor distance.
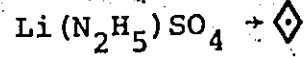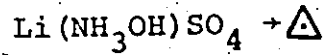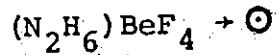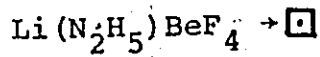
$Li(N_2H_5)BeF_4 \rightarrow \boxdot$

$(N_2H_6)BeF_4 \rightarrow \odot$

$Li(NH_3OH)SO_4 \rightarrow \triangle$

$Li(N_2H_5)SO_4 \rightarrow \diamondsuit$

Bifurcated bonds indicated by

Trifurcated bonds indicated by

N-H....N bonds indicated by §

O-H....O bond indicated by †

All bonds are those determined by X-ray diffraction.
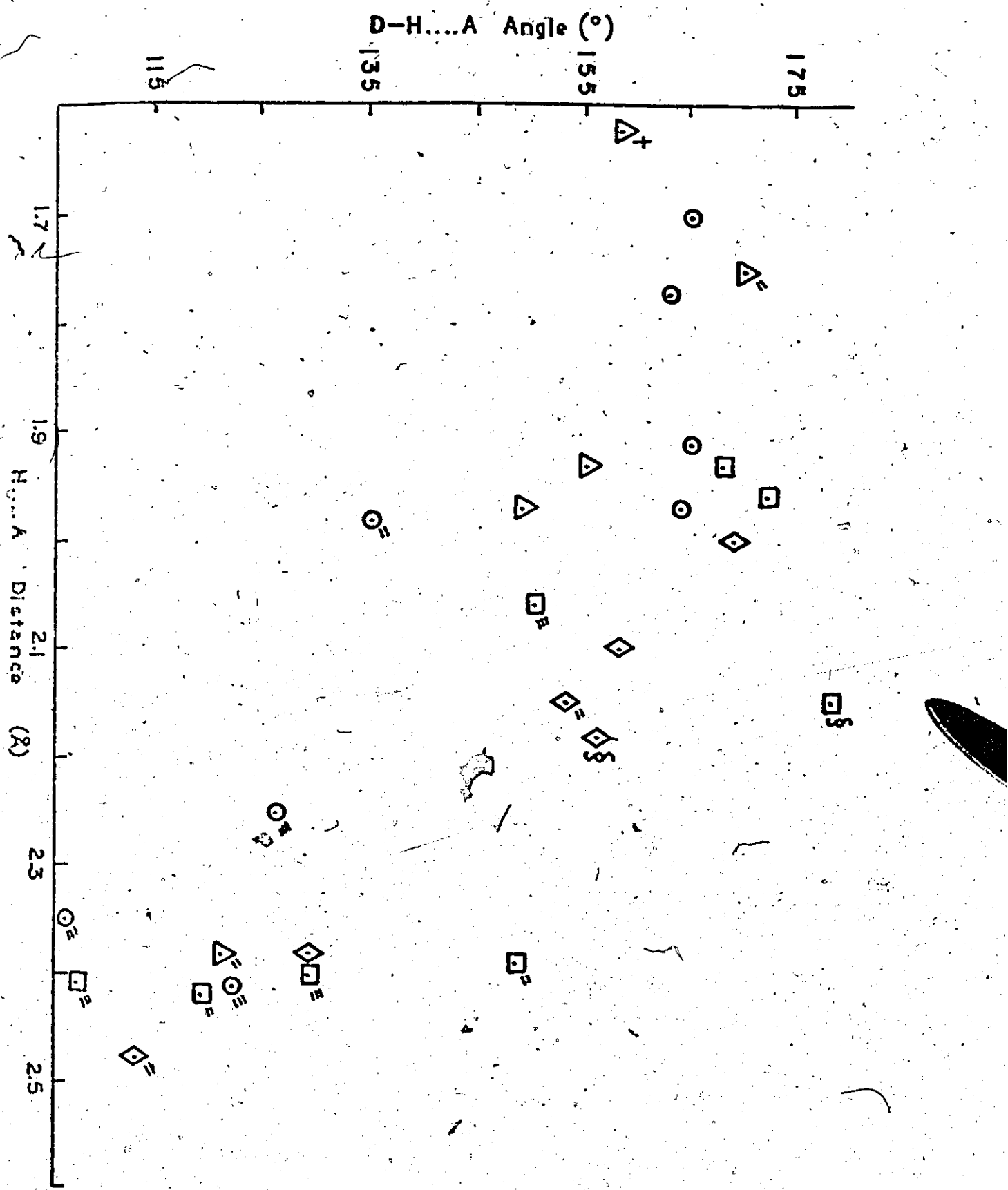
bonds. With the exception of the N(1)-H(1)....O(4) bond in Li(N$_2$H$_5$)SO$_4$, all the single hydrogen bonds had bond angles > 148°, and the bifurcated and trifurcated bonds with three exceptions were < 148°. There is a slight tendency for the neutron diffraction results to give a smaller angle; this is caused by the longer N-H distances. The hydrogen-bond angles in Li(NH$_3$OH)SO$_4$ were consistently lower than those of the X-ray determination of Li(N$_2$H$_5$)SO$_4$ because of the anomalously long N-H and O-H distances in the former compound at 1.00(4) Å and 1.08(6) Å respectively. It is also of note that while all the N-N-H and O-N-H angles were close to the tetrahedral value of 109.5°, the N-O-H angle in Li(NH$_3$OH)SO$_4$ is quite low at 89(3)°.

CHAPTER XI

SUMMARY

Although we have demonstrated that $Li(N_2H_5)SO_4$ is not a ferroelectric, it does have the very interesting property of an anisotropic electrical conductivity. The conductivity is highest in the $\underline{c}$ direction and is caused by proton transfer along the chains of hydrogen bonded hydrazinium ions. The same type of chain (cf. Figure 1-2a) is found in the isostructural compound $Li(N_2H_5)BeF_4$ and would indicate that similar electrical properties should exist in this compound.

The substitution of the monovalent cation, NH_3OH^+, for M in the $LiMSO_4$ series of framework structures produces a totally different type of structure. The size and shape of this cation are such that the framework type of structure is impossible; it should be pointed out that the oxygen atom of an O-H group is not always a good acceptor of hydrogen bonds, and the possibility of hydrogen bonded chains of NH_3OH^+ ions was unlikely. The hydrogen positions in $Li(NH_3OH)SO_4$ were easily located in the X-ray work, as they were for the other compounds investigated by this method. It would appear that all hydrogen atoms can be located by X-ray methods when there are no very heavy atoms present, provided that a diffrac-tometer is used and that sufficient care is taken in

the collection and correction of the measurements. Neutron diffraction will, of course, provide more accurate positions and temperature factors of the hydrogen atoms and will locate hydrogen atoms in a heavy atom environment.

The hydrogen bonding arrangements of the compounds were fully investigated and showed that single, bifurcated and trifurcated bonds existed. The hydrogen bonding did not appear to distort the almost perfect tetrahedral geometry of the $-NH_3^+$ and $-NH_2....H'$ groups or appreciably affect the staggered configuration of the $N_2H_5^+$ and $N_2H_6^{2+}$ ions.

Comparison of the X-ray and neutron diffraction structures of $Li(N_2H_5)SO_4$ and $Li(N_2H_5)BeF_4$ clearly showed the effects of both bonding electrons and of the problem of using the free atom atomic form factors for bonded atoms. The effect of systematically larger X-ray temperature factors of the heavy atoms was observed for the sulphate but not for the fluoroberyllate. Problems in the refinement of this structure, especially extinction, are thought to be caused by an underestimation of the absorption. High absorption could be caused by the large incoherent cross-section of the hydrogen atoms which are a high atomic percentage of this crystal. This would not only introduce absorption problems, but also the problem of anisotropic extinction. Such problems would not occur in $Li(N_2D_5)SO_4$ as deuterium has a negligible incoherent scattering cross-section. Although this problem has been noted by other

workers, no satisfactory solution has been proposed; and
we would suggest that for neutron diffraction investigations
of structures, deuterated crystals should always be used
when there is a high atomic percentage of hydrogen present.

APPENDIX A

TABLES OF OBSERVED AND CALCULATED STRUCTURE

FACTORS AND CALCULATED PHASES

For the non-centro-symmetric structure (Tables A-1, A-2, A-3), the phase factor (α) is given in millicycles; for the centro-symmetric structures (Tables A-4, A-5), the phase factor (± 1) is indicated by the sign of the calculated structure factor.

* Reflections where $F_o < 3\sigma_{Fo}$ are regarded as unobserved and are marked with an asterisk.

E Table A-3. If the integrated intensity of a reflection was negative, it was regarded as extinct, and the reflection was marked with an E.

h	$|F_o|$	$|KF_c|$	α
H,0,0			
2	213	194	500
4	289	264	0
6	487	502	0
8	116	114	500
10	114	115	500
12	165	160	0
14	47*	47	0
H,1,0			
1	271	245	0
2	338	335	500
3	617	513	500
4	433	400	0
5	374	381	0
6	84	77	500
7	109	110	0
8	155	155	500
9	155	152	500
10	53	59	500
11	89	85	0
12	20*	20	0
13	83	83	0
14	171	172	500
15	29*	29	500
H,2,0			
0	130	141	500
1	466	435	500
2	154	154	500
3	32	38	500
4	134	134	500
5	321	324	0
6	232	227	0
7	240	238	500
8	98	100	500
9	58	57	500
10	101	101	0
11	173	171	0
12	25*	22	500
13	53	54	500
14	38*	39	500
H,3,0			
1	241	228	500
2	413	432	500
3	32	7	0
4	25*	23	500
5	124	114	500
6	72	72	500
7	338	345	500
8	262	262	500
9	75	76	0
10	89	89	0
11	42	40	500
12	13*	4	500
13	140	139	500
14	44*	44	500
H,4,0			
1	54	61	0
2	158	152	500
3	226	230	0
4	243	238	0
5	68	64	0

h	$|F_o|$	$|KF_c|$	α
7	443	453	500
	122	122	
8	29*	28	500
9	82	83	0
10	113	116	0
11	23*	22	500
12	163	162	500
13	41	39	0
14	14*	18	500
H,5,0			
1	118	114	500
2	306	311	0
3	297	300	0
4	127	132	500
5	0*	1	500
6	65	64	500
7	43	39	500
8	267	275	0
9	175	173	0
10	128	128	500
11	19*	13	0
12	28*	24	500
13	96	98	500
H,6,0			
1	356	362	0
2	69	68	0
3	89	95	500
4	57	65	500
5	315	319	500
6	92	92	0
7	193	191	0
8	17*	10	0
9	71	73	0
10	45	43	0
11	108	110	500
12	25*	17	0
13	83	84	0
H,7,0			
1	321	327	0
2	248	252	0
3	115	113	500
4	223	225	500
5	173	183	0
6	56	61	0
7	94	95	0
8	85	83	0
9	80	81	500
10	48	48	500
11	12*	13	500
12	44*	45	500
H,8,0			
1	18*	3	0
2	241	253	500
3	11*	1	500
4	88	84	500
5	4*	3	0
6	155	165	0
7	0*	2	500
8	37*	35	500
9	109	103	500
10	101	101	500
11	25*	27	500

h	$|F_o|$	$|KF_c|$	α
12	79	79	0
H,9,0			
1	7*	10	0
2	172	175	500
3	219	219	500
4	117	119	0
5	73	73	0
6	56	48	0
7	54	52	0
8	107	109	500
9	79	77	500
10	45*	39	0
11	44*	41	0
H,10,0			
1	160	163	500
2	4*	7	500
3	84	82	500
4	15*	7	500
5	151	155	0
6	14*	16	500
7	133	136	500
8	112	110	500
9	68	68	500
10	45*	47	0
H,11,0			
1	73	76	500
2	77	76	500
3	59	57	0
4	118	117	0
5	12*	9	0
6	50	52	0
7	166	170	500
8	66	67	500
H,12,0			
1	19*	13	500
2	22*	22	0
3	56	54	0
4	148	149	0
5	25*	18	500
6	88	89	500
7	22*	19	0
H,13,0			
1	32*	31	500
2	68	68	0
3	57*	55	0
4	85	86	500
H,0,1			
2	493	506	996
4	267	266	998
6	107	99	915
8	185	175	42
10	84	82	116
12	162	151	967
14	142	143	972

h	$|F_o|$	$|KF_c|$	α

H,1,1

h	$|F_o|$	$|KF_c|$	α
0	360	346	8
1	326	335	1000
2	356	368	994
3	76	77	6
4	107	102	780
5	130	127	36
6	291	292	48
7	195	193	1
8	157	167	914
9	122	125	990
10	87	86	951
11	49	48	30
12	153	150	939
13	71	69	5
14	42*	41	955

H,2,1

h	$|F_o|$	$|KF_c|$	α
1	604	577	10
2	207	203	20
3	232	230	137
4	179	174	948
5	268	265	75
6	130	126	1000
7	336	338	970
8	49	47	46
9	188	188	13
10	53	55	894
11	33*	31	150
12	63	62	911
13	180	175	974
14	50*	51	919

H,3,1

h	$|F_o|$	$|KF_c|$	α
0	333	333	179
1	277	271	191
2	250	248	770
3	152	147	854
4	340	338	961
5	243	246	18
6	211	208	14
7	141	140	79
8	118	116	63
9	181	185	936
10	149	147	969
11	114	112	962
12	110	109	989
13	98	97	977
14	35*	35	962

H,4,1

h	$|F_o|$	$|KF_c|$	α
1	93	93	937
2	237	239	154
3	80	82	140
4	295	290	157
5	63	57	154
6	284	281	903
7	16*	8	813
8	296	298	965
9	22*	24	906
10	97	97	9
11	22*	26	786
12	59	59	957
13	27*	29	85
14	146	146	978

H,5,1

h	$|F_o|$	$|KF_c|$	α
0	337	342	29
1	253	250	154
2	256	247	933
3	197	190	921
4	80	81	922
5	51	46	180
6	290	295	977
7	131	133	124
8	21*	19	103
9	152	134	900
10	80	81	21
11	127	126	950
12	103	104	996
13	17*	13	17

H,6,1

h	$|F_o|$	$|KF_c|$	α
1	131	124	18
2	154	151	902
3	253	255	32
4	109	108	807
5	118	121	29
6	75	77	847
7	209	211	989
8	124	126	996
9	95	96	30
10	33*	34	244
11	20*	18	800
12	89	88	902
13	124	125	979

H,7,1

h	$|F_o|$	$|KF_c|$	α
0	145	145	30
1	313	324	353
2	184	190	5
3	65	62	152
4	99	97	40
5	160	156	9
6	74	73	131
7	155	157	969
8	48	50	212
9	49	50	112
10	109	109	953
11	136	134	32
12	64	68	978

H,8,1

h	$|F_o|$	$|KF_c|$	α
1	30*	29	176
2	257	261	990
3	61	60	887
4	230	238	979
5	79	77	873
6	38*	36	209
7	73	70	56
8	173	171	28
9	60	56	954
10	52	51	73
11	11*	13	933
12	69	67	974

H,9,1

h	$|F_o|$	$|KF_c|$	α
0	288	295	974
1	104	106	29
2	33*	32	808
3	13*	15	76
4	38*	38	179
5	155	167	999
6	172	131	13
7	71	69	14
8	40*	36	954
9	14*	15	956
10	105	105	1
11	66	67	999

H,10,1

h	$|F_o|$	$|KF_c|$	α
2	20*	21	942
3	150	151	23
4	18*	17	870
5	43	38	876
6	16*	14	-167
7	95	94	977
8	45	44	15
9	145	146	995
10	52*	49	973

H,11,1

h	$|F_o|$	$|KF_c|$	α
0	65	64	784
1	71	74	55
2	46	46	159
3	35*	32	908
4	83	82	962
5	164	164	993
6	70	72	20
7	44*	44	0
8	18*	14	241

H,12,1

h	$|F_o|$	$|KF_c|$	α
1	58	58	951
2	139	139	23
3	40*	37	897
4	55*	57	96
5	25*	32	880
6	44*	42	901

H,13,1

h	$|F_o|$	$|KF_c|$	α
0	107	102	982
1	59	60	71
2	44*	46	984
3	15*	9	192

H,0,2

h	$|F_o|$	$|KF_c|$	α
0	746	797	906
2	406	438	108
4	205	202	241
6	310	311	988
8	93	95	66
10	233	240	29
12	191	189	6
14	57	58	993

H,1,2

h	$|F_o|$	$|KF_c|$	α
1	117	113	820
2	140	138	941
3	220	224	882
4	172	171	899
5	160	159	223
6	128	125	125
7	243	250	28

h	$\lvert F_o \rvert$	$\lvert KF_c \rvert$	α		h	$\lvert F_o \rvert$	$\lvert KF_c \rvert$	α		h	$\lvert F_o \rvert$	$\lvert KF_c \rvert$	α
	H,1,2				7	61	30	981		1	152	153	30
8	207	211	38		8	214	220	961		2	70	71	37
9	135	133	5		9	152	150	2		3	77	75	952
10	65	60	862		10	83	85	931		4	32*	28	760
11	41	40	759		11	41	43	945		5	137	136	994
12	34*	37	943		12	74	73	101		6	90	88	65
13	149	147	28		13	104	107	972		7	116	116	0
14	163	166	969			**H,6,2**				8	58	50	786
										9	71	68	992
	H,2,2				0	8*	7	144					
0	275	272	989		1	181	186	943			**H,11,2**		
1	128	138	950		2	42	39	782		1	101	100	21
2	35	29	21		3	42	40	786		2	46	48	39
3	170	163	990		4	43	42	839		3	139	141	54
4	124	118	856		5	271	268	0		4	78	75	17
5	215	214	991		6	96	96	863		5	81	82	83
6	126	125	823		7	99	100	962		6	70	68	959
7	97	93	959		8	51	47	195		7	113	112	940
8	99	101	185		9	130	129	16					
9	153	156	7		10	54	51	842			**H,12,2**		
10	58	57	772		11	134	133	22		0	136	132	58
11	203	202	7		12	27*	25	66		1	47	46	53
12	18*	20	193							2	82	81	92
13	46	46	943			**H,7,2**				3	28*	26	880
14	29*	30	947		1	247	255	966		4	120	114	961
					2	118	119	936		5	23*	20	331
	H,3,2				3	68	68	843					
-1	193	190	10		4	77	79	849			**H,13,2**		
2	170	171	996		5	115	118	870		1	25*	28	39
3	187	182	151		6	74	74	122		2	79	82	2
4	164	159	956		7	142	141	50					
5	163	162	68		8	115	115	41			**H,0,3**		
6	55	53	913		9	95	96	36		2	315	318	902
7	265	265	954		10	25*	29	65		4	182	171	805
8	221	225	957		11	20*	21	53		6	193	195	163
9	51	52	993		12	72	72	977		8	239	246	31
10	51	52	812							10	117	115	27
11	29*	27	964			**H,8,2**				12	110	112	19
12	81	81	82		0	180	188	874					
13	129	126	981		1	87	88	11			**H,1,3**		
14	92	92	43		2	128	130	853		0	315	315	878
					3	35*	34	943		1	167	160	843
	H,4,2				4	146	146	69		2	195	192	853
0	349	359	95		5	49	50	91		3	119	117	77
1	180	177	23		6	121	123	1000		4	182	181	130
2	220	216	793		7	71	68	47		5	127	123	972
3	116	112	946		8	33*	32	69		6	293	305	1
4	164	156	910		9	49	48	925		7	128	131	901
5	39	38	12		10	143	143	22		8	43	44	895
6	328	330	970		11	43*	43	957		9	145	147	47
7	140	147	990							10	61	62	71
8	76	75	972			**H,9,2**				11	88	87	59
9	31*	30	963		1	43	43	31		12	125	125	991
10	132	133	0		2	181	184	1		13	70	70	967
11	8*	6	131		3	92	93	910					
12	143	141	979		4	137	136	7			**H,2,3**		
13	28*	27	951		5	60	58	93		1	424	447	968
					6	41	40	72		2	170	166	500
	H,5,2				7	103	101	16		3	222	219	977
1	78	73	24		8	116	116	27		4	37	34	212
2	255	252	1		9	60	59	951		5	243	247	937
3	187	184	29		10	71	72	71		6	109	110	958
4	125	125	40							7	234	234	3
5	68	64	900			**H,10,2**							
6	55	53	937		0	104	104	25					

h	$|F_O|$	$|KF_C|$	α	h	$|F_O|$	$|KF_C|$	α	h	$|F_O|$	$|KF_C|$	α
	H,2,3			11	20*	19	840	4	96	94	27
				12	31*	26	229				
8	62	59	97						**H,0,4**		
9	181	180	999		**H,7,3**			0	419	443	997
10	52	54	180	0	145	149	848	2	136	141	895
11	51	49	856	1	140	141	950	4	155	152	78
12	47	48	206	2	144	150	865	6	320	326	25
13	131	134	19	3	103	101	20	8	87	87	170
				4	136	134	52	10	142	143	963
	H,3,3			5	143	142	29	12	134	136	972
0	324	331	994	6	97	96	14				
1	309	318	12	7	91	92	976		**H,1,4**		
2	190	192	56	8	51	50	930				
3	49	51	38	9	85	83	5	1	95	89	25
4	168	152	941	10	72	71	28	2	157	159	27
5	225	225	999	11	150	150	12	3	233	240	73
6	177	178	923					4	162	159	2
7	182	181	982		**H,8,3**			5	76	78	119
8	113	115	895					6	62	61	35
9	60	60	964	1	20*	22	952	7	147	154	946
10	125	122	54	2	177	178	969	8	189	191	9
11	59	59	39	3	51	49	168	9	114	112	20
12	94	95	11	4	139	139	936	10	59	62	143
13	70	71	950	5	19*	15	94	11	23*	17	59
				6	96	97	83	12	21*	22	45
	H,4,3			7	80	79	963				
1	53	48	930	8	196	195	21		**H,2,4**		
2	302	307	997	9	40*	41	853				
3	90	90	896	10	71	70	30	0	163	161	777
4	343	352	997					1	284	288	30
5	49	47	899		**H,9,3**			2	98	101	133
6	19*	17	865					3	52	49	812
7	29*	33	208	0	202	205	975	4	73	71	172
8	172	176	960	1	72	74	952	5	207	208	22
9	11*	10	226	2	16*	17	21	6	22*	20	102
10	80	82	931	3	13*	11	791	7	153	156	12
11	18*	21	54	4	77	76	87	8	59	59	964
12	65	69	148	5	135	137	966	9	56	56	901
13	41*	35	964	6	152	149	28	10	9*	12	830
				7	52	52	896	11	131	130	9
	H,5,3			8	39*	35	248	12	13*	7	925
0	310	320	8	9	44*	42	114				
1	272	284	954						**H,3,4**		
2	96	97	7.96		**H,10,3**						
3	56	55	93					1	157	159	976
4	39	37	825	1	81	81	996	2	224	237	22
5	78	75	24	2	39	39	104	3	219	213	15
6	194	195	940	3	178	174	13	4	133	133	98
7	175	174	975	4	40*	40	119	5	176	176	962
8	47	47	107	5	25*	22	118	6	88	89	62
9	30*	30	172	6	0*	10	208	7	144	142	980
10	96	94	51	7	62	63	963	8	111	109	953
11	71	71	23	8	43*	39	7	9	61	61	65
12	90	90	990					10	16*	19	912
					H,11,3			11	43	40	923
	H,6,3			0	64	65	68	12	50*	49	9
				1	129	129	56				
1	111	111	948	2	74	72	6		**H,4,4**		
2	34*	34	169	3	30*	30	167				
3	229	232	966	4	52*	53	908	0	428	446	11
4	79	77	888	5	135	133	990	1	50	46	943
5	119	123	878	6	67	68	949	2	197	205	51
6	42	42	822					3	79	79	955
7	193	190	17		**H,12,3**			4	52	51	15
8	96	97	928					5	38	39	979
9	106	107	32	1	35*	37	2	6	269	267	977
10	54	51	46	2	153	151	5	7	60	61	923
				3	28*	28	196	8	14*	17	98

Table A-1 (Continued)

h	$\|F_O\|$	$\|KF_C\|$	α		h	$\|F_O\|$	$\|KF_C\|$	α		h	$\|F_O\|$	$\|KF_C\|$	α
					7	57	57	919		11	78	78	63
H,4,4					8	114	115	5		**H,4,5**			
9	54	54	19							1	48	49	866
10	76	76	57		**H,10,4**					2	152	152	392
11	17*	16	56		0	61	62	774		3	9*	8	795
12	97	98	3		1	171	170	22		4	154	150	580
					2	39*	38	249		5	17*	22	775
H,5,4					3	35*	35	892		6	74	73	36
1	116	118	985		4	49*	44	118		7	20*	20	973
2	208	209	5		5	108	110	939		8	127	125	935
3	247	253	5		6	70	65	961		9	0*	3	985
4	145	143	41							10	20*	22	62
5	75	77	999		**H,11,4**								
6	14*	11	977		1	77	74	976		**H,5,5**			
7	33*	30	174		2	81	80	39		0	217	224	997
8	135	134	967		3	113	110	986		1	70	66	939
9	139	140	17		4	119	114	19		2	44	44	156
10	36*	37	984							3	86	86	999
11	28*	26	120		**H,0,5**					4	26*	24	146
					2	159	155	49		5	52	56	47
H,6,4					4	116	117	219		6	99	101	977
0	47	49	927		6	114	114	937		7	62	54	374
1	182	185	12		8	138	136	970		8	43	41	959
2	58	59	803		10	83	82	33		9	65	66	14
3	14*	18	817							10	87	87	18
4	22*	23	152		**H,1,5**								
5	242	239	9		0	58	55	39		**H,6,5**			
6	52	53	147		1	115	120	149		1	56	56	22
7	117	117	28		2	28*	32	203		2	69	69	30
8	89	87	2		3	70	68	876		3	133	132	40
9	73	72	957		4	145	143	31		4	53	54	66
10	35*	37	60		5	84	84	25		5	11*	10	3
11	102	102	17		6	197	197	988		6	51	46	23
					7	66	64	89		7	163	163	975
H,7,4					8	35	55	851		8	29*	29	924
1	155	158	973		9	119	116	922		9	80	38	35
2	126	126	20		10	59	60	15					
3	43	40	178		11	65	65	952		**H,7,5**			
4	87	89	27							0	44	43	787
5	6*	10	942		**H,2,5**					1	125	128	29
6	23*	22	989		1	209	210	981		2	18*	16	246
7	138	135	992		2	80	81	877		3	64	62	927
8	108	106	24		3	137	142	84		4	116	112	989
9	98	98	15		4	57	58	137		5	119	118	36
10	70	68	52		5	75	74	18		6	65	67	58
					6	60	60	790		7	83	85	13
H,8,4					7	177	179	971		8	19*	21	194
0	90	91	23		8	73	69	35					
1	32*	30	227		9	122	121	9		**H,8,5**			
2	38*	40	61		10	44*	42	973		1	10*	15	250
3	29*	29	164		11	22*	17	39		2	133	132	40
4	146	148	25							3	55	55	946
5	40*	40	6		**H,3,5**					4	103	102	66
6	143	143	25		0	182	188	18		5	56	53	849
7	29*	26	906		1	130	134	961		6	77	72	928
8	39*	39	209		2	107	112	77		7	47*	46	991
9	59	-59	998		3	29*	25	174					
					4	77	76	995		**H,9,5**			
H,9,4					5	151	151	998		0	146	145	961
1	37*	38	763		6	55	56	28		1	84	83	124
2	132	134	939		7	86	85	942		2	11*	5	945
3	119	115	43		8	7*	13	194		3	22*	25	161
4	89	88	997		9	83	80	13					
5	55	55	203		10	117	118	984					
6	59	58	50										

h	$|F_O|$	$|KF_C|$	α	h	$|F_O|$	$|KF_C|$	α	h	$|F_O|$	$|KF_C|$	α
	H,9,5			8	86*	39	16		**H,0,7**		
4	71	70	32	9	49*	53	38	2	187	182	983
5	76	77	986					4	133	134	9
	H,10,5				**H,4,6**			6	26*	25	802
1	63	51	977	0	130	185	917		**H,1,7**		
2	43*	37	877	1	64	64	50				
3	128	127	1	2	69	67	875	0	106	105	21
	H,0,6			3	30*	31	866	1	137	138	975
0	266	269	976	4	85	85	74	2	70	69	52
2	52	50	824	5	27*	27	832	3	22*	18	835
4	106	109	16	6	137	136	950	4	77	78	998
6	208	205	973	7	50*	47	24	5	85	87	9
8	34*	37	922	8	58	56	56	6	140	136	955
	H,1,6				**H,5,6**				**H,2,7**		
1	63	68	965	1	49	51	891	1	143	139	965
2	81	82	933	2	141	139	990	2	0*	5	130
3	162	159	6	3	84	82	908	3	151	152	8
4	79	80	943	4	96	95	8	4	64	64	908
5	49	51	929	5	60	61	120	5	92	92	938
6	70	76	20	6	21*	27	160	6	21*	13	861
7	85	87	981	7	77	78	60		**H,3,7**		
8	135	135	974		**H,6,6**						
9	75	76	14	0	72	76	33	0	163	163	943
	H,2,6			1	101	99	986	1	81	80	1
0	41	43	81	2	70	70	67	2	84	82	950
1	133	135	934	3	26*	24	110	3	19*	14	65
2	80	80	955	4	34*	30	878	4	70	69	74
3	50	47	33	5	163	164	987	5	101	102	1
4	35*	33	970	6	17*	17	162		**H,4,7**		
5	139	139	998	7	69	68	971				
6	16*	16	224		**H,7,6**			1	21*	20	834
7	81	82	903	1	114	113	972	2	115	117	992
8	22*	24	846	2	66	64	973	3	20*	25	846
9	73	74	49	3	88	87	69	4	115	118	971
	H,3,6			4	32*	33	933	5	8*	16	988
2	117	118	934	5	50*	48	23		**H,5,7**		
3	85	84	957		**H,8,6**			0	147	144	958
4	46	47	834	0	101	98	14	1	75	72	984
5	69	66	807	1	27*	27	107	2	26*	28	7
6	53	51	248	2	54	54	49	3	41*	38	960
7	130	131	995	3	0*	3	993		**H,6,7**		
								1	58	58	4

h	|F$_o$|	|KF$_c$|	α	h	|F$_o$|	|KF$_c$|	α	h	|F$_o$|	|KF$_c$|	α
H,0,0				13	0*	22	0	8	18*	5	500
2	117	116	500					9	28*	1	500
4	617	628	0	**H,5,0**							
6	316	310	0	1	63	67	500	**H,10,0**			
8	72	77	500	2	145	139	0	1	13*	16	0
10	127	126	0	3	155	154	0	2	51	49	500
12	19*	21	0	4	30*	31	500	3	94	91	500
				5	45	47	500	4	20*	1	500
H,1,0				6	9*	9	0	5	26*	21	0
1	178	180	0	7	51	55	0	6	10*	3	0
2	103	95	500	8	76	78	0	7	57	58	500
3	474	464	500	9	34*	36	0	8	73	64	500
4	379	392	0	10	98	94	500				
5	412	420	0	11	19*	3	0	**H,11,0**			
6	124	129	500	12	23*	12	0	1	15*	15	500
7	66	59	500					2	24*	25	500
8	82	77	0	**H,6,0**				3	68	65	500
9	18*	23	0	0	162	162	500	4	37*	35	0
10	80	87	500	1	286	290	0	5	18*	18	0
12	19*	2	500	2	53	59	0	6	0*	1	500
13	0*	6	0	3	214	213	500				
				4	44	48	500	**H,12,0**			
H,2,0				5	85	88	500	0	0*	7	0
0	87	97	500	6	55	50	0	1	40*	40	500
1	186	183	500	7	64	63	0	2	23*	4	500
2	183	191	500	8	38*	37	0	3	65	58	0
3	68	65	0	9	56	47	500				
4	100	104	500	10	50*	49	0	**H,0,1**			
5	128	125	0	11	15*	27	0	2	229	231	977
6	209	209	0	12	19*	16	0	4	100	101	916
7	39*	36	500					6	136	133	916
8	87	88	500	**H,7,0**				8	113	117	894
9	56	59	0	1	237	243	0	10	64	54	761
10	90	95	0	2	153	157	0	12	114	114	949
12	26*	14	500	3	40*	46	0				
13	14*	24	0	4	179	182	500	**H,1,1**			
				5	181	181	0	0	129	110	999
H,3,0				6	125	125	0	1	83	81	7
1	111	117	500	7	29*	18	500	2	260	253	993
2	226	219	500	8	0*	13	500	3	32	34	70
3	309	311	500	9	72	67	0	4	226	227	928
4	195	190	500	10	10*	22	0	5	48	48	912
5	39	35	500	11	20*	10	500	6	152	152	98
6	84	82	500					7	48	49	19
7	258	264	500	**H,8,0**				8	174	173	924
8	138	137	500	0	223	213	0	9	51	52	987
9	19*	31	500	1	50	46	0	10	68	68	61
10	15*	26	0	2	101	99	500	12	77	71	976
12	34*	29	500	3	19*	23	0	13	22*	13	59
13	53*	58	500	4	73	73	0				
				5	27*	25	500	**H,2,1**			
H,4,0				6	0*	29	0	1	529	513	20
0	0*	2	0	7	51	49	0	2	193	190	25
1	36	35	500	8	0*	4	500	3	426	433	896
2	339	335	500	9	74	71	500	4	127	127	950
3	194	195	0	10	20*	11	0	5	251	254	118
4	21*	19	0					6	134	131	9
5	0*	11	0	**H,9,0**				7	245	247	925
6	285	296	500	1	39*	37	500	8	30*	17	126
7	91	90	0	2	13*	8	0	9	27*	13	100
8	84	88	500	3	89	94	500	10	27*	35	851
9	29*	23	0	4	17*	4	0	12	64	48	905
10	58	53	500	5	45*	35	0	13	70	67	935
11	8*	19	500	6	57	56	0				
12	84	81	500	7	0*	15	0				

h	$|F_O|$	$|KF_C|$	α

H,3,1

h	$|F_O|$	$|KF_C|$	α
0	424	420	782
1	390	397	830
2	391	399	845
3	202	203	819
4	210	208	894
5	109	110	972
6	74	76	14
7	56	61	756
8	79	83	135
9	88	89	853
10	62	61	868
12	58	57	921
13	37*	43	915

H,4,1

h	$|F_O|$	$|KF_C|$	α
1	47	51	871
2	281	279	853
3	96	99	162
4	288	291	756
5	76	73	131
6	304	305	880
7	8*	18	215
8	127	129	859
9	0*	18	856
10	59	57	934
11	11*	26	808
12	27*	9	226

H,5,1

h	$|F_O|$	$|KF_C|$	α
0	194	193	39
1	219	219	233
2	330	325	960
3	157	156	886
4	88	85	64
5	108	108	953
6	145	148	946
7	89	98	208
8	42*	44	48
9	109	110	874
10	29*	31	905
11	44*	47	819
12	45*	39	987

H,6,1

h	$|F_O|$	$|KF_C|$	α
1	74	72	998
2	108	109	833
3	23*	21	246
4	127	131	835
5	123	126	984
6	80	82	807
7	76	69	16
8	48	46	65
9	85	80	942
10	14*	18	800
11	0*	19	146

H,7,1

h	$|F_O|$	$|KF_C|$	α
0	10*	11	95
1	228	237	900
2	116	118	13
3	97	97	824
4	18*	24	204
5	33*	33	788
6	36*	40	816
7	43*	40	950
8	41*	43	837
9	41*	48	898
10	11*	21	816
11	52*	41	109

H,8,1

h	$|F_O|$	$|KF_C|$	α
1	43	43	84
2	84	83	985
3	52	51	855
4	71	70	950
5	72	72	865
6	45	49	918
7	42*	39	151
8	41*	34	145
9	79	74	945
10	30*	21	754

H,9,1

h	$|F_O|$	$|KF_C|$	α
1	55	53	782
2	71	70	8
3	35*	39	765
4	72	70	951
5	72	70	981
6	47*	48	45
7	32*	30	35
8	69	68	957
9	0*	14	868

H,10,1

h	$|F_O|$	$|KF_C|$	α
1	16*	23	107
2	22*	12	195
3	61	62	839
4	29*	27	112
5	79	75	889
6	13*	19	837
7	53	48	857
8	0*	16	12

H,11,1

h	$|F_O|$	$|KF_C|$	α
0	81	82	852
1	45	49	902
2	51	48	803
3	28*	24	773
4	33*	28	893
5	76	75	956
6	0*	11	212

H,12,1

h	$|F_O|$	$|KF_C|$	α
1	37*	42	942
2	45*	30	41
3	30*	29	245

H,0,2

h	$|F_O|$	$|KF_C|$	α
0	731	725	835
2	664	655	92
4	323	326	842
6	161	161	967
8	123	123	54
10	96	91	160
12	104	96	43

H,1,2

h	$|F_O|$	$|KF_C|$	α
1	130	129	183
2	146	144	106
3	221	222	160
4	151	151	764
5	208	203	190
6	148	149	154
7	171	177	64
8	82	87	179
9	33*	30	130
10	61	66	874
11	60	50	895
12	32*	20	230
13	67	61	48

H,2,2

h	$|F_O|$	$|KF_C|$	α
0	291	283	2
1	176	180	26
2	43	46	952
3	107	104	975
4	112	106	882
5	56	59	902
6	112	112	826
7	87	82	55
8	96	92	166
9	50	47	70
10	43*	46	236
11	80	83	1
12	23*	26	92
13	0*	16	50

H,3,2

h	$|F_O|$	$|KF_C|$	α
1	104	103	17
2	11*	18	200
3	194	192	835
4	275	271	971
5	154	149	101
6	57	52	802
7	163	167	889
8	120	120	911
9	78	75	52
10	54	52	173
11	47*	52	920
12	47*	44	143

H,4,2

h	$|F_O|$	$|KF_C|$	α
0	217	217	175
1	144	142	71
2	282	284	855
3	83	84	868
4	126	125	132
5	44	44	119
6	177	177	926
7	97	68	976
8	123	120	988
9	0*	9	32
10	26*	29	7
11	31*	10	174
12	68	66	929

H,5,2

h	$|F_O|$	$|KF_C|$	α
1	29*	26	848
2	76	73	981
3	28*	25	977
4	9*	7	65
5	49	49	44

h	$|F_O|$	$|KF_C|$	α		h	$|F_O|$	$|KF_C|$	α		h	$|F_O|$	$|KF_C|$	α

H,5,2

h	$|F_O|$	$|KF_C|$	α
6	19*	18	786
7	0*	13	858
8	50	57	895
9	35*	41	59
10	58	60	888
11	0*	18	919
12	47*	38	147

H,6,2

h	$|F_O|$	$|KF_C|$	α
0	54	59	967
1	160	161	225
2	38	42	190
3	118	108	795
4	30*	31	795
5	90	89	34
6	53	53	840
7	40*	32	134
8	48	44	108
9	51	48	122
10	54	45	902
11	48*	38	133

H,7,2

h	$|F_O|$	$|KF_C|$	α
1	172	172	946
2	75	74	213
3	141	145	73
4	105	102	174
5	114	114	821
6	91	88	174
7	81	84	131
8	70	65	95
9	51	49	801
10	19*	23	897

H,8,2

h	$|F_O|$	$|KF_C|$	α
1	77	71	16
2	111	112	141
3	68	67	955
4	63	62	231
5	35*	36	179
6	12*	5	979
7	57	50	146
8	39*	44	20
9	26*	29	235

H,9,2

h	$|F_O|$	$|KF_C|$	α
1	83	81	15
2	44	43	70
3	37*	34	140
4	74	72	71
5	79	74	42
6	9*	17	804
7	70	64	993
8	0*	8	31

H,10,2

h	$|F_O|$	$|KF_C|$	α
1	74	73	168
2	53	56	75
3	64	66	863
4	10*	22	978
5	37*	22	226
6	33*	41	71
7	47*	47	987

H,11,2

h	$|F_O|$	$|KF_C|$	α
1	38*	41	34
2	0*	9	121
3	47*	44	202
4	0*	13	71
5	76	75	88

H,12,2

h	$|F_O|$	$|KF_C|$	α
0	20*	24	57
1	17*	25	161

H,0,3

h	$|F_O|$	$|KF_C|$	α
2	160	162	760
4	206	202	168
6	172	176	161
8	98	98	152
10	88	78	52
12	46*	49	975

H,1,3

h	$|F_O|$	$|KF_C|$	α
0	249	248	781
1	122	120	157
2	163	163	766
3	85	88	93
4	135	135	243
5	20*	14	783
6	182	185	3
7	46	51	784
8	38*	40	929
9	76	75	76
10	79	76	924
11	34*	24	197
12	45*	54	4

H,2,3

h	$|F_O|$	$|KF_C|$	α
1	359	358	958
2	141	141	977
3	10*	8	228
4	11*	15	882
5	274	273	946
6	109	108	941
7	68	69	969
8	44*	44	166
9	16*	16	885
10	56	48	144
11	66	66	918
12	53*	35	195

H,3,3

h	$|F_O|$	$|KF_C|$	α
0	316	310	997
1	227	231	22
2	176	173	61
3	135	138	19
4	50	50	182
5	62	61	944
6	81	83	838
7	69	68	966
8	94	91	931
9	38*	41	995
10	22*	29	785
11	31*	27	997
12	0*	17	960

H,4,3

h	$|F_O|$	$|KF_C|$	α
1	8*	9	34
2	128	125	987
3	117	115	923
4	267	270	991
5	84	81	896
6	72	68	31
7	44*	41	761
8	69	60	65
9	27*	27	155
10	32*	32	773
11	21*	27	77

H,5,3

h	$|F_O|$	$|KF_C|$	α
0	166	167	11
1	225	222	903
2	139	139	902
3	67	68	235
4	101	100	33
5	42	46	889
6	75	71	839
7	114	112	969
8	67	63	30
9	34*	31	859
10	39*	24	221
11	29*	33	888

H,6,3

h	$|F_O|$	$|KF_C|$	α
1	57	59	839
2	55	55	889
3	55	53	198
4	77	77	876
5	110	112	812
6	69	67	864
7	98	102	55
8	58	58	888
9	50	46	815
10	33*	29	104

H,7,3

h	$|F_O|$	$|KF_C|$	α
1	60	58	173
2	94	96	818
3	92	89	54
4	76	74	104
5	44*	43	102
6	28*	25	7
7	23*	19	42
8	0*	18	851
9	0*	9	17

H,8,3

h	$|F_O|$	$|KF_C|$	α
1	45	45	975
2	43	42	930
3	31*	21	216
4	20*	33	784
5	12*	3	855
6	14*	30	145
7	54	49	986
8	58	63	41

H,9,3

h	$|F_O|$	$|KF_C|$	α
1	39*	35	42
2	50	54	944

h	$|F_o|$	$|KF_c|$	α		h	$|F_o|$	$|KF_c|$	α		h	$|F_o|$	$|KF_c|$	α
	H,9,3				7	37*	28	946		2	29*	27	892
					8	22*	31	207		3	67	68	129
3	30*	32	69		9	58	63	931		4	34*	41	925
4	37*	36	902		10	45*	40	16		5	60	59	208
5	49*	49	912		11	22*	33	922					
6	63	66	18								H,10,4		
7	43*	31	845			H,4,4							
										0	40*	53	226
	H,10,3				0	271	264	1000		1	90	86	18
					1	39	37	963		2	38*	41	206
1	44	41	981		2	114	115	82		3	0*	15	146
2	18*	19	775		3	31*	37	938					
3	58	52	81		4	113	115	962			H,0,5		
4	7*	25	849		5	46	44	25					
5	37*	31	89		6	100	100	955		2	52	55	830
6	0*	19	170		7	31*	32	918		4	139	137	883
					8	50	45	891		6	109	104	890
	H,11,3				9	13*	22	42		8	51	58	880
					10	54	54	945		10	58	42	935
0	19*	38	0										
1	37*	48	161			H,5,4					H,1,5		
2	45*	46	971										
3	60	53	91		1	45	45	952		2	81	79	910
					2	68	68	43		3	53	52	823
	H,0,4				3	93	92	22		4	55	56	14
					4	50	45	146		5	13*	17	19
0	211	219	61		5	34*	31	964		6	85	88	937
2	297	297	906		6	30*	36	107		7	29*	27	832
4	29*	31	823		7	26*	32	928		8	58	55	938
6	160	162	22		8	28*	19	784		9	67	61	902
8	89	91	239		9	49*	50	68					
10	50*	39	777		10	20*	10	901			H,2,5		
	H,1,4					H,6,4				2	51	54	840
										3	82	84	919
1	40	36	134		0	64	67	960		4	70	72	100
2	41	38	809		1	46	41	793		5	40*	43	905
3	153	155	198		2	26*	29	240		6	42	42	756
4	42	49	59		3	11*	3	172		7	78	81	941
5	103	102	192		4	22*	22	133		8	53	57	34
6	61	57	974		5	94	91	14		9	18*	12	768
7	98	101	829		6	39*	39	103					
8	56	60	21		7	22*	36	185			H,3,5		
9	0*	6	916		8	69	70	1					
10	38*	26	171		9	37*	25	798		2	23*	22	55
11	0*	28	991							3	38*	40	768
						H,7,4				4	12*	19	762
	H,2,4									5	38*	32	992
					1	81	86	959		6	18*	28	12
0	170	171	241		2	45	39	176		7	25*	20	204
1	143	139	105		3	117	117	948		8	0*	10	825
2	138	141	129		4	55	53	224		9	39*	31	107
3	66	68	139		5	19*	17	5					
4	73	71	158		6	43*	32	797			H,4,5		
5	34*	30	34		7	69	76	962					
6	11*	9	982		8	43*	43	955		2	33*	35	121
7	37*	31	202							3	15*	15	157
8	53	55	907			H,8,4				4	55	54	819
9	31*	39	121							5	15*	19	971
10	0*	29	242		1	74	72	162		6	67	67	73
11	21*	30	891		2	70	69	863		7	39*	38	998
					3	43	44	201		8	28*	21	235
	H,3,4				4	32*	29	35					
					5	31*	33	1			H,5,5		
1	86	84	946		6	33*	30	23					
2	121	125	57		7	42*	22	851		2	48	46	903
3	52	52	35							3	104	100	5
4	85	83	207			H,9,4				4	65	66	937
5	144	142	949							5	17*	16	919
6	127	129	53		1	44	43	878					

h	$|F_o|$	$|KF_c|$	α		h	$|F_o|$	$|KF_c|$	α		h	$|F_o|$	$|KF_c|$	α
	H,5,5				4	23*	24	950			**H,5,6**		
					6	94	94	913		1	25*	25	238
6	9*	8	910							2	45*	50	973
7	37*	21	819			**H,1,6**				3	15*	27	215
8	46*	45	910							4	23*	30	969
					2	21*	14	90		5	55	57	94
	H,6,5				3	83	78	973					
					4	26*	25	848			**H,6,6**		
2	50	46	43		5	62	67	900					
3	59	62	869		6	39*	40	2		0	32*	23	48
4	69	72	37		7	21*	5	929		1	19*	17	27
5	32*	28	958							2	52	50	27
6	65	56	39			**H,2,6**				3	0*	11	977
7	98	92	929							4	36*	24	900
					1	70	70	779					
	H,7,5				2	92	94	926			**H,0,7**		
					3	42*	34	218					
0	102	103	922		4	33*	35	886		2	62	62	995
1	36*	49	144		5	12*	23	989					
2	43	46	848		6	41*	25	115			**H,1,7**		
3	41*	42	872		7	37*	29	216					
4	59	55	948							0	32*	41	134
5	21*	23	999			**H,3,6**				1	66	63	946
6	24*	4	148							2	49*	55	120
					1	35*	28	805		3	38*	29	897
	H,8,5				2	61	59	835					
					3	28*	33	97			**H,2,7**		
1	0*	20	68		4	67	67	164					
2	34*	33	106		5	65	53	244		1	66	67	944
3	32*	34	881		6	75	68	811		2	8*	14	227
4	30*	27	212										
						H,4,6					**H,3,7**		
	H,9,5												
					0	104	105	773		0	53*	63	921
0	65	59	878		1	57	51	46		1	27*	15	196
1	37*	33	134		2	52	51	182					
					3	10*	13	250					
	H,0,6				4	57	51	768					
					5	34*	25	903					
2	57	59	887		6	48*	50	906					

h	$|F_o'|$	$|KF_c|$	α

H,0,0

h	$|F_o'|$	$|KF_c|$	α
2	130	125	500
4	513	509	0
6	287	285	0
8	220	235	500
10	-50	90	0
12	69E	95	0

H,1,0

h	$|F_o'|$	$|KF_c|$	α
1	153	149	0
2	285	288	500
3	485	473	500
4	473	468	0
5	229	225	0
6	198	196	500
7	79	59	0
8	255	266	500
9	69	84	0
10	491	196	500
11	120	156	0
12	53*	49	500

H,2,0

h	$|F_o'|$	$|KF_c|$	α
0	43	8	500
1	367	374	500
2	66	70	500
3	139	135	500
4	73	73	500
5	294	239	0
6	342	343	0
7	137	131	500
8	35	40	0
9	164	175	0
10	206	202	0
11	252	226	0
12	115	75	500

H,3,0

h	$|F_o'|$	$|KF_c|$	α
1	52	37	0
2	261	262	500
3	323	324	0
4	43*	33	500
5	24*	37	0
6	304	315	500
7	526	544	500
8	410	419	500
9	29*	8	0
10	221	205	0
11	228	229	500
12	119	75	500

H,4,0

h	$|F_o'|$	$|KF_c|$	α
0	294	292	500
1	153	152	500
2	343	344	500
3	361	357	0
4	94	76	500
5	404	391	0
6	537	534	500
7	215	224	0
8	200	196	500
9	175	152	0
10	91	32	500
11	27E	36	0
12	314	334	500

H,5,0

h	$|F_o|$	$|KF_c|$	α
1	222	239	500
2	190	191	0
3	131	177	0
4	55*	16	500
5	102	104	0
6	48*	27	0
7	221	225	0
8	238	235	0
9	179	181	0
10	249	257	500
11	82	80	0

H,6,0

h	$|F_o|$	$|KF_c|$	α
0	292	274	500
1	413	416	0
2	145	138	500
3	339	395	500
4	223	237	500
5	548	544	500
6	59*	15	0
7	79	79	500
8	71	19	500
9	77	48	500
10	177	171	0

H,7,0

h	$|F_o|$	$|KF_c|$	α
1	644	634	0
2	252	254	0
3	94	80	0
4	279	275	500
5	426	439	0
6	286	307	0
7	56*	23	500
8	137	80	0
9	62E	26	500
10	107	66	0

H,8,0

h	$|F_o|$	$|KF_c|$	α
0	576	575	0
1	109	132	0
2	268	251	500
3	150	158	0
4	35E	82	0
5	103	62	0
6	312	312	0
7	119	143	0
8	135	110	500
9	283	285	500

H,9,0

h	$|F_o|$	$|KF_c|$	α
1	200	181	500
2	42E	4	0
3	468	466	500
4	91	33	0
5	97	131	0
6	221	210	0
7	154	163	0
8	23E	28	0

H,10,0

h	$|F_o|$	$|KF_c|$	α
0	211	236	0
1	89	68	500
2	36E	59	500
3	361	343	500
4	45E	58	0
5	68E	13	0
6	79*	28	0

H,11,0

h	$|F_o|$	$|KF_c|$	α
1	71	72	500
2	87	53	500
3	168	145	500
4	61*	100	0

H,0,1

h	$|F_o|$	$|KF_c|$	α
2	410	404	995
4	233	231	38
6	157	155	776
8	249	236	917
10	277	272	25
12	364	396	952

H,1,1

h	$|F_o|$	$|KF_c|$	α
0	262	267	986
1	240	244	999
2	306	309	4
3	65	59	963
4	177	187	149
5	145	101	950
6	346	340	993
7	377	380	28
8	482	470	938
9	172	168	19
10	122	97	140
11	61*	27	7
12	257	263	982

H,2,1

h	$|F_o|$	$|KF_c|$	α
1	451	466	20
2	45	36	68
3	451	468	952
4	338	342	971
5	400	403	81
6	256	253	8
7	401	405	947
8	83	103	805
9	73	110	11
10	81	65	33
11	72	78	996
12	184	206	920

H,3,1

h	$|F_o|$	$|KF_c|$	α
0	208	206	808
1	239	237	804
2	354	355	817
3	192	193	237
4	387	389	905
5	383	383	982
6	137	117	975
7	133	113	182
8	149	128	35
9	253	250	896
10	239	236	911
11	236	240	920
12	106	153	909

h	$\lvert F_O \rvert$	$\lvert KF_C \rvert$	α		h	$\lvert F_O \rvert$	$\lvert KF_C \rvert$	α		h	$\lvert F_O \rvert$	$\lvert KF_C \rvert$	α
					0	366	377	500		3	199	172	56
					1	106	117	886		4	408	396	970
	H,4,1				2	98	185	4		5	291	277	88
1	223	202	901		3	65*	110	164		6	335	330	53
2	272	277	221		4	174	172	910		7	449	444	947
3	70	70	849		5	253	238	0		8	469	467	392
4	371	345	122		6	255	235	4		9	129	121	148
5	158	153	176		7	55*	55	940		10	120	172	796
6	601	595	926							11	150	156	955
7	177	198	994			**H,10,1**							
8	282	282	874		1	165	179	46			**H,4,2**		
9	177	153	18		2	74	64	896		0	207	180	135
10	177	105	973		3	122	101	166		1	117	94	207
11	109	107	868		4	16*	3	66		2	248	244	783
					5	223	180	862		3	220	201	972
	H,5,1				6	92	81	918		4	114	125	165
0	499	510	25							5	318	317	11
1	280	270	157			**H,11,1**				6	540	529	943
2	286	293	970		0	127	147	750		7	173	173	971
3	298	307	943		1	50E	97	872		8	308	299	955
4	102	106	774		2	118	102	212		9	38E	87	116
5	372	355	964		3	69*	90	108		10	50*	53	802
6	433	398	2							11	56E	72	957
7	415	395	70			**H,0,2**							
8	77	30	786		0	636	615	917			**H,5,2**		
9	325	305	909		2	622	656	75		1	57*	43	982
10	77	28	77		4	453	454	964		2	224	206	906
11	94	161	880		6	295	280	68		3	171	154	938
					8	196	194	157		4	152	106	937
	H,6,1				10	356	348	101		5	235	236	44
1	97	122	871		12	223	248	30		6	57*	29	883
2	51*	63	119							7	53E	34	911
3	258	230	39			**H,1,2**				8	140	145	924
4	232	225	755		1	222	226	120		9	138	142	975
5	391	381	992		2	65	119	205		10	145	200	901
6	119	125	335		3	272	266	909					
7	355	367	991		4	427	427	932			**H,6,2**		
8	147	125	102		5	402	396	129		0	282	268	931
9	13*	101	890		6	262	226	70		1	238	258	807
10	167	131	29		7	320	292	46		2	298	276	36
					8	298	281	42		3	206	219	813
	H,7,1				9	61*	42	996		4	156	155	8
0	168	149	248		10	156	201	813		5	340	369	993
1	323	340	904		11	67E	72	795		6	84	103	829
2	312	356	967		12	88	61	77		7	112	83	113
3	117	150	105							8	65*	69	20
4	222	206	2			**H,2,2**				9	225	225	78
5	163	170	935		0	328	343	983		10	154	184	905
6	119	65	794		1	157	135	25					
7	95	84	957		2	66	69	761			**H,7,2**		
8	91	86	834		3	143	141	13		1	476	496	983
9	76*	102	887		4	112	120	773		2	76	117	220
10	43E	74	775		5	358	350	18		3	188	167	63
					6	318	307	886		4	162	214	245
	H,8,1				7	150	169	129		5	246	297	877
1	239	305	8		8	352	338	49		6	164	164	201
2	207	241	974		9	11E	43	822		7	186	194	118
3	229	270	960		10	138	124	839		8	177	221	54
4	101	131	957		11	329	359	1		9	183	164	172
5	44E	84	778		12	51E	107	113					
6	45*	47	217								**H,8,2**		
7	152	152	123			**H,3,2**				0	369	358	844
8	209	178	66		1	241	243	71		1	104	94	60
9	279	255	961		2	249	309	987		2	99	126	245
	H,9,1												

h	$|F_O|$	$|KF_C|$	α		h	$|F_O|$	$|KF_C|$	α		h	$|F_O|$	$|KF_C|$	α

H,8,2

3	175	157	973
4	140	140	105
5	80	116	177
6	180	175	29
7	140	155	139
8	27E	39	750

H,9,2

1	138	134	965
2	95	97	123
3	187	168	881
4	154	178	34
5	9*	76	57
6	107	105	926
7	252	278	14

H,10,2

0	153	117	112
1	245	176	113
2	143	145	87
3	233	228	929
4	24*	11	947
5	47*	78	250

H,11,2

| 1 | 126 | 134 | 23 |

H,0,3

2	407	406	991
4	237	200	198
6	271	234	214
8	309	289	139
10	322	324	500

H,1,3

0	363	350	137
1	218	193	909
2	429	427	952
3	155	111	20
4	344	361	99
5	113	57	881
6	385	383	969
7	328	329	0
8	216	225	937
9	196	227	35
10	123	174	966
11	78E	70	143

H,2,3

1	504	515	946
2	252	259	996
3	124	118	920
4	373	370	3
5	444	435	960
6	372	332	972
7	205	223	953
8	158	131	113
9	78*	80	153
10	57E	29	897
11	134	156	877

H,3,3

0	428	424	36
1	332	301	13
2	168	140	30
3	190	174	58
4	176	174	885
5	223	218	905
6	123	123	122
7	180	207	21
8	236	264	894
9	32*	11	137
10	104	113	997

H,4,3

1	135	150	9
2	206	213	49
3	166	228	138
4	577	611	993
5	224	227	974
6	136	152	943
7	126	152	60
8	53*	112	158
9	78*	62	990
10	71E	112	847

H,5,3

0	639	619	1
1	416	379	931
2	318	314	903
3	89	84	84
4	129	172	977
5	137	114	860
6	277	264	933
7	346	361	982
8	55*	42	115
9	13*	48	938
10	59E	104	104

H,6,3

1	125	125	954
2	192	176	914
3	245	239	883
4	135	155	918
5	224	260	938
6	121	112	873
7	337	323	40
8	111	148	968
9	57*	127	182

H,7,3

0	162	124	795
1	123	198	209
2	228	260	844
3	192	175	54
4	162	162	68
5	32*	133	106
6	167	179	8
7	69E	38	883
8	38E	53	198

H,8,3

1	165	142	959
2	198	185	949
3	111	106	143

4	73*	53	801
5	53*	100	825
6	129	106	128
7	158	168	970

H,9,3

0	373	333	33
1	66*	62	27
2	133	141	935
3	86	95	51
4	85	88	895
5	158	179	898

H,10,3

1	219	187	0
2	85E	51	200
3	245	223	44

H,0,4

0	575	559	953
2	640	630	940
4	204	207	889

H,1,4

1	124	139	775
1	113	139	775
2	33*	20	11
3	141	149	38
4	285	284	0

H,2,4

0	195	207	928
1	298	324	90
2	202	245	95
3	90	65	54

H,3,4

1	178	224	948
1	178	224	948
2	266	370	6
3	127	166	100

H,4,4

0	368	391	17
1	53E	20	171
2	145	207	44
3	74*	118	947

H,5,4

1	72*	40	994
2	59E	138	998
3	144	224	992

H,6,4

0	149	170	869
1	41E	17	809
2	15E	140	57
3	82	44	151

Table A-3 (Continued)

h	$|F_O|$	$|KF_C|$	α	h	$|F_O|$	$|KF_C|$	α	h	$|F_O|$	$|KF_C|$	α
					H,8,4				H,9,4		
	H,7,4			0	131	131	107	1	84*	90	821
1	245	297	962	1	180	103	129	2	68*	87	8
2	65*	55	85	2	79*	89	805				
3	70*	205	859	3	93	100	750				

Table A-4. Observed and calculated structure factors and calculated phases for the X-ray measurements on Li(NH₃OH)SO₄

Table A-4. Observed and calculated structure factors and calculated phases for the X-ray measurements on $Li(NH_3OH)SO_4$

h	$|F_o|$	KF_c	h	$|F_o|$	KF_c	h	$|F_o|$	KF_c
H,0,0			14	27*	-47	**H,1,1**		
2	461	-423	16	51*	-36			
4	937	-1021	18	124	126	1	236	249
6	769	792	20	153	158	2	980	-1019
8	1398	-1382	22	109	-122	3	993	-1013
10	1046	-1066				4	1234	1274
12	812	777	**H,5,0**			4	1239	1274
14	272	287				5	209	212
16	533	-534	2	184	-175	6	573	587
18	496	409	4	19*	34	7	355	376
20	299	283	6	102	90	8	455	-476
22	380	-382	8	444	-441	9	206	-194
24	220	216	10	113	-113	10	384	375
26	127	149	12	355	368	11	274	278
			16	132	-125	12	240	228
H,1,0			20	221	-212	13	384	384
			22	285	-278	14	731	-740
2	284	-309				15	208	-202
4	374	382	**H,6,0**			16	145	-151
6	21*	21				17	197	-204
8	572	554	0	253	-272	18	343	348
10	0*	-19	2	407	404	19	70	73
12	27*	-29	4	239	234	20	205	-203
14	100	-124	6	369	-376	21	113	-106
16	480	-493	8	103	-92	22	63*	56
18	267	263	10	127	131	23	78	-69
20	51*	-66	12	349	-364	24	346	327
22	69	79	14	28*	22	25	141	142
24	163	142	16	209	207			
			18	56*	-6	**H,2,1**		
H,2,0			20	47*	11			
						0	1078	-1055
0	1370	1479	**H,7,0**			1	543	-557
2	130	144				2	123	-90
4	1141	-1129	2	126	-127	3	613	-610
6	1133	1138	4	295	293	4	203	217
8	370	-374	6	132	118	5	330	-313
10	993	-870	8	242	-245	6	209	179
12	756	735	10	126	-137	7	131	-145
14	9*	-34	12	247	238	8	258	262
16	372	-361	14	183	-183	9	0*	14
20	128	114	16	44*	5	10	103	129
22	193	-209	18	256	254	11	285	293
24	0*	-1				12	126	-119
			H,8,0			13	166	181
H,3,0						14	287	-295
			0	315	-321	15	205	-206
2	0*	-32	2	370	374	16	227	-230
4	453	-421	4	304	308	17	110	118
6	524	521	6	647	-635	18	49	39
8	34*	-22	8	0*	-11	19	91	89
10	40*	-25	10	224	229	21	150	-145
12	422	424	12	230	-226	22	139	121
14	437	-437	14	55*	-39	23	70	74
16	207	-227	16	328	336	24	24*	-45
18	185	185				25	14*	25
20	59*	53	**H,9,0**					
22	176	-175				**H,3,1**		
24	315	307	2	49*	-55			
			4	36*	38	1	237	248
H,4,0			6	163	156	2	0*	-28
			8	104	-105	3	85	-96
0	165	170	10	95	108	4	440	439
2	503	-495	12	5*	-13	5	93	64
4	135	157				6	426	427
6	388	381	**H,10,0**			7	270	258
8	118	134				8	642	-613
10	147	-137	0	313	-312	9	395	-393
12	47*	-71	2	134	140			
			4	234	238			

h	$|F_O|$	KF_C	h	$|F_O|$	KF_C	h	$|F_O|$	KF_C
H,1,2			8	204	213	3	387	389
24	0*	-21	9	123	-135	4	181	-174
25	194	-175	10	181	176	5	173	-182
			11	118	-122	6	59	-44
H,2,2			12	158	164	7	341	-342
0	354	-377	13	97	106	8	155	152
1	8*	-36	14	48*	-51	9	238	240
2	399	-388	15	66	-50	10	39*	-50
3	285	-269	16	33*	-33	11	71	60
4	86	69	17	136	132	12	17*	-40
5	167	175	18	131	-123	13	168	-165
6	112	95	19	36*	18	14	77	86
7	114	87	20	147	-129	15	155	161
8	15*	-16	21	189	-187	16	0*	-19
9	471	-470	22	54*	31	17	94	95
10	470	463	23	49*	15	18	96	-83
11	513	509						
12	82	-83	**H,5,2**			**H,8,2**		
13	44*	-56	1	443	-434	0	59	68
14	78	-88	2	198	203	1	173	179
15	199	-197	3	687	692	2	103	-99
16	64	62	4	418	-426	3	132	-145
17	140	129	5	344	-339	4	45*	-41
18	107	-96	6	101	-106	5	252	-246
19	110	100	7	451	-443	6	100	92
20	174	-164	8	216	210	7	31*	47
21	212	-221	9	561	570	8	81	80
22	79	73	10	69	-87	9	223	226
23	0*	15	11	179	177	10	90	-89
24	72	60	12	36*	-35	11	98	-91
			13	361	-360	12	0*	22
H,3,2			14	212	208	13	41*	-32
1	571	-567	15	290	296	14	86	70
2	379	387	16	36*	-34	15	180	169
3	742	731	17	64	52			
4	55	-64	18	82	-77	**H,9,2**		
5	142	147	19	387	-390	1	0*	-12
6	89	-96	20	66*	69	2	7*	37
7	604	-589	21	58*	49	3	63*	40
8	337	337	22	0*	12	4	29*	28
9	691	695				5	48*	56
10	260	-263	**H,6,2**			6	47*	-11
11	205	-220	0	55	-52	7	76	-67
12	91	-83	1	34*	-40	8	0*	42
13	578	-586	2	23*	-22	9	0*	22
14	168	170	3	0*	24	10	62*	-25
15	311	316	4	84	-86	11	56*	-53
16	64	-74	5	227	-231			
17	189	189	6	90	89	**H,10,2**		
18	66	-64	7	33*	1	0	34*	-21
19	213	-210	8	35*	38	1	95	82
20	62*	66	9	15*	7			
21	163	153	10	31*	-12	**H,1,3**		
22	47*	-9	11	36*	-14	1	196	-222
23	99	110	12	18*	25	2	133	-130
24	47*	-35	13	22*	22	3	154	183
			14	58	50	4	111	-101
H,4,2			15	142	157	5	271	266
0	318	-323	16	71	-79	6	44	40
1	53	47	17	27*	3	7	130	-130
2	205	-208	18	54*	-31	8	4*	8
3	272	274	19	62*	-67	9	80	-84
4	32*	-44	20	0*	39	10	28*	85
5	393	386				11	166	168
6	25*	-15	**H,7,2**			12	102	109
7	171	-191	1	101	-107			
			2	111	126			

h	$|F_O|$	KF_C	h	$|F_O|$	KF_C	h	$|F_O|$	KF_C
H,3,1			**H,6,1**			7	200	-196
10	76	78	0	323	-316	8	356	365
11	140	-137	1	177	-175	9	157	158
12	143	122	2	308	319	10	99	-95
13	61	50	3	174	176	11	45*	31
14	269	-267	4	138	125	12	197	-194
15	136	-126	5	314	316			
16	123	130	6	394	-399	**H,10,1**		
17	85	81	7	64	-71	0	91	-86
18	132	134	8	56	-41	1	34*	-38
19	148	149	9	189	-187	2	0*	-13
20	110	-107	11	83	72	3	38*	-29
21	43*	42	12	45*	3	4	0*	11
22	83	-86	13	0*	32			
23	85	-86	14	155	-165	**H,0,2**		
24	163	150	15	203	-203	0	561	-564
			16	256	254	1	930	-976
H,4,1			17	145	157	2	40	-28
0	101	-97	18	92	-102	3	910	-910
1	0*	-11	19	59*	63	4	162	159
2	62	-61	20	252	-234	5	374	-326
3	131	-130				6	18*	-46
4	402	384	**H,7,1**			7	330	-341
5	372	371	1	194	-193	8	47	47
6	267	-273	2	400	391	9	188	182
7	24*	24	3	191	189	10	83	74
8	176	-164	4	242	-251	11	342	347
9	270	-262	5	131	-146	12	0*	-1
10	426	417	6	101	104	13	432	453
11	290	287	7	46*	-46	14	328	-331
12	313	-319	8	303	300	15	523	-533
13	57	-67	9	201	209	16	242	248
14	110	-107	10	67	-76	17	208	201
15	251	-259	11	92	92	18	24*	-1
16	238	235	12	218	-220	19	215	213
17	128	130	13	54*	-49	20	193	-193
18	30*	-23	14	68	67	21	351	-342
19	86	77	15	0*	30	22	179	183
20	168	-167	16	53*	-49	23	153	152
21	169	-172	17	1*	1	24	0*	-16
22	153	153	18	215	-217	25	112	113
23	53*	81						
			H,8,1			**H,1,2**		
H,5,1			0	142	-127	1	405	-400
1	75	-74	1	50*	-46	2	525	518
2	214	205	2	44*	-23	3	901	878
3	7*	-37	3	101	-95	4	90	-78
4	349	341	4	126	138	5	295	-283
5	156	149	5	67	69	6	331	330
6	58	-63	6	126	-126	7	165	154
7	40*	-25	7	64	-72	8	8*	-21
8	144	157	8	55*	-26	9	73	-76
9	89	109	9	98	-101	10	71	-67
10	221	-228	10	215	221	11	153	-152
11	74	-78	11	138	132	12	117	-115
12	113	-119	12	111	-130	13	368	-374
13	102	-109	13	0*	-2	14	25*	10
14	90	86	14	31*	-6	15	99	92
15	34*	38	15	31*	-29	16	19*	-11
16	53*	-64				17	224	234
17	50*	-23	**H,9,1**			18	67	-68
18	56*	5	1	72	-70	19	55	-53
19	72	74	2	253	250	20	57	47
20	0*	-22	3	195	188	21	101	111
21	0*	5	4	176	-182	22	26*	9
22	31*	13	5	40*	-61	23	50*	49

h	$|F_O|$	KF_C
H,1,3		
13	454	-450
14	75	-77
15	26*	-6
16	79	-74
17	468	475
18	48*	61
19	223	-220
20	37*	-29
21	23*	-38
22	0*	-29
23	262	253
24	53*	60
H,2,3		
0	536	-533
1	1029	995
2	207	-204
3	172	160
4	67	61
5	610	-591
6	78	71
7	412	403
8	260	259
9	81	-87
10	187	185
11	506	-507
12	33*	-37
13	227	223
14	37*	-36
15	414	411
16	19*	12
17	229	-244
18	65	-57
19	28*	13
20	0*	-32
21	125	124
22	0*	-0
23	257	-240
24	51*	-27
H,3,3		
1	240	239
2	207	-217
3	40*	79
4	291	-291
5	67	82
6	239	-239
7	565	-565
8	202	-208
9	74	69
10	0*	18
11	132	109
12	187	192
13	172	-174
14	152	150
15	133	143
16	115	112
17	111	115
18	83	71
19	121	-129
20	89	-80
21	20*	-53
22	109	-107
23	223	203

h	$|F_O|$	KF_C
H,4,3		
0	70	-61
1	640	636
2	149	146
3	252	247
4	107	107
5	862	-856
6	156	-159
7	529	545
8	36*	-36
9	345	343
10	36*	25
11	789	-793
13	352	363
14	28*	5
15	237	238
15	240	238
16	81	77
17	380	-372
18	0*	4
19	80	77
20	0*	7
21	223	221
22	18*	44
H,5,3		
2	47*	-53
3	231	248
4	58	-49
5	293	-297
6	95	-96
7	49*	-40
8	75	-78
9	118	-128
10	32*	-13
11	34*	5
12	63	55
13	85	76
14	78	71
15	33*	25
16	83	78
17	36*	46
18	31*	19
19	86	-96
20	36*	-41
21	55*	65
H,6,3		
0	52	42
1	611	606
2	133	135
3	100	-107
4	66	61
5	548	-547
6	172	-172
7	461	471
8	58	-63
9	211	208
10	27*	2
11	312	-310
12	46*	-45
14	44*	12
15	190	196
16	78	68
17	350	-351
18	0*	-19
19	36*	-20

h	$|F_O|$	KF_C
H,7,3		
1	69	63
2	21*	10
3	149	-146
4	44*	-9
5	102	104
6	23*	-0
7	78	64
8	27*	41
9	27*	-17
10	45*	29
11	184	-189
12	59*	-39
13	82	84
14	0*	-1
15	71	70
16	25*	-4
17	162	-161
H,8,3		
0	82	-71
1	79	82
2	13*	-8
3	89	68
4	0*	1
5	185	-192
6	18*	-16
7	82	77
8	29*	22
9	148	138
10	60*	57
11	199	-198
12	0*	6
13	80	91
14	46*	11
H,9,3		
2	15*	-21
3	115	-119
4	74	-87
5	34*	-24
6	56*	-72
7	243	250
8	61*	35
9	143	-148
H,0,4		
0	743	-745
1	688	691
2	248	255
3	89	-108
4	287	291
5	252	-250
6	93	-81
7	107	100
8	33*	20
9	10*	-8
10	216	215
11	244	-254
12	297	-298
13	0*	9
14	297	-296
15	348	358
16	364	377
17	123	-123

h	$\lvert F_O \rvert$	KF_C	h	$\lvert F_O \rvert$	KF_C	h	$\lvert F_O \rvert$	KF_C
	H,0,4		9	381	-372	7	13*	-7
18	56	43	10	221	-239	8	59	9
19	106	-93	11	96	-90	9	80	-71
20	142	-151	12	206	-204	10	134	-128
21	194	203	13	400	398	11	74	76
22	247	237	14	313	310	12	72	56
23	159	-150	15	230	-231	13	40*	-28
			16	36*	-9	14	37*	56
	H,1,4		17	61	-70	15	42*	-44
			18	75	-76	16	52*	-45
1	425	415	19	164	160	17	0*	16
2	330	325	20	50*	45			
3	235	-221	21	21*	-7		**H,7,4**	
5	111	112	22	23*	23			
6	36*	39				1	80	77
7	158*	-163		**H,4,4**		2	125	123
8	28*	-49				4	210	-220
9	200	-191	0	73	56	5	87	83
10	146	-145	1	259	274	6	50*	-55
11	58	-53	2	277	289	7	160	159
12	24*	-32	3	0*	11	8	184	179
13	58	72	4	16*	-15	9	79	-88
14	99	106	5	98	108	10	18*	19
15	83	63	6	206	-231	11	93	-101
16	133	141	7	199	221	12	109	-106
17	149	-154	8	155	-152	13	167	160
18	117	-107	9	111	115	14	107	107
19	213	201	10	36*	51	15	95	-99
20	68	60	11	126	-125			
21	57*	-57	12	24*	3		**H,8,4**	
23	0*	-14	13	135	-135			
			14	35*	33	0	156	153
	H,2,4		15	89	-91	1	145	-142
			16	82	79	2	66	-65
0	26*	15	17	122	-110	3	13*	12
1	73	78	18	24*	-46	4	106	-98
2	55	54	19	50*	3	5	213	214
3	402	401	20	73	-70	6	205	207
4	383	376	21	162	159	7	125	-125
5	235	-229				8	0*	9
6	320	-328		**H,5,4**		9	117	-99
7	263	283				10	184	-184
8	139	-124	1	63	60	11	77	80
9	189	193	2	285	279			
10	225	228	3	429	-434		**H,9,4**	
11	394	-395	4	277	-282			
12	249	-253	5	126	122	1	0*	41
13	17*	2	6	85	-74	2	46*	31
14	110	-105	7	409	405	3	47*	40
15	77	73	8	366	370	4	22*	36
16	261	264	9	194	-196	5	54*	-68
17	177	-171	10	92	-101			
18	36*	-24	11	29*	-4		**H,1,5**	
19	0*	10	12	139	-146			
20	84	-91	13	238	245	1	20*	39
21	146	147	14	126	123	2	938	928
22	142	152	15	123	-128	3	248	-249
23	0*	16	16	41*	-35	4	402	-395
			17	209	-206	5	126	133
	H,3,4		18	175	-187	6	35*	-4
			19	228	236	7	151	153
1	352	333				8	583	590
2	444	426		**H,6,4**		9	68	-76
3	294	-273				10	416	-423
4	100	-87	0	152	148	11	62	60
5	75	-86	1	99	-102	12	350	-352
6	126	-123	3	13*	19	13	80	67
7	289	288	4	38*	-38	14	412	431
8	254	242	5	58	51	15	89	-112
			6	38*	21			

h	$|F_O|$	KF_C	h	$|F_O|$	KF_C	h	$|F_O|$	KF_C
H,1,5			12	158	165	5	48*	31
			13	30*	24	6	100	116
16	82	-76	14	167	159	7	0*	29
17	60*	-41	15	38*	-46	8	92	82
18	296	-290	16	208	-212			
19	26*	46	17	42*	57	**H,0,6**		
20	266	253	18	38*	1			
21	54*	-35	19	41*	34	0	766	764
						1	202	198
H,2,5			**H,5,5**			2	407	-417
						3	10*	-9
0	271	244	1	46*	-44	4	508	-505
1	35*	-21	2	70	-67	5	297	-301
2	109	-108	3	63	-61	6	622	620
3	93	88	4	87	-98	7	32*	36
4	189	-178	5	48*	44	9	35*	-31
5	136	125	6	113	117	10	180	-185
6	38*	-6	7	11*	-10	11	126	-131
7	40*	43	8	-74	-66	13	176	167
8	65	64	9	103	96	14	192	200
9	44*	-42	11	42*	35	15	234	211
10	15*	-8	12	4*	31	16	467	-461
11	14*	-16	13	34*	6	17	0*	-38
12	157	152	14	137	-131	18	107	109
13	34*	8	15	0*	10	19	0*	-13
14	252	254	16	0*	8	20	82	92
15	109	-114	17	81	-70			
16	262	-253	18	13*	-50	**H,1,6**		
17	25*	35						
18	139	-121	**H,6,5**			1	105	108
19	0*	38				2	239	-238
20	88	95	0	260	266	3	12*	-0
21	56*	-66	1	92	-84	4	36*	23
			2	153	-154	5	38*	-53
H,3,5			3	14*	-32	6	162	-170
			4	98	-85	7	55	-60
1	103	-120	5	15*	2	8	69	81
2	189	195	6	231	239	9	6*	-37
3	142	-161	7	50*	-37	10	41*	-38
4	315	-325	8	54*	48	11	18*	-21
5	12*	10	9	52*	-15	12	167	156
6	207	-215	10	243	-237	13	74	78
7	210	212	11	47*	32	14	22*	-23
8	468	465	12	55*	-54	15	26*	12
9	32*	33	13	88	74	16	87	-89
10	119	-134	14	171	168	17	55*	-40
11	124	132	15	54*	-77	18	126	126
12	117	-118				19	43*	11
13	83	90	**H,7,5**					
14	231	231				**H,2,6**		
15	87	-163	1	77	-69			
16	129	-139	2	248	-245	0	444	456
17	69	-55	3	101	102	1	137	122
18	99	-102	4	404	398	2	176	-165
19	60*	-55	5	69	-59	3	57	-60
20	118	122	6	93	74	4	321	-322
			7	0*	5	6	370	373
H,4,5			9	73	59	7	44*	44
			10	68	74	8	28*	21
0	140	128	11	0*	-1	10	440	-446
1	0*	2	12	86	-82	11	84	-87
2	72	81	13	19*	-32	12	415	412
3	100	-104				13	117	117
4	266	-260	**H,8,5**			14	0*	-18
5	42*	25				15	106	96
7	0*	-13	0	40*	19	16	231	-228
8	117	121	1	47*	20	17	25*	-44
9	123	-122	2	0*	-14	18	145	144
10	369	-367	3	29*	-11	19	37*	-13
11	125	126	4	117	-122			

h	$\|F_o\|$	KF_c	h	$\|F_o\|$	KF_c	h	$\|F_o\|$	KF_c
H,3,6			9	0*	-5	11	74	-62
			10	173	161	12	80	83
1	117	122	11	101	92	13	94	86
2	168*	-160	12	113	-107	14	95	-94
3	40*	-25	13	0*	19	15	59*	-57
4	92	-101						
5	73	-77	**H,7,6**			**H,4,7**		
6	197	201						
7	0*	9	1	0*	3	0	158	-164
8	238	-230	2	126	-143	1	201	-200
9	85	-82	3	78	-75	2	8*	27
10	87	78	4	150	139	3	115	-111
11	43*	-36	5	49*	33	4	167	167
12	227	212	6	91	70	5	261	251
13	105	121	7	93	98	6	184	-189
14	161	-156	8	191	-186	7	134	-141
16	104	-99	9	52*	-38	8	33*	-1
17	83	-86				9	170	-178
18	187	179	**H,1,7**			10	199	203
						11	285	285
H,4,6			1	333	341	12	168	-164
			2	219	-211	13	47*	-55
0	63	74	3	224	-225	14	60*	3
1	24*	-27	4	153	156			
2	28*	-38	5	38*	-0	**H,5,7**		
3	89	-92	6	84	84			
4	49*	-52	7	69	68	1	35*	-6
5	104	-115	8	191	-196	2	12*	3
6	168	171	9	310	-306	3	26*	21
7	32*	28	10	58	32	4	34*	16
8	57	-65	11	103	-93	5	65*	57
9	54*	69	12	159	160	6	86	-84
10	55*	-55	13	230	239	7	44*	-49
11	62	44	14	172	-169	8	73	69
12	74	-76	15	71	-56	9	0*	26
13	37*	17	16	55*	-34	10	44*	-52
14	41*	38	17	70	-93	11	84	-82
15	54*	-5				12	0*	-11
16	42*	-47	**H,2,7**					
17	0*	-42				**H,6,7**		
			0	213	-205			
H,5,6			1	205	-200	0	235	-234
			2	93	92	1	216	-214
1	14*	-1	3	29*	-42	2	137	139
2	151	-145	4	79	79	3	48*	11
3	84	-87	5	207	200	4	93	91
4	235	242	6	117	-114	5	228	227
5	29*	20	7	44*	-19	6	179	-179
6	145	150	8	31*	36	7	176	-179
7	130	128	9	21*	-8	8	39*	41
8	205	-193	10	83	63			
9	41*	-35	11	145	150	**H,0,8**		
10	27*	-52	12	55*	-59			
11	86	-70	13	75	-61	0	68*	-81
12	191	193	14	15*	-55	1	261	-251
13	93	86	15	247	-241	2	0*	10
14	176	-176	16	92	99	3	35*	28
15	20*	-31				4	34*	-36
			H,3,7			5	187	187
H,6,6						6	0*	3
			1	53*	32	7	68	45
0	254	-245	2	66	-48	8	0*	26
1	73	-77	3	108	-110	9	109	-105
2	0*	15	4	12*	25	10	52*	52
3	88	-80	5	0*	17	11	124	130
4	163	158	6	106	109	12	81	69
5	0*	4	7	201	187	13	0*	32
6	228	-219	8	160	-158			
7	89	-85	9	133	-136			
8	106	116	10	42*	26			

Table A-4 (Continued)

h	$|F_O|$	KF_C	h	$|F_O|$	KF_C	h	$|F_O|$	KF_C
	H,1,8			**H,3,8**		3	401	396
						4	40*	3
1	168	-165	1	231	-240	5	147	-140
2	32*	-14	2	0*	-16			
3	199	196	3	351	350		**H,1,9**	
4	106	-97	4	70	-55			
5	81	-72	5	37*	-45	1	122	-129
6	0*	-5	6	24*	-40	2	140	-137
7	27*	-9	7	252	-249	3	146	148
8	60*	-8	8	30*	47	4	0*	-13
9	114	122	9	315	323	5	39*	-7
10	36*	21	10	0*	0	6	14*	26
11	33*	-23	11	0*	-24	7	98	-100
12	29*	38						
13	103	-92		**H,4,8**			**H,2,9**	
			0	21*	-21	0	137	-135
	H,2,8		1	57*	-67	1	229	225
			2	37*	25	2	50*	53
0	56*	41	3	113	108	3	53*	40
1	26*	0	4	0*	3	4	86	89
2	46*	-40	5	90	90	6	77	-68
3	109	-95	6	26*	33			
4	30*	33	7	49*	-11		**H,3,9**	
5	247	238	8	0*	4			
6	0*	2	9	79	-86	1	105	-89
7	0*	-17				2	0*	-31
8	0*	-18		**H,5,8**				
9	160	-163						
10	38*	32	1	179	-176			
11	158	154	2	70*	67			
12	10*	-20						

Table A-9.   Observed and Calculated structure
factors and calculated phases for the
X-ray measurements on $(N_2H_6)BeF_4$

185

ℓ	|Fo|	KFc	ℓ	|Fo|	KFc	ℓ	|Fo|	KFc
0,0,L			5	187	-181	8	36*	-25
			6	67	-59	9	11*	-22
2	44	17	7	29*	-29	10	18*	10
4	665	-683	8	49	-51	11	48*	34
6	270	-264	9	25*	45			
8	236	-228				**1,2,L**		
10	102	108	**0,6,L**					
						-11	0*	23
0,1,L			0	319	307	-10	49	37
			1	110	100	-9	0*	15
1	0*	8	2	82	75	-8	92	-98
2	110	-79	3	67	70	-7	78	76
3	61	75	4	141	-137	-6	34*	-26
4	392	-392	5	69	-65	-5	23*	16
5	74	-74	6	139	-144	-4	229	233
6	16*	6	7	59	63	-3	161	165
7	49	-50	8	16*	-10	-2	0*	-13
8	116	107				-1	380	-383
9	100	105	**0,7,L**			0	0*	-5
10	92	95				1	436	-435
11	32*	-22	1	31*	-10	2	27*	36
			2	182	-182	3	364	359
0,2,L			3	31*	-30	4	103	-97
			4	89	-83	5	18*	13
0	502	-476	5	92	90	6	19*	-22
1	117	116	6	16*	-27	7	100	95
2	286	-288				8	32*	-20
3	667	-681	**0,8,L**			9	71	67
4	190	193				10	23*	-29
5	273	-278	0	153	-152			
6	310	313	1	17*	16	**1,3,L**		
7	319	318	2	33*	-28			
8	19*	1	3	97	-97	-11	0*	-1
9	153	151	4	86	90	-10	54	-37
10	50	-44				-9	81	-84
11	0*	15	**1,0,L**			-8	14*	-10
						-7	93	-94
0,3,L			-10	18*	-0	-6	79	82
			-8	72	-55	-5	38*	-16
1	406	-405	-6	23*	0	-4	167	-168
2	55	51	-4	275	291	-3	225	235
3	374	368	-2	440	-431	-2	77	94
4	303	296	0	0*	4	-1	360	360
5	35*	24	2	422	417	0	248	248
6	56	53	4	570	-574	1	492	-499
7	28*	9	6	143	149	2	154	-154
8	161	-157	8	239	238	3	71	-71
9	35*	-21	10	69	-54	4	107	-110
10	35*	-24				5	176	180
			1,1,L			6	40*	40
0,4,L						7	68	-66
			-11	52	-48	8	15*	-12
0	270	-265	-10	52	38	9	51	42
1	226	227	-9	87	88	10	29*	16
2	48	-52	-8	167	-168			
3	275	280	-7	178	180	**1,4,L**		
4	38*	48	-6	198	-198			
5	18*	10	-5	279	-285	-10	74	72
6	169	165	-4	150	-155	-9	55	49
7	87	-87	-3	108	-111	-8	31*	-26
8	38*	35	-2	301	293	-7	14*	-29
9	155	-149	-1	58	-38	-6	67	58
10	105	-101	0	151	124	-5	60	-69
			1	47	39	-4	92	-82
0,5,L			2	290	286	-3	132	133
			3	221	233	-2	205	-213
1	223	220	4	39	-38	-1	35*	31
2	158	-148	5	53	47	0	48	57
3	70	-68	6	219	-223	1	61	51
4	196	191	7	113	-114			

ℓ	|F_o|	KF_c		ℓ	|F_o|	KF_c		ℓ	|F_o|	KF_c
1,4,L				**1,8,L**				6	67	64
								7	100	-99
2	99	100		-4	61	56		8	29*	13
3	33*	24		-3	80	71		9	73	79
4	126	115		-2	147	140		10	59	-70
5	101	-99		-1	21*	-3				
6	47*	-5		0	51*	-50		**2,3,L**		
7	42*	-47		1	39*	-37				
8	40*	-29		2	90	-86		-10	41*	8
9	0*	14		3	57	53		-9	32*	38
				4	30*	2		-8	64	-70
1,5,L								-7	257	261
				2,0,L				-6	137	109
-9	21*	-35						-5	254	258
-8	23*	25		-10	99	112		-4	113	108
-7	73	76		-8	0*	-11		-3	70	-67
-6	171	173		-6	68	-62		-2	205	-200
-5	101	92		-4	61	-64		-1	389	-399
-4	29*	10		-2	23*	-23		0	172	155
-3	0*	-19		0	148	-138		1	368	-376
-2	202	-209		2	380	389		2	24*	-2
-1	37*	14		4	4*	-12		3	131	-122
0	92	89		6	315	-311		4	167	-151
1	19*	-14		8	146	146		5	444	451
2	153	-152		10	67	68		6	65	48
3	96	-93						7	196	198
4	54	40		**2,1,L**				8	33*	21
5	56	-73						9	122	-126
6	188	185		-11	108	107				
7	25*	20		-10	33*	6		**2,4,L**		
8	94	-83		-9	129	-124				
9	70	73		-8	286	-288		-10	33*	31
				-7	62	-51		-9	71	66
1,6,L				-6	99	-95		-8	44*	-11
				-5	142	-143		-7	177	180
-8	25*	34		-4	525	545		-6	128	-131
-7	106	-108		-3	270	-253		-5	232	-229
-6	25*	-5		-2	348	361		-4	126	115
-5	48	-39		-1	612	647		-3	271	-274
-4	16*	-42		0	150	-108		-2	33*	16
-3	74	80		1	242	243		-1	37*	-26
-2	17*	-24		2	566	-573		0	22*	21
-1	108	-104		3	183	-170		1	92	90
0	27*	17		4	178	-181		2	88	61
1	42*	35		5	122	-119		3	273	270
2	40*	46		6	121	126		4	122	-104
3	82	89		7	150	-137		5	95	95
4	54	-50		8	151	155		6	45*	-20
5	73	-70		9	25*	14		7	78	-84
6	0*	5		10	89	85		8	24*	13
7	32*	-42						9	74	-76
8	41*	34		**2,2,L**						
								2,5,L		
1,7,L				-11	26*	15				
				-10	25*	-32		-9	39*	-25
-6	21*	18		-9	12*	3		-8	82	82
-5	91	-86		-8	72	65		-7	108	-101
-4	33*	-19		-7	106	-107		-6	34*	23
-3	47	-36		-6	57	-51		-5	67	-59
-2	26*	-27		-5	43	32		-4	127	-127
-1	68	-79		-4	174	170		-3	72	-11
0	61	69		-3	142	140		-2	269	-259
1	118	118		-2	65	51		-1	100	97
2	-41*	-14		-1	236	231		0	46*	44
3	81	82		0	328	-336		1	218	213
4	10*	-4		1	231	-232		2	324	325
5	19*	1		2	35*	-15		3	51	8
6	27*	33		3	119	-117		4	14*	-13
				4	119	118		5	139	-144
				5	60	55		6	37*	-9

ℓ	$\|F_O\|$	KF_C	ℓ	$\|F_O\|$	KF_C	ℓ	$\|F_O\|$	KF_C
	2,5,L		-4	13*	-0	-1	90	-86
			-3	84	-81	0	164	-171
7	65	-69	-2	44	35	1	98	-92
8	62	-52	-1	168	-172	2	129	-127
	2,6,L		0	178	-172	3	39*	-36
			1	165	162	4	0*	-17
-8	20*	-43	2	21*	21	5	97	97
-7	28*	9	3	132	-132	6	0*	-9
-6	21*	-8	4	46	44	7	0*	35
-5	21*	-6	5	23*	13	8	79	86
-4	61	-69	6	91	91			
-3	277	279	7	76	78		3,5,L	
-2	45*	15	8	23*	-1			
-1	86	82	9	16*	-16	-8	29*	-39
0	90	94				-7	0*	-8
1	243	-252		3,2,L		-6	0*	2
2	79	59				-5	56	-62
3	71	-71	-10	73	-70	-4	42*	47
4	42*	-33	-9	42*	5	-3	84	-85
5	30*	-34	-8	16*	15	-2	24*	-4
6	94	-100	-7	171	-166	-1	96	-100
7	0*	1	-6	72	-60	0	44*	-48
			-5	277	-275	1	30*	40
	2,7,L		-4	97	-97	2	54	56
			-3	171	164	3	152	152
-6	42*	-49	-2	221	225	4	37*	5
-5	65	-53	-1	320	326	5	0*	26
-4	119	121	0	0*	-9	6	83	-95
-3	29*	3	1	196	192	7	27*	-30
-2	29*	42	2	103	-105			
-1	36*	44	3	160	-158		3,6,L	
0	10*	-20	4	60	59			
1	49*	-51	5	90	-98	-7	39*	43
2	34*	-50	6	0*	17	-6	32*	-8
3	26*	19	7	42*	-47	-5	0*	-21
4	66	-69	8	0*	9	-4	29*	-18
5	18*	-39	9	44*	-38	-3	89	-98
						-2	104	-106
	2,8,L			3,3,L		-1	111	116
			-10	22*	-18	0	36*	23
-3	27*	-15	-9	81	-87	1	47*	-51
-2	38*	-12	-8	18*	15	2	80	69
-1	47*	47	-7	9*	37	3	0*	-4
0	45*	-48	-6	37*	-27	4	32*	34
1	50*	-35	-5	33*	7	5	135	131
2	81	-100	-4	142	142			
			-3	0*	3		3,7,L	
	3,0,L		-2	75	-78			
			-1	103	101	-5	23*	37
-10	140	136	0	145	-142	-4	0*	13
-8	167	168	1	37	89	-3	0*	32
-6	84	-90	2	156	159	-2	47*	60
-4	88	-100	3	82	-82	-1	44*	46
-2	207	-203	4	47*	-36	0	30*	-13
0	44	-46	5	99	-104	1	21*	-24
2	179	185	6	0*	-23	2	16*	14
4	236	234	7	52	61	3	72	-76
6	174	-167	8	48*	48			
8	139	-145					4,0,L	
				3,4,L				
	3,1,L					-10	39*	-18
			-9	91	-73	-8	74	-76
-11	20*	39	-8	23*	-12	-6	280	-273
-10	79	80	-7	171	176	-4	140	-137
-9	24*	5	-6	40*	37	-2	427	421
-8	137	140	-5	192	195	0	314	316
-7	101	-98	-4	88	85	2	41*	-11
-6	162	-163	-3	183	-180	4	155	-150
-5	213	215	-2	209	213	6	168	-157

ℓ	|F_o|	KF_c		ℓ	|F_o|	KF_c		ℓ	|F_o|	KF_c
	4,0,L			-6	89	86			5,2,L	
8	100	-97		-5	81	82				
				-4	30*	-23		-8	91	-90
	4,1,L			-3	150	-149		-7	32*	-28
				-2	66	-72		-6	71	67
-10	47*	-49		-1	130	-131		-5	0*	4
-9	90	84		0	5*	-1		-4	107	106
-8	27*	4		1	189	191		-3	94	-100
-7	33*	-26		2	73	-63		-2	41*	-35
-6	32*	8		3	79	71		-1	33*	-36
-5	59	-56		4	100	100		0	60	61
-4	55	-31		5	19*	-29		1	91	91
-3	110	109		6	22*	49		2	35*	-19
-2	282	283						3	16*	-15
-1	175	-168			4,5,L			4	105	-116
0	51	22						5	26*	5
1	46*	32		-7	66	-79				
2	191	-191		-6	39*	-26			5,3,L	
3	109	109		-5	71	-59				
4	90	-84		-4	55	50		-7	66	-62
5	86	-85		-3	46*	44		-6	16*	16
6	38*	-23		-2	0*	-3		-5	47*	54
7	45*	26		-1	75	79		-4	33*	14
8	62	61		0	85	-75		-3	164	161
				1	27*	11		-2	15*	18
	4,2,L			2	27*	1		-1	51	-59
				3	39*	-35		0	26*	14
-9	131	-126		4	60	65		1	73	-65
-8	62	60		5	30*	-48		2	74	-80
-7	16*	-10						3	45*	-31
-6	206	211			4,6,L			4	0*	3
-5	96	86						5	17*	-8
-4	65	-58		-5	16*	-3				
-3	128	123		-4	18*	-15			5,4,L	
-2	144	-143		-3	24*	-51				
-1	133	130		-2	100	95		-6	54	-54
0	66	-63		-1	0*	2		-5	70	64
1	182	-179		0	72	61		-4	24*	-3
2	125	-131		1	92	91		-3	114	111
3	195	-197		2	41*	38		-2	39*	-33
4	91	86		3	78	-72		-1	105	-109
5	18*	5						0	19*	31
6	133	128			5,0,L			1	19*	-26
7	148	151		-8	12*	14		2	46*	50
				-6	71	77		3	54	67
	4,3,L			-4	126	-130		4	52	-31
				-2	99	-97				
-9	50	-53		0	42*	43			5,5,L	
-8	67	45		2	31*	-42				
-7	40*	-40		4	65	73		-5	16*	-18
-6	65	-54		6	88	88		-4	52	-43
-5	132	130						-3	0*	23
-4	146	-143			5,1,L			-2	36*	-18
-3	0*	-13						-1	22*	-6
-2	21*	7		-8	93	-83		0	100	-97
-1	66	-46		-7	34*	37		1	28*	-41
0	48*	-35		-6	115	-115		2	24*	-26
1	0*	3		-5	114	-114				
2	115	115		-4	79	-85			6,0,L	
3	18*	1		-3	39*	-45				
4	134	136		-2	104	101		-6	57*	-38
5	9*	-2		-1	44*	53		-4	0*	1
6	100	-89		0	284	287		-20	91	-96
7	21*	33		1	39*	-26		0	49*	46
				2	14*	-17		2	0*	39
	4,4,L			3	110	108				
				4	113	-113				
-8	0*	-0		5	0*	-1				
-7	30*	11		6	66	-49				

Table A-5 (Continued)

ℓ	$\lvert F_O \rvert$	KF_C	ℓ	$\lvert F_O \rvert$	KF_C	ℓ	$\lvert F_O \rvert$	KF_C
	6,1,L			6,2,L			6,3,L	
-5	51	-44	-5	38*	-42	-4	44*	19
-4	65	56	-4	77	80	-3	57	-41
-3	27*	12	-3	72	65	-2	0*	-4
-2	29*	-14	-2	47*	-32	-1	106	-102
-1	111	116	-1	30*	-7	0	31*	-6
0	0*	-31	0	73	-63	1	120	-113
1	0*	22	1	47*	-21			
2	38*	-23	2	61	67			
3	81	-73						

APPENDIX B

COMPUTER PROGRAMMES USED IN THIS WORK

All calculations were carried out on the CDC 6400 computer at the University's computer centre. The punched paper control tapes for the neutron diffractometer were made on the PDP 9 and PDP 15 computers in the University's Tandem van der Graaff Accelerator Laboratory by kind permission of its director.

The FORTRAN programmes MACDIF and DIFDAT, used in the running of the neutron diffractometer, were written by us; and the MACRO programme ASTIG, for punching the paper tape, was written by Dr. L. Hughes and modified by Dr. J. C. Tippett. For the crystallographic calculations, extensive use was made of the University of Maryland's (1967, 1971) computing system XRAY 67 and XRAY 71. In addition, the local crystallographic least-squares programme CUDLS, written by Dr. J. S. Stephens, was used for refinements involving extinction. Some of the molecular geometry calculations and the thermal ellipsoid plot were made using ORTEP, the Oak Ridge National Laboratory's (1965) thermal ellipsoid plotting programme. The bond-strength summation programme BOST was written in FORTRAN by Dr. I. D. Brown.

REFERENCES

Anderson, M.R. and Brown, I.D. (1972) Acta Cryst. A28, 663.

Adrian, H. W. W. & Feil, D. (1969). Acta Cryst. A25, 438.

Ahmed, N. A. K., Liminga, R. & Olovsson, I. (1968).
Acta Chem. Scand. 22, 88.

Bacon, G. E. (1962). Neutron Diffraction., Second Edition.
Oxford University Press, London.

Bacon, G. E. & Pease, R. S.' (1955). Proc. Roy. Soc. London.
A230, 359.

Baur, W. H. (1965). Acta Cryst. 19, 909.

Baur, W. H. (1972). Acta Cryst. B28, 1456.

Bradley, A. J. (1925). Phil. Mag. 49, 1225.

Brown, I. D. (1964). Acta Cryst. 17, 654.

Brown, I. D. (1973). Private communication.

Brown, I. D. & Shannon, R. D. (1973). Acta Cryst. A29, 266.

Chung, S. J. & Hahn, Th. (1972). Mat. Res. Bull. 7, 1209.

Coppens, P. (1970). Thermal Neutron Diffraction
(Willis, B. T. M., Editor). Oxford University Press,
London.

Coster, D., Knol, K. S. & Prims, J. A. (1930). Z. Phys.
63, 345.

Cromer, D. T. & Mann, J. B. (1968). Acta Cryst. A24, 321.

Cuthbert, J. D. & Petch, H. E. (1963). Can. J. Phys.
41, 1629.

Dawson, B. (1970). Thermal Neutron Diffraction
(Willis, B. T. M., Editor). Oxford University Press,
London.

Dollase, W. A. (1969). Acta Cryst. B25, 2298.

Habuda, S. P. & Gagarinsky, Yu. V. (1971). Acta Cryst. B27, 1677.

Hahn, Th., Lohre, G. & Chung, S. J. (1969). Naturwissenschaften. 56, 459.

Hainsworth, F. N. & Petch, H. E. (1965). Solid State Comm. 3, 315.

Hamilton, W. C. (1964). Statistics in Physical Science. Ronald Press, New York.

Hamilton, W. C. & Ibers, J. A. (1968). Hydrogen Bonding in Solids. W. A. Benjamin, New York.

Hastings, R. N. & Oja, T. (1972). J. Chem. Phys. 57, 2139.

Howell, F. L. & Schmidt, V. H. (1969). J. Chem. Phys. 51, 1983.

Ibers, J. A. (1964). J. Chem. Phys. 40, 402.

International Tables for X-ray Crystallography (1952). Vol. I. Kynoch Press, Birmingham.

Johnson, C. K. (1970). Thermal Neutron Diffraction (Willis, B. T. M., Editor). Oxford University Press, London.

Jönsson, P.-G. & Hamilton, W. C. (1970). Acta Cryst. B26, 536.

Knispel, R. R. & Petch, H. E. (1970). Can. J. Phys. 49, 870.

Larson, A. C. (1967). Acta Cryst. 23, 664.

LeRoy, J. & Aléonard, S. (1972). Acta Cryst. B28, 1383.

Liminga, R. (1965). Acta Chem. Scand. 19, 1629.

Liminga, R. (1967). Acta Chem. Scand. 21, 1217.

Liminga, R. (1968). Arkiv Kemi. 28, 483.

Liminga, R. & Lundgren, J.-O. (1965). Acta Chem. Scand. 19, 1612.

Lipscomb, W. N. (1972). Trans. Am. Cryst. Assoc. 8, 79.

Lundgren, J.-O., Liminga, R. & Olovsson, I. (1968).
Arkiv Kemi. 30, 81.

MacClement, W. D., Pintar, M. & Petch, H. E. (1967).
Can. J. Phys. 45, 3257.

McGaw, B. L. & Ibers, J. A. (1963). J. Chem. Phys. 39,
2677.

Matthias, B. T. & Remeika, J. P. (1956). Phys. Rev.
103, 262.

Neutron Diffraction Commission (G. E. Bacon, Chairman).
(1969). Acta Cryst. A25, 391.

Neutron Diffraction Commission (G. E. Bacon, Chairman).
(1972). Acta Cryst. A28, 357.

Niizeki, N. & Koizumi, H. (1964). J. Phys. Soc. Japan.
19, 132.

Nilsson, Å., Liminga, R. & Olovsson, I. (1968).
Acta Chem. Scand. 22, 719.

Oak Ridge National Laboratory. (1965). Report No. ORNL-3794.
Johnson, C. K.

Padmanabhan, V. M. & Balasubramanian, R. (1967). Acta Cryst.
22, 532.

Parker, R. S. & Schmidt, V. H. (1971). Bull. Am. Phys. Soc.
16, 94.

Patterson, A. L. (1934). Phys. Rev. 46, 372.

Pauling, L. (1960). The Nature of the Chemical Bond.,
Third Edition. Cornell University Press, Ithica.

Pepinsky, R., Vedam, K., Okaya, Y. & Hoshino, S. (1958).
Phys. Rev. 111, 1467.

Pepinsky, R., Vedam, K., Okaya, Y. & Hoshino, S. (1958a).
Phys. Rev. 111, 1508.

Ross, F. (1970). Private communication.

Sakurai, K. & Tomiie, Y. (1952). Acta Cryst. 5, 289.

Sayre, D. (1952). Acta Cryst. 5, 60.

Schlemper, E. O. & Hamilton, W. C. (1966). J. Chem. Phys.
44, 4498.

Schmidt, V. H., Drumheller, J. E. & Howell, F. L. (1971). Phys. Rev. B4, 4582.

Sommer, F. & Weise, K. (1916). Z. anorg. Chem. 94, 51.

Stout, G. H. & Jensen, L. H. (1968). X-ray Structure Determination. The Macmillan Co., London.

Tédenac, J. C., Vilminot, S., Cot, L., Norbert, A. & Maurin, M. (1971). Mat. Res. Bull. 6, 183.

University of Maryland. (1967). University of Maryland's Crystallographic Computing System. Kundell, F. A., Chastain, R. V. & Stewart, J. M., Editors.

University of Maryland. (1971). University of Maryland's Crystallographic Computing System. Stewart, J. M., Kruger, G. J., Kundell, F. A. & Baldwin, J. C., Editors.

Van den Hende, J. H., & Boutin, H. P. (1964). Acta Cryst. 17, 660.

Vanderkooy, J., Cuthbert, J. D. & Petch, H. E. (1964). Can. J. Phys. 42, 1871.

Wells, A. F. (1954). Acta Cryst. 7, 545.

Willis, B. T. M. (1970). Thermal Neutron Diffraction (Willis, B. T. M., Editor). Oxford University Press, London.

Woolfson, M. M. (1961). Direct Methods in Crystallography. Oxford University Press, New York.